4-9-2010

Synthesis, Structure, Function and Biomedical Studies of Nucleic Acid Derivatized with Selenium

Lina Lin
Georgia State University

SYNTHESIS, STRUCTURE, FUNCTION AND BIOMEDICAL STUDIES OF NUCLEIC ACID DERIVATIZED WITH SELENIUM

by

LINA LIN

Under the Direction of Professor Zhen Huang

ABSTRACT

Nucleic acids are macromolecules in cells for storing and transferring genetic information. Moreover, nucleic acids, especially RNAs, can fold into well-defined 3D structures and catalyze biochemical reactions. As ubiquitous biological molecules in all living systems, nucleic acids are important drug targets, and they can also be used in diagnostics and therapeutics. Structural information of nucleic acids provides the foundation for DNA and RNA function studies. X-ray crystallography has been a useful tool for structural studies of bio-macromolecules at atomic level. There are two major problems in macromolecular crystal structure determination: phasing and crystallization. Although selenium derivatization is routinely used for solving novel protein structures through the MAD phasing technique, the phase problem is still a

critical issue in nucleic acid crystallography. The covalent selenium-derivatization of nucleic acids has been proven to be a useful strategy for solving the phase problem in nucleic acid X-ray crystallography. Besides the facilitation of nucleic acid crystallography, there is also a wide range of other applications for selenium-derivatized nucleic acids (SeNA).

The investigation presented in this dissertation mainly focuses on the following research subjects

(1) Synthesis and characterization of selenium-derivatized nucleic acids for X-ray crystallography, especially phosphoroselenoate RNAs. They are generated and used for crystallization.

(2) Application of selenium-derivatized RNA for RNA interference. Phosphoroselenoate RNAs are tested for RNAi activities.

(3) Synthesis and characterization of the uridine 5'-triphosphate modified with selenium at position 4.

(4) Facile synthesis and antitumor activities of selenium modified deoxyribonucleosides. MeSe-thymidine nucleosides have shown antitumor activity in cell assays.

. .

INDEX WORDS: Selenium, Nucleic acids, RNA, DNA, PSe-RNA, X-ray crystallography, Anti-cancer drug, siRNA, RNA interference,

SYNTHESIS, STRUCTURE, FUNCTION AND BIOMEDICAL STUDIES OF NUCLEIC ACID DERIVATIZED WITH SELENIUM

by

LINA LIN

A Dissertation Submitted in Partial Fulfillment of the Requirements for the

Degree of

Doctor of Philosophy

in the College of Arts and Sciences

Georgia State University

2010

SYNTHESIS, STRUCTURE, FUNCTION AND BIOMEDICAL STUDIES OF NUCLEIC ACID DERIVATIZED WITH SELENIUM

by

LINA LIN

Committee Chair: Zhen Huang

Committee: Phang C. Tai
Irene T. Weber

Electronic Version Approved:

Office of Graduate Studies
College of Arts and Sciences
Georgia State University
May 2010

DEDICATION

This thesis is dedicated to my parents Kaiming Lin and Meizhen Xie, who are the initial sources for my creativity and independent thinking. I am deeply indebted to them for their continued love, support and unwavering faith in me.

ACKNOWLEDGEMENTS

All the work in this dissertation was carried out under the direction of Prof. Zhen Huang. I am deeply indebted to Prof. Zhen Huang, whose valuable suggestions and tireless encouragement helped me during all the time that I carried out this research. His enthusiasm and love for science have been major driving forces through my graduate career. I would like to thank Prof. Phang C. Tai and Prof. Irene T. Weber who gave me their full support and guidance in performing this research. I am obliged to Dr. Julianne Caton-Williams, Dr. Jia Sheng, Dr. Jozef Salon, Dr. Abdalla E. A. Hassan, Sarah Spencer, Wen Zhang and other lab members for their daily discussions and helps in lab research. Especially, I would like to thank Andres M. Patino and Jaya Punetha as research assistants, who helped me to finish the projects on time. Many people from the faculty, staff and colleagues of the Department of Biology and Chemistry have helped and encouraged me in various ways during my graduate years. I gladly express my gratitude to them for their help, support, interest and valuable discussions. This work is supported by grants from the NIH (GM069703) and NSF (CHE-0750235, MCB-0517092, and MCB-0824837).

TABLE OF CONTENTS

LIST OF TABLES

LIST OF FIGURES

LIST OF ABBREVIATIONS

4-Se-UTP	4-Se-uridine 5’- triphosphate
4-Se-T	4-Se- thymidine
ATPαSe	Adenosine 5’-(alpha-P-seleno)triphosphate
BTSe	3H-1,2-benzothaselenol-3-one
CTPαSe	Cytidine 5’-(alpha-P-seleno)triphosphate
DMAP	4-Dimethylaminopyridine
DMF	Dimethylformamide
DMTr	Dimethoxytrityl
DNA	Deoxyribonucleic acid
dsDNA	Double stranded DNA
dNTP	Deoxyribonucleotide triphosphate
DTT	Dithiothreitol
EDTA	Ethylenediaminetetraacetic acid
ESI	Electrospray ionization
FPLC	Fast protein liquid chromatography
GPx	Glutathione peroxidase
GSH	Glutathione
GTPαSe	Guanosine 5’-(alpha-P-seleno)triphosphate
HDV	Hepatitis delta virus
HHM	Hammerhead ribozyme mutant
HHN	Native hammerhead ribozyme
HR-MS	High resolution mass spectrum
MAD	Multi-wavelength anomalous dispersion
MALDI	Matrix-Assisted Laser Desorption/ionization
MeSe	Methylselenol
MIR	Molecular isomorphorous replacement
mnm5se2U	5-[(methylamino)methyl]-2-selenouridine
MR	Molecular replacement
$NaBH_4$	Sodium borohydride
NCR	Noncoding region
NMR	Nuclear magnetic resonance
NTPαSe	5’-(alpha-P-seleno)triphosphate
PAGE	Polyacrylamide gel electrophoresis
PCR	Polymerase chain reaction
PEG	Poly ethylene glycol
PKM2	Pyruvate kinase type M2
PS	Phosphothioate
PSe-RNA	Phosphoroselenoate RNA
PTGS	Post transcriptional gene silencing
RNA	Ribonucleic acid
RNase	Ribonuclease
RNAi	RNA interference
RISC	RNA-induced silencing complex
RP-HPLC	Reverse phase high-performance liquid chromatography

rRNA	Ribosomal RNA
RT	Room temperature
SAD	Single-wavelength anomalous dispersion
SeCys/Sec	Selenocysteine
SeMet/SeM	Selenomethionine
SeNA	Selenium modified nucleic acids
SIR	Single isomorphous replacement
SIRAS	Single isomorphous replacement with anomalous scattering
siRNA	Small interfering RNA
SL	Stem-loop
ssDNA	Single stranded DNA
TBDMS	*tert*-butyldimethylsilyl
TCA	Trichloroacetic acid
TEA	Triethylamine
TEAAc	Triethylamine-acetic acid buffer
TEABC	Triethylamine bicarbonate buffer
TFA	Trifluoroacetic acid
THF	Tetrahedrofuran
TIBSCl	2,4,6-(Triisopropylbenzene)sulfonyl chloride
TLC	Thin layer chromatography
Tm	Melting temperature
TMP	Trimethyl phosphate.
tRNA	Transfer RNA
UV	Ultraviolet
UTPαSe	Uridine 5’-(alpha-P-seleno)triphosphate
WNV	West Nile virus

1. INTRODUCTION

1.1 RNA crystallography

In 1953, the DNA double helix model was proposed by Watson and Crick, while at that time scientists still had no clue about the structure and function of the RNA molecule.[1] Until 1974, after the X-ray crystal structure of L-shaped transfer RNA (tRNA) was determined, the role of RNA in protein biosynthesis started to be revealed.

RNA is an important mediator of gene expression. mRNA transfers genetic information out of the nucleus and serves as a template to guide the synthesis of corresponding proteins. There are also other RNA species playing important roles in the protein synthesis machinery, such as rRNA and tRNA. In biological regulation, researchers previously focused more on protein biology, because protein possesses more diverse structures and biological functions. However, since massive discoveries on non-coding and regulatory RNA molecules, like microRNA [2] and riboswitch,[3] researchers found that nature has very smart and much varied designs for the regulation. Beside regulation of proteins, RNAs, especially mRNAs, are also regulated.[4] These RNA regulations can be performed by both protein and RNA. Furthermore, non-coding RNAs, such as microRNAs, can also regulate proteins expression through RNA-protein interactions.[5] The study of the function and structure of these non-coding and regulatory RNA molecules has become an increasingly active research field.

Like proteins, RNA molecules also have complicated structures and

abilities to catalyze enzymatic reactions.[6] Understanding the biological activities of RNA molecules also requires the knowledge about the structure and conformational dynamics of these molecules. Another important advance in RNA crystallography after the tRNA structure was the crystal structure of several types of ribozymes, such as hammerhead ribozyme (1994),[7] P4-P6 domain of the *Tetrahymena* group I intron (1996),[8] and hepatitis delta virus (HDV) ribozyme (1998),[9] which represented a growing interest in the RNA crystallography field. After that, many more crystal structures of functional RNAs were determined, such as ribosomal RNA, [10] hepatitis C virus ribosome entry site [11] and riboswitches.[12] With the assistance of these RNA structures, scientists are able to discover more insights into biological systems.

In biomacromolecular X-ray crystallography, crystallization and phasing problem are the two major limiting factors. Crystallization of biomacromolecules is the most unpredictable step in determining the structure of the biomacromolecules. Comparing with protein crystallization, RNA crystallization has some unique difficulties. A crystal is regularly assembled by a large numbers of molecules, which are held by non-covalent interactions (crystal contacts).[13] While proteins have a variety of structural and chemical groups on the surface to make crystal contacts, the surface of a RNA molecule is full of negatively charged repetitive phosphate groups, which make the crystal packing much more difficult. Moreover, crystal diffraction signals are usually weaker from the RNA crystals due to the loose packing and higher solvent content in the RNA crystals. In addition, RNA typically has weaker tertiary interactions, which result in higher

flexibility of structures; thus it is more difficult to prepare conformationally homogeneous RNA samples. Besides crystallization, the other difficulty in nucleic acid crystallography is how to solve the phase problem.[14] Several methods have been developed for solving the phase problem. [15] The major technical breakthrough for solving the protein phase problem was MAD (multi-wavelength anomalous dispersion) phasing technique with selenomethionine (SeMet) derivatized protein.[16] For nucleic acids, due to the lack of convenient heavy atom derivatization with high stability, the phase problem is still a bottleneck.

Our group pioneered and developed selenium derivatized nucleic acid (SeNA) strategy to solve the phase problem in nucleic acid crystallography, through the MAD phasing technique. What the phase problem is and how selenium-derivatization facilitates the RNA crystallography are explained in detail in the following sections.

1.2 Selenium derivatization for nucleic acid crystallography - why we need selenium derivatization for nucleic acids X-ray crystallography and how to introduce selenium into RNA?

1.2.1 The phase problem in X-ray crystallography

In a biomacromolecular X-ray crystallography experiment, there are three major steps, crystallization, data collection and data analysis (Figure 1.1) [17]. Firstly, enough of pure macromolecules has to be prepared and crystallized, then the X-ray diffraction data of the crystals can be collected. If good quality X-ray

diffraction data is obtained; it can be analyzed and refined to reconstruct the electron density map of the macromolecule.

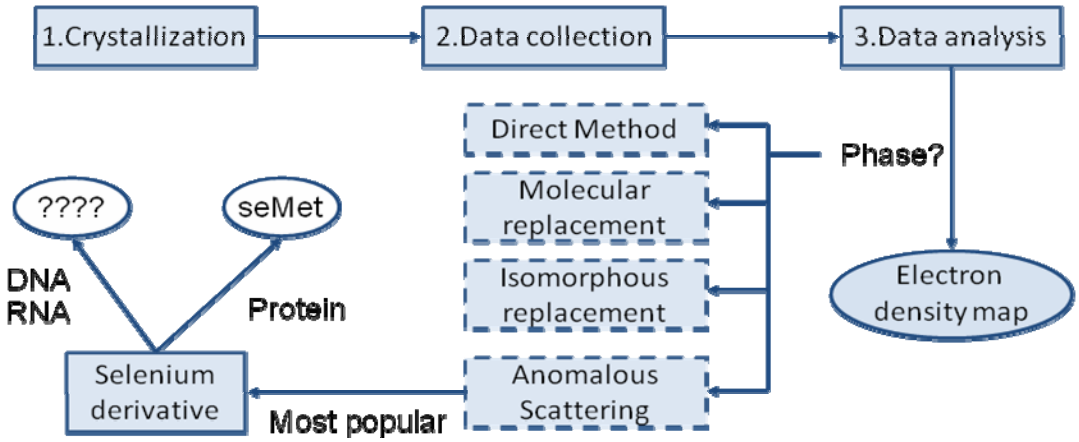

Figure1.1 Steps for solving a novel macromolecular X-ray crystal structure. Illustration of why selenium derivatization is needed for nucleic acids X-ray crystallography.

In the data analysis step; the reconstruction of the electron density map in order to acquire the electron density at a position (*xyz*) from the diffraction data requires us to apply Fourier transformation (equation expressed as following) [15].

$$\rho(xyz) = 1/V \Sigma \left| F_{hkl} \right| \exp(i\alpha_{hkl}) \exp(-2\pi i hx+ky+lz)$$

Two components on the right side of the equation, structure-factor amplitude $\left| F_{hkl} \right|$ and phase α_{hkl} associated with $\left| F_{hkl} \right|$, are needed for calculation of the electron density at a position (*xyz*). The amplitude $\left| F_{hkl} \right|$ can be measured from the reflection intensity. However, the phase information α_{hkl} is not directly available from the experiment. This problem is called the phase problem of X-ray crystallography.

Phase is a descriptive term for electromagnetic (EM) waves, such as X-ray.

For two waves with same or similar wavelength, when they are added together, there will be interference. Depending on their relative phases, the interference could be either constructive or destructive. There is either constructive or destructive interference among crystal diffracted X-ray beams. The phase information of diffracted beams is required for determination of the atom position in the structure. In fact, the phase information is very important to produce the right structure. [15] For example, if an electron density map for protein A is desired and is calculated by combining the amplitude of protein A and phase of protein B, a structure like protein B could be generated for protein A, which actually is a wrong structure for protein A.

1.2.2 Methods to solve the phase problem

There are several methods to solve the phase problem in X-ray crystallography: direct methods, molecular replacement, isomorphous replacement and anomalous scattering. [15]

Direct methods [15]

In the beginning, the molecules crystallographers were working on were usually simple molecules and crystallographers could often make a good guess on the conformation of the molecule. Then the guess could be analyzed by calculating a diffraction pattern and comparing it to the observed one. This method requires high resolution data (<1.2 Å) and could be used for small molecules (<1000 non-hydrogen atoms). Currently, programs like *Shake-and-*

Bake, *SHELXD* and *SHARP*, are still using direct methods to find the substructure of heavy-atom.

Molecular replacement

To carry out the molecular replacement method, a good homolog model for the unknown molecule has to be available. [18] As a rule of thumb, the model normally has to share at least 25% sequence similarity to that of the unknown molecule, usually much greater similarity is required for success. Patterson method is usually used first to determine the orientation of the model in the new unknown molecule. The oriented model can be then placed into the crystallographic unit cell with the translation function. The phase information can then be extracted from the model.

Isomorphous replacement

Isomorphous derivatives are the derivatives that have same space group and unit cell as native molecule. If one or several heavy-atoms could be introduced into native molecules at specific binding site(s) without changing the crystalline order, such isomorphous heavy-atom derivatives can be used to solve the phase problem of the native molecule. [15, 17] The principle of isomorphous replacement is that isomorphous heavy-atom derivatization will introduce an intensity difference, which can be measured and used to estimate the position of the heavy-atom using the direct method or Patterson method. Once the position of the heavy-atom is located, its corresponding phase can be calculated and

used to solve the phase of the native molecule.

Soaking the crystal in a solution containing heavy-atom compound can introduce the heavy-atom into the crystal. Another method to introduce the heavy-atom to crystal is growing the crysal with heavy-atom containing molecules[18]. Using one type of heavy-atom derivative in single isomorphous replacement (SIR) alone will acquire two possible solutions to the phase. This is called phase ambiguity. More than one type of heavy-atom derivatives are needed to acquire the only one solution of the phase. This method is called multiple isomorphous replacements (MIR).

Anomalous scattering [15, 17]

Similar to what happens in isomorphous replacement, introducing of heavy-atom to the crystal also results in considerable differences in structure-factor amplitudes due to anomalous scattering. These differences could be used to solve the phase of the original molecule. Compared with isomorphous replacement, differences in structure-factor amplitudes generated by anomalous scattering are usually smaller. Therefore, anomalous scattering has higher requirement on preciseness of intensities measurement. However, the advantage of the anomalous scattering is that there is no need to grow several different heavy-atom derivatized crystals. Different X-ray wavelengths can be used in anomalous scattering on one heavy-atom derivatized crystal to obtain several different sets of data. Anomalous scattering can be combined with SIR to break the phase ambiguity in SIR, and this method is called SIRAS (single

isomorphous replacement with anomalous scattering). Generally, at least three different X-ray wavelengths are needed in anomalous scattering to solve the phase problem and this method is called multiple wavelength anomalous diffraction (MAD).

1.2.3 Selenium derivatization of macromolecules and MAD phasing

Molecular replacement is the most convenient method for structure determination, if a good homology model is available, and then there will be no need to obtain a heavy-atom derivative. On the other hand, for new structures, the phase problem has to be solved through heavy-atom methods. Then the question is should we go for isomorphous replacement or anomalous scattering?

With isomorphous replacement, there are several problems. [15] First, different heavy-atom derivatives and native molecule crystals have to be obtained. Second, there could be nonisomorphism among these crystals. Third, all heavy atom positions have to be located and refined. While with MAD technique, it is unable to help on all of the problems of isomorphous replacement. However, it can overcome the nonisomorphism problem since only one type of heavy-atom derivative is needed.

There are many particular heavy-atoms that could be used for MAD phasing.[16, 19] The choice of atoms is mainly limited by the absorption edge of the element, which is related with the practical wavelengths of X-ray used in the diffraction experiments. The most popular anomalous scattering atom used for proteins is selenium. Because, firstly, the K absorption edge of selenium is

0.9795 Á, which is an ideal wavelength for X-ray diffraction experiments in most synchrotron radiation sources. [15] Secondly, selenium is within the same group as oxygen and sulfur in periodic table, which means there will be insignificant structure perturbation.[20] Thirdly, the building block (amino acid) selenium analog is available, which is selenomethionine (SeMet) with selenium substitution of sulfur in methionine.[21] Fourthly, SeMet can be conveniently incorporated into proteins by expressing proteins in Met^- strain with selenomethionine rich media.[22] Therefore, with advances in the instruments and technical details for MAD, the majority of novel protein structures are now solved by the MAD phasing technique.

1.2.4 The advantages of SeNA for nucleic acids X-ray crystallography

The phase problem of nucleic acid X-ray crystallography can also be solved by these protein techniques stated above. The comparison of these techniques for solving nucleic acid phase problem is shown in Table 1.1. In order to use direct method, high resolution diffraction data is required, which usually does not happen on a regular basis.[14] Molecular replacement is the most convenient method and can be applied for low resolution data; though, comparing with protein, it is less successful for structures that have highly repetitive units stacked together, especially in DNA. For novel structures, MAD phasing technique provides a good solution to the phase problem of nucleic acid X-ray crystallography. A specific U1A method for RNA MAD phasing, in which RNA was co-crystallized with SeMet protein U1A (a RNA binding protein), was

reported by Ferre-D' Amare and Doudna group.[9, 23] Although the U1A method has been used to solve two ribozyme structures, it is a considerably labor-intensive approach. Direct and convenient heavy atom derivatization methods for nucleic acids have not been well developed yet.

Without methods to prepare selenium nucleic acid derivatives, bromine (K edge 0.9202 Å) derivatives are usually used for nucleic acid crystallography to solve the phasing problem.[24] Halogen derivatives work fine with B-form DNA. However, in A-form DNA or RNA, halogen derivatives generate significant structural perturbations. Furthermore, due to the chemical properties of halogens, there are limited sites on nucleic acids suitable for halogen modification, usually at the 5-position of pyrimidines. It was also found that the bromine modification was not very stable during X-ray radiation. Debromination can happen with a mild dose of X-ray radiation.

Compared with traditional halogen derivatization, selenium derivatization is more stable under X-ray exposure. [25] In addition, the anomalous diffraction signals from bromine and selenium are comparable, thus the phasing power of selenium atoms for nucleic acid derivatizations are similar to bromine.[26] Since selenium is in the same group with oxygen in the periodic table, there are more site choices for selenium derivatization on nucleic acids. There are many oxygen atoms on nucleic acids, which in principle can all be selenium incorporation sites. It has been observed from nucleic acid crystal structures with selenium modifications, that selenium did not induce significant structure perturbation in the structure.[27] We also found that the high quality 2'MeSe-derivatized DNA

crystals can be obtained overnight. [20]

Nucleic acids are easier to prepare and purify in comparison with proteins. Se-derivatized RNA and DNA can also facilitate solving the phase problem of proteins that bind with nucleic acid. For enzymes in the nucleotidyl transferases superfamily, instead of mutating the protein active site, selenium atomic mutation on DNA or RNA may also be an option to inactivate the enzymes, plus phase information could be obtained without expressing proteins in Met^- strain. More detailed information about the relationship of selenium and nucleotidyl transferases is discussed in instruction 1.3.1.

Table 1.1 Methods to solve the phase problem for nucleic acid crystal structures

Methods	Requirement	Techniques	Problems
Direct Method	High resolution diffraction data		Unpredictable
Molecular Replacement	Good homolog model		Availability of model Less successful for structures with highly repetitive units
MAD	Heavy atom derivative	Bromine derivative	Photolabile Structure perturbation Limited sites
		seMet protein U1A method	Labor-intensive
		Selenium derivative	Availability of selenium analog and technique

1.2.5 Methods for introducing selenium into RNA

As described above, to determine the phase by isomorphous replacement or anomalous scattering in nucleic acid crystallography, heavy atoms have to be introduced into nucleic acid crystals. [15] There are several techniques to introduce the heavy atoms into nucleic acids, including enzymatic incorporation,

synthetic incorporation, soaking, and co-crystallization. [28] A comparison of these methods is shown in Table 1.2. The problem with soaking method is that there is non-specific binding of heavy-atom compounds to nucleic acids, while co-crystallization may also change the structure of nucleic acid due to ion replacement. [28] The benefit of covalent incorporation, like enzymatic incorporation and synthetic incorporation, is that the position of heavy atom is known, which is very important for initial localization of the heavy atom. However, these are no natural building block analogs available to nucleic acids, like selenomethionine (SeMet) to proteins. Artificial heavy-atom derivatized nucleic acids have to be specially prepared.

In the terms of preparing large scale RNA for crystallization, enzymatic incorporation and synthetic incorporation methods both have advantages and disadvantages.[29] For synthetic incorporation with the solid phase synthesizer, the advantage is the convenience to prepare a large quantity of oligonucleotides and also the capability for almost any types of modifications. The primary disadvantage is the limit on length (<50 nt) due to significantly low yield for longer oligonucleotides. Considering the length of most structurally interesting RNA molecules and demands on the equipment for most laboratories that are not equipped with solid phase synthesizers, enzymatic synthesis is the generally preferred procedure in most RNA laboratories. Very long RNA strands and a large quantity of RNA molecules could be obtained from enzymatic synthesis. For the enzymatic method, in order to get modified RNA, modified NTP analogs have to be prepared. Moreover, the modification can be inserted into RNA only if

the RNA polymerase is able to take the modified NTP analogs in as substrate.

T7 RNA polymerase from bacteriophages is the most commonly used RNA polymerase for *in vitro* preparation of RNA. The polymerase domain of T7 RNA polymerase is homologous to that of polymerases found in DNA polymerase I family, and shares the catalytic mechanism. [30] The two metal ions catalytic mechanism of T7 RNA polymerase is illustrated in Figure 1.2. T7 RNA polymerase catalysis is an S_N2 nucleophilic reaction. In the active site, metal ion A lowers the pKa of 3'-OH thus increasing its nucleophilicity. Metal ion B helps to bring in NTP, stabilizing the negative charge on the oxygens and facilitates the pyrophosphate release.[31] When preparing modified RNAs by enzymatic synthesis, the mechanism of T7 RNA polymerization should be definitely considered.

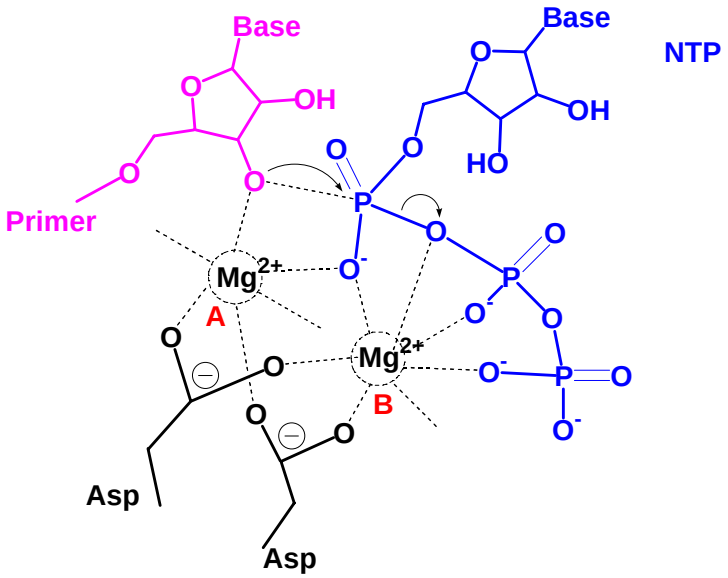

Figure 1.2. T7 RNA polymerase polymerization mechanism

When comparing 5'-(alpha-P-seleno)triphosphates (NTPαSe) to native

NTP, there was not much difference on the yield of radioactive labeled RNA. In the large scale preparation of RNA with much higher NTP concentrations, there was a difference in the yields for both native RNA and PSe-RNA, especially when dsDNA templates were used. Therefore, the protocol for large scale preparation of PSe-RNA has to be optimized from the native NTP condition. It was suspected that the lower affinity of magnesium to selenium was the reason for the lower yield of PSe-RNA. Therefore, manganese ions were tested in the transcription and indeed improved the transcription yield.

Table 1.2. Methods for introducing selenium into nucleic acid

Methods	Techniques	Advantages	Problems
Soaking		No need for building block analog	Non-specific binding
Co-crystallization		No need for building block analog	Structure change
Covalent incorporation	Enzymatic	Heavy atom position is known Common equipment requirement Good for longer nucleic acid	Analog not accepted by RNA polymerase
	Synthetic	Heavy atom position is known Capable for all types of modifications	Length limit (<40nt) Need solid phase synthesizer

1.3 Other applications of Se-derivatized nucleic acids

1.3.1 Investigation of nucleotidyl-transfer reactions

Nucleotidyl-transfer reaction, in which nucleic acids get synthesized, degraded or rearranged, is an essential chemical reaction happening in all life forms. As a result of this reaction, genetic information gets replicated, transferred, or destroyed, which represents the most basic cycle of the life. According to the "RNA world hypothesis", this reaction is one of the most ancient and fundamental

events in the beginning of life.

The typical catalytic mechanism of nucleotidyl-transfer reaction, whether by cleavage or ligation, usually involves one or two metal ions. A similar intermediate structure is shared among these nucleotidyl-transferases using two metal ion catalysis, like DNA or RNA polymerase, some nucleases and ribozymes.[32] In the active site(s), metal ions are coordinated by the scissile phosphate and also nearby amino acid residues (protein) or bases (ribozyme) to promote the nucleophilic attack. Examples of the catalytic mechanism for nucleotidyl-transfer reactions are illustrated in the following sections with discussions later about how selenium modified nucleic acids could be used for investigation of the nucleotidyl-transfer reaction. Moreover, as discussed in 1.2.5, the mechanism of nucleotidyl-transfer reaction must be considered for preparation and application of selenium modified DNA and RNA.

1.3.1.1 Ribonuclease catalytic mechanism and inhibition of RNase by selenium modification

Ribonuclease catalytic mechanism

Ribonuclease (RNase) is a type of nuclease that catalyzes the degradation of ribonucleic acids (RNA). These enzymes could digest a variety of RNA substrates, including dsRNA, ssRNA or RNA in RNA/DNA duplex. For instance, RNase H that can degrade RNA in the RNA/DNA duplex, is required in DNA replication to remove RNA primers from Okazaki fragments.[33] The function of RNase III like domain in Dicer is to produce small interfering RNAs (siRNA) in

RNA induced post transcriptional gene silence mechanism.[34] RNases are also applied to many analytical purposes, such as RNA sequencing, mapping, and quantitation[35]. Some RNase domains are proposed drug targets in RNA virus infections, such as the RNase H domain in retroviral reverse transcriptase.[36] Advances in the knowledge about the catalysis of RNases provide opportunities for better control of many essential biological processes.

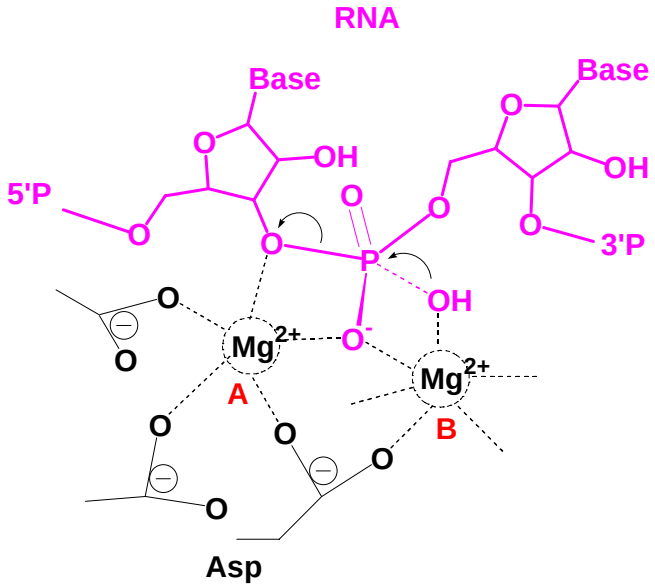

Figure 1.3. RNase H cleavage mechanism

Stepwise models for several important RNases with two metal ions catalysis have been built based on X-ray crystal structures. A diagram for RNase H catalysis is shown in Figure 1.3. [32] The two metal ions, A and B, which usually are Mg^{2+} in physiological conditions, are present in the active site to coordinate the negatively charged phosphate backbone of RNA substrates and acidic residues of the enzyme. Metal ion B deprotonates the nucleophilic water and may assist in bringing the nucleophilic water close to the scissile phosphate

[36]. The negative charge generated on the oxygen is stabilized by Metal ion A and this may destabilize the substrate and promote nucleophilic attack. Later, the substrate release may require dissociation of the metal ion B.

Inhibition of RNase by selenium modification

Extensive studies have been carried out on how to control the RNA hydrolysis process, either to accelerate or to delay it. Recently, due to the great desire of extending siRNA lifetime in mammalian cells for therapeutic purposes; studies on inhibiting RNase activities with modified RNA substrate attracted lots of research interests. A variety of chemical modifications have been tested on RNA for RNase resistance and higher base-pairing fidelity.[37]

Our group reported previously that selenium modification at the position of the non-bridging oxygen of RNA phosphate backbone would inhibit the RNase activity.[38] This mechanism is proposed as reduction of magnesium ion affinity to selenium compared with oxygen. Although due to differences in electronegativity, selenide (Se^-) should be more stable than oxide (O^-) in the intermediate structure; magnesium ions have much lower affinity to selenium than to oxygen,[38] which may result in lose of magnesium ion interaction with RNA and a significantly reduced turnover rate of the enzyme. Based on the RNA interference experiment in Chapter 3, the RNA interference strength from siRNAs with selenium modification at phosphate backbone was enhanced about one fold comparing with native siRNA.

1.3.1.2 Self-cleavage mechanisms of ribozymes and selenium as an atomic probe for ribozyme catalytic studies

Ribozyme self-cleavage mechanism

The catalytic mechanism of the hammerhead ribozyme is mainly discussed here as an example. Hammerhead ribozymes are small self-cleaving RNAs that first were discovered in a self-cleavage sequence in small RNA satellites of plant viruses [39]. A full-length active hammerhead ribozyme contains three base-paired stems and 15 highly conserved nucleotides.[40] A proposed one metal ion mechanism in hammerhead ribozyme catalysis is shown here (Figure 1.4). The metal ion stabilizes the negative charge generated in the 2' oxygen in the proposed general acid G-8 to promote nucleophilic in-line attack. [41]

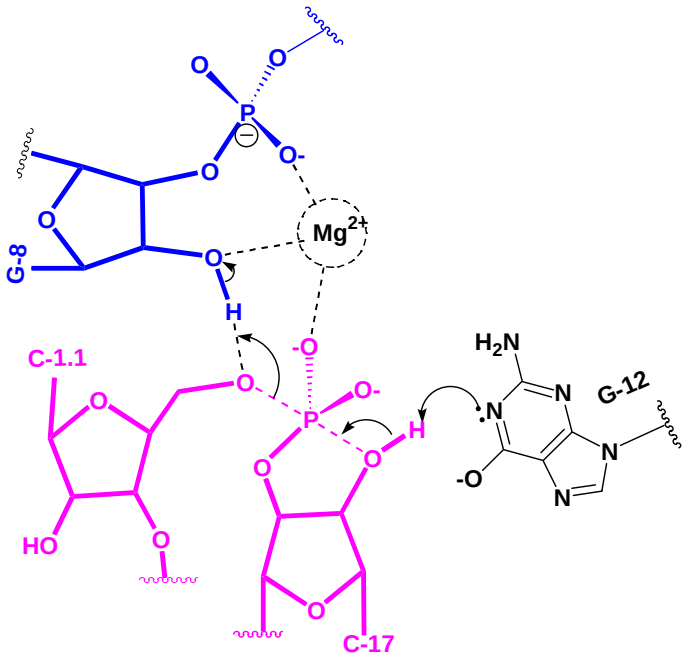

Figure 1.4. Metal ion mechanism in hammerhead ribozyme catalysis [41].

Selenium as an atomic probe for ribozyme studies

In ribozyme studies, it is very important to discover which chemical groups play the main role in structural conformation and which directly participate in chemical catalysis.[42] To answer this question, insertion of chemically modified nucleotides into ribozyme as probe is a very useful strategy. Atomic mutation with elements in the same group is an ideal choice because less perturbation is expected on ribozyme structure. Changes in ribozyme turn-over rate will mainly come from the mutation site.

Originally, there was a strong disagreement on hammerhead ribozyme catalytic mechanism derived from biochemistry studies and the structural data. It was caused by the absence of tertiary interaction of active site in the hammerhead ribozyme structures.[43] Scott and coworkers published a *Schistosma* hammerhead ribozyme structure in 2006, which basically solved most of the structure-function conflicts and organized the majority of the biochemical data.[43] However, in Scott's structure, no metal ion was found in the active site.[40]

Based on other biochemical data, the metal ion should be involved in the active site of the hammerhead ribozyme. [44-45] A previous experiment from our lab carried out with an RNA substrate that had several selenium modifications on the non-bridging oxygens of the phosphate backbone, also showed that metal ions played an important role in catalysis. With selenium modification at phosphate backbone and the presence of Mg^{2+} containing buffer, self-cleaving activity of hammerhead ribozyme was inhibited; while with Mn^{2+} substitution of

Mg^{2+}, the activity was rescued.[38] Selenium on the phosphate backbone was considered to produce no significant perturbation in the structures, if the phosphate was exposed to solvent.[27] The inhibition of cleavage activity was caused by the atomic mutation. This is an example of how selenium modified nucleotides can be used as an atomic mutation to probe the function of chemical groups for ribozymes.

1.3.2 Selenium and diseases

Selenium is an unusual trace element. Discovered in 1818, and named after the goodness of the moon, this element was only known for its toxicity and as a possible carcinogen for a long period of time.[46] The essentiality of selenium for life rather than a hazard was primarily recognized in the late 1950s, which was almost one and a half centuries after the identification of selenium element. The systematically documented diseases caused by selenium deficiency in humans were rare, except for the well known severe heart failure in Keshan disease.[47] However, there is evidence from both laboratory and observational studies suggesting that selenium may affect human health from diverse aspects, such as immune responses, cancer, HIV infection, cardiomyopathy, rheumatoid arthritis, asthma and Alzheimer's disease.[48]

There were two famous randomized controlled clinical trials concerning the investigation of selenium health benefits in the US. However, the results coming out of these two trials were different from each other. The first study was from Nutritional Prevention of Cancer (NPC), the result of which showed that

prostate cancer risk was reduced by 63% for selenium enriched yeast. [49] In contrast, the more recent and larger scale clinical trial result for Selenium and Vitamin E Cancer Prevention Trial (SELECT), funded by the National Cancer Institute (NCI) and the National Institutes of Health (NIH) showed that selenium and vitamin E supplements, either alone or in combination, did not prevent prostate cancer.[50] These results seem suggest that selenium may only benefit people who have low serum selenium level. Although the result from SELECT was a huge disappointment, as a trace element, the essentiality of selenium to life was still indisputable.

The biological effects of selenium on life are exerted through a variety of selenium-containing molecules in cells:

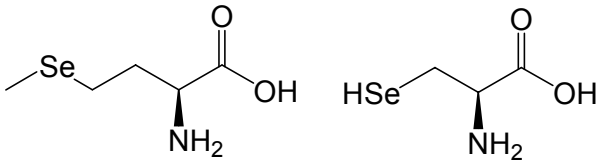

SeMet SeCys

Figure 1.5. Selenomethionine and Selenocysteine

In protein, selenium is inserted in two forms, selenomethionine (SeM, SeMet) and selenocysteine (Sec, SeCys) (Figure 1.5). [51] No physiological function differences were observed between proteins with selenomethionine or methionine. [21] Selenoenzymes, the majority of which are involved in catalyzing redox reactions, are generally referred as enzymes with Sec in the active sites for specific functions. In the human genomes, there are 25 genes encoding for 30 selenoproteins.[52] The most well studied selenoenzyme is glutathione

peroxidase (GPx), which catalyzes the reduction of hydrogen peroxide or phospholipid peroxide to water or corresponding alcohols using glutathione (GSH).[53] GPxs constitute an important part of the cell antioxidant defense system and have also been related with oxidative stress recovery, reduction of UV-induced DNA damage, protection against neurodegenerative diseases and cancer prevention. [54]

Selenium levels in the body are mainly determined by the dietary selenium content. The major natural selenium species in selenium rich plants are selenate, SeMet, SeCys, Se-methyl-selenocysteine (MeSeCys) and g-glutamyl-Semethyl-Selenocysteine (GluMeSeCys). [55] In general selenium metabolic pathways, selenium containing amino acids from food, such as SeMet and SeCys are metabolized to hydrogen selenide (H_2Se) through enzymatic reactions (Figure 1.6).[56] Selenomethionine could also be incorporated into ordinary proteins through the normal protein synthesis pathway in the place of methionine. Inorganic selenite (SeO_3^{2-}) and selenate (SeO_4^{2-}) are also reduced to H_2Se through several metabolic steps involving glutathione and NADPH-dependent reductases.[57-58] H_2Se is an intermediate among several selenium pathways, such as selenium reductive pathway, synthetic metabolism and methylation metabolism. H_2Se can be incorporated into phosphate by selenophosphate synthetase.[59] The selenophosphate (H_3PO_3Se) is used to synthesize sec-tRNA, which conducts insertion of selenocysteine into selenoproteins through the UGA code. H_2Se could also be methylated by thiol S-methyltransferase to mono-, di- and tri- methylated forms, which would get out of body though breath or urine. [57]

Nevertheless, as first proposed by Ip and coworkers, methylselenol (MeSe, CH_3SeH) was considered to be the most active metabolite of selenium compounds in selenium chemoprevention.[60] There were many researches on the chemprevention activities of MeSe.

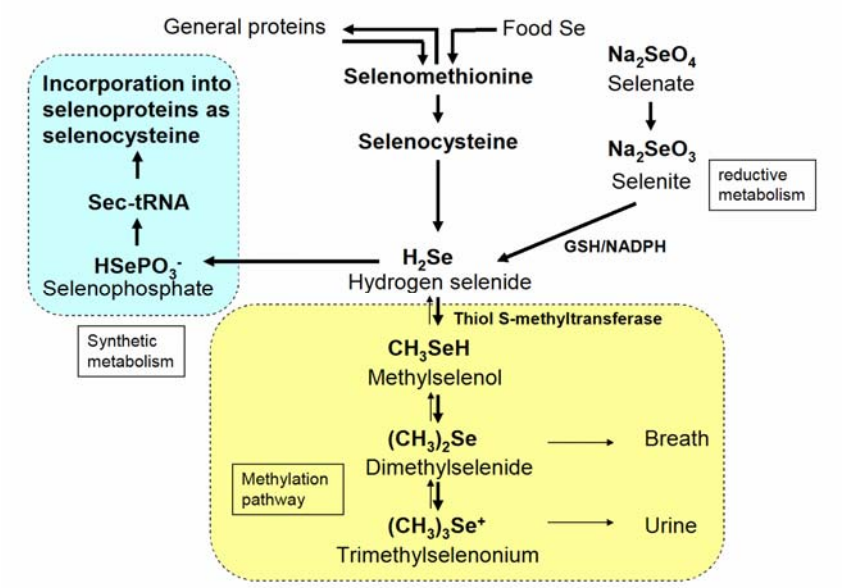

Figure 1.6. Selenium metabolism pathways

Compared with the most extensively studied selenoproteins and small selenium metabolites, it is not well-known that selenium also naturally occurs in bases of tRNA, usually in the wobble base position, which may have some special functions. [61] However, detailed studies about the natural Se-derivatized RNAs are rather limited. Selenium was found in tRNAs, mainly in the forms of 2-selenouridine and 5-[(methylamino)methyl]-2-selenouridine (mnm5se2U), as shown in Figure 1.7. These seleno-tRNAs are usually found in species such as *Escherichia coli*, *Clostridium sticklandii*, *Methanococcus vannielii*, and *Salmonella* typhimurium.[62-65] Se-derivatization of tRNA was also surprisingly found in mouse leukemia cells [66] and bovines. [67]

It is reasonable that the essentiality of selenium for life could be the combined effects from selenoproteins, seleno-nucleic acids and selenium metabolites in body, which increases the complexity of the evaluation of selenium biological activities.

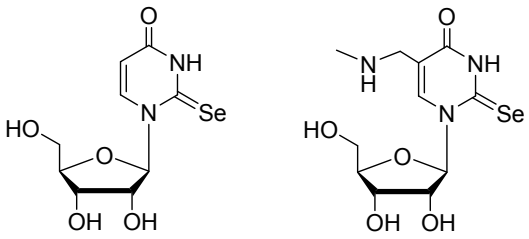

Figure 1.7. 2-selenouridine and 5-[(methylamino)methyl]-2-selenouridine (mnm5se2U)

In our lab, many selenium-containing nucleosides, nucleotides and nucleic acids have been made. Considering the possible therapeutic activity of selenium compounds, these nucleosides, nucleotides and nucleic acids have been sent for primary anticancer, antimicrobial screenings. Some of them indeed shown biological activities.[68] Further investigation on selenium-containing molecules for health will definitely offer more information about this type of molecule.

1.4 Current development of SeNA for X-ray crystallography

Selenium can be incorporated in to a variety of sites of nucleic acids, including the sugar, phosphate and base (Figure 1.8). Since 1998, our lab has pioneered the technique advancing in this field.[69] Here is a brief summary of the current stage of SeNA development for nucleic acid X-ray crystallography.

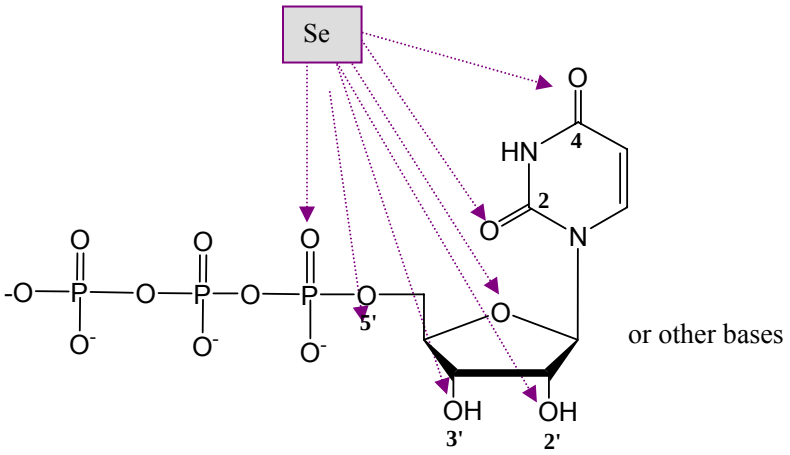

Figure 1.8. Atom specific selenium replacement of oxygen in nucleic acids

1.4.1 Selenium modification at sugar

Selenium substitution of oxygen at 5' of A, C, G, T and U as methylselenol, was the first attempt of derivatizing nucleic acid with selenium for X-ray crystal structure studies. [69] This modification was designed for terminal selenium derivatization of nucleic acid. Selenium containing phosphoramidites were prepared and selenium was introduced into nucleic acids through a solid phase synthesizer. The successful synthesis of selenium containing oligonucleotides proved that it was possible to incorporate selenium into nucleic acid through solid phase synthesizer.

Selenium was also introduced to 2'-position of nucleic acid as methylselenol group through solid phase synthesis.[20, 26, 70-73] This modification later turned out to be a great success, even more than expected. Selenium modified DNA grew crystals in many buffer conditions of the Hampton kit

overnight. [20] The comparison results showed that DNA derivatized with selenium at 2'-position could crystallize at broader buffer condition and had better crystallizability than native or bromine modified DNA. A high resolution selenium derivatized small DNA duplex structure (1.28 Å) was solved by MAD with 2'-methylseleno modification. Selenium derivatization was also present in the minor groove of DNA and did not affect minor groove hydration significantly.

Micura's group in Austria has developed strategies for solid phase synthesis of RNA with 2'-methylseleno modifications.[74-76] The shorter RNA strands prepared by solid phase synthesis with site specific 2'-methylseleno modification were linked together to form longer RNA (up to 100 nt) by T4 RNA ligase.[75] A ligated 49 nt RNA with 6 selenium atoms was crystallized in the same conditions as native and the crystals diffracted at about 3 Å resolution. It was stated that, with site specific insertion, 2'-methylseleno modification did not significantly change the global folding of RNA. As with what happened in DNA, a crystallization screening showed that 2'-methylseleno modified RNA was able to crystallize at broader buffer conditions than the nonmodified counterpart. Crystal packing analysis suggested that selenium atoms may contribute to bring RNA molecules closer to each other. [76]

1.4.2 Selenium modification at non-bridging phosphate

Egli and co-worker from Vanderbilt University developed a solid phase synthesis method to derivatize DNA with selenium at the non-bridging phosphate position [27]. DNA phosphoroselenoate (PSe-DNA) was demonstrated to be stable

under crystallization conditions for months. It was reported that selenium modification close to the 5' end was more stable than inside positions. There were only minimal differences between PSe-DNA structure and the native DNA structure. The Mg^{2+} ion coordination was identical to that in original native DNA structure. The PSe-DNA generated from solid phase synthesis method was a mixture of *Rp* and *Sp* diastereomers for phosphorous chiral center and needed further purification. Diastereomeric pure PSe-DNA could be made from enzymatic synthesis [77-78]. Our group reported a synthesis method for all nucleoside 5'-(α-P-seleno)triphosphates and also incorporation of one of the two NTPαSe diastereomers into RNA [38]. RNase resistance was observed for PSe-RNA.

1.4.3 Selenium modification at nucleobase

Derivatives of DNA at the 4-position of thymidine (4-Se-T) have been prepared through both solid phase synthesis and enzymatic incorporation. [79-80] Crystallization was attempted for solid phase synthesized 4-Se-DNA. A selenium mediated hydrogen bond was observed in the 4-Se-DNA duplex with distance of 2.87 Å.[80] The UV-melting experiment showed that the 4-selenium modification did not significantly affect the melting point of a 9mer DNA comparing with the native DNA duplex, which indicated that there was not much perturbation on base pairing.

In order to investigate whether a C-H (or CH_3) group can form a hydrogen bond with the phosphate backbone of nucleic acids, selenium was inserted into

the 5-methyl group of thymidine.[81] A DNA duplex crystal was obtained with selenium at 5-methyl position of thymidine from solid phase synthesis In the crystal structure, the selenium linker extended the methyl group toward the phosphate and the distance between the methyl and phosphate was only 2.93 Å, which is within the normal hydrogen bond distance. The possible interaction between methyl and phosphate was suspected to be involved in DNA duplex unwinding by reducing the energy barrier.

Selenium was also introduced into the 6-position of guanine (6-Se-G).[82] 6-Se-DNA was co-crystallized with RNA and RNase H and the crystal structure was determined, which was the first nucleic acid–protein complex structure with phase solved by selenium derivatization on nucleic acid. The base pair between 6-Se-G and C was similar to a normal G-C pair with a shift of about 0.3 Å. The overall structure of 6-Se-DNA was very similar to native DNA duplex.

2 PREPARATION OF PHOSPHOROSELENOATE RNA FOR X-RAY CRYSTALLOGRAPHY

2.1 Introduction

The explosive discoveries on RNA in recent years, such as small regulatory RNA [2, 83] and the riboswitch, [3] lead to a great demand for structural insights of RNA and RNA related molecules. Compared with protein crystallography, RNA crystallography has some unique problems (as discussed in the introduction). One major problem is lack of a well developed heavy atom derivatization method to solve the phase problem.[13] In the case of novel protein structure, the phase problem is usually solved by selenomethionine (SeMet) derivative via MAD phasing technique.[16, 19] Halogen derivatives have been traditionally used for nucleic acid heavy atom derivatization. However, halogen derivatives usually produce crystal structures that are different from native structures and are unstable during X-ray radiation.[24] Since 1998, Huang's research group has pioneered the development of selenium derivatization of nucleic acids for X-ray crystallography. [69] It was found that selenium derivatives are much more stable than halogen derivatives under X-ray radiation and less structural perturbation has been observed for the selenium derivatives.[20, 25]

Heavy atoms can be introduced into nucleic acid through several different ways - soaking, co-crystallization and covalent incorporation.[28] The difficulty with the soaking method is that many heavy atom compounds do not bind well to nucleic acids at specific sites. A co-crystallization method, using SeMet derivatized U1A protein (a RNA binding protein), was reported by Ferre-D'

Amare and Doudna groups.[9, 23] Although this U1A method has been used to solve two ribozyme structures, it is a labor-intensive approach. For direct covalent incorporation of a heavy atom into nucleic acids, there are two methods - enzymatic (RNA polymerase) and synthetic (solid phase synthesis).[29] A drawback of solid phase synthesis for large-scale RNA preparation is that the length of RNA is limited (<50 nt). To solve this problem, a T4 RNA ligase method for RNA 2'-methylseleno modification was developed by Micura's group to produce longer selenium derivatized RNA.[75] For most laboratories that are not equipped with a solid phase synthesizer and not familiar with organic synthesis, enzymatic incorporation is a much more accessible method. A large quantity of long RNA molecules can be obtained using enzymatic synthesis by RNA polymerase. In addition to assisting in RNA crystallography, phosphoroselenoate RNA (PSe-RNA) was also reported to be RNase resistant,[38] as such it serves as a potential application for RNA interference therapeutics.

To incorporate selenium into RNA through RNA polymerase, the 5'-(alpha-P-seleno) triphosphates (NTPαSe) have to be prepared and must be capable of being accepted as substrate by RNA polymerase. We have reported previously a method to prepare NTPαSe with protective groups on the sugar moiety, [38, 78] and their incorporation into RNA by T7 RNA polymerase. Considering the general applications of these NTPαSe, it is necessary to simplify the synthesis method, improve the yield and carry out a full scale characterization for these NTPαSe. In this section of the dissertation, a new synthesis method is described in detail for preparation of NTPαSe without any

protective groups, which greatly reduced efforts for purification and increased the yield of NTPαSe and PSe-RNA. All of the nucleoside 5'-(α-P-seleno)triphosphate diastereomers synthesized by the new method were characterized by NMR, MS and HPLC and tested for RNA incorporation on multiple types of DNA templates. Different DNA template preparation methods (single strand, plasmid and PCR) for RNA crystallization are also described in detail to standardize the protocol. All of the NTPαSe were purified by RP-HPLC or boronate column and purified NTPαSes were tested for several RNA incorporations through different types of DNA template. The PSe-RNA was purified and the selenium derivatization was confirmed by MALDI-TOF.

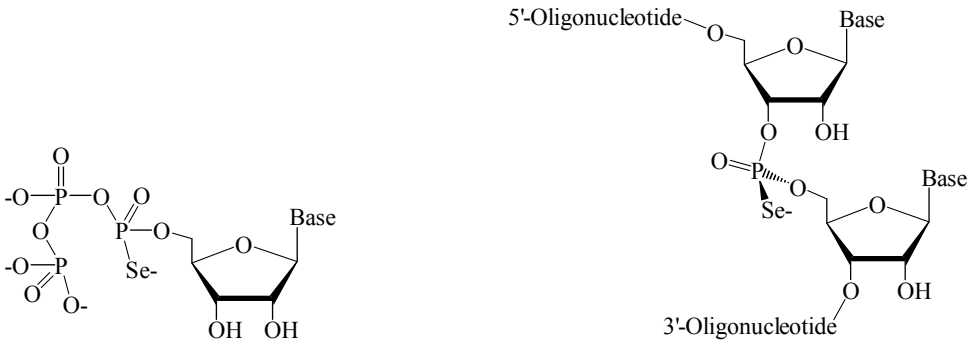

Figure 2.1. (A) NTPαSe structure. (B) Structure of *Rp* phosphoroselenoate RNA.

2.1.1 Brief introduction about the functional RNA molecules in this dissertation

Hammerhead ribozyme

The hammerhead ribozyme is the smallest nucleolytic ribozyme, which can perform a site specific self-cleavage.[84] The hammerhead ribozyme was initially found in several plant viruses for rolling cycle replication.[40] The minimal

hammerhead ribozyme has of three base-paired stems and a conserved core of 15 nucleotides (shown in grey in Figure 2.2). The catalytic mechanism of the hammerhead ribozyme has been discussed in detail in the Introduction 1.3.1.2 *Self-cleavage mechanisms of ribozymes and selenium as an atomic probe for ribozyme catalytic studies.* Basically, the nucleophilic attack starts from the 2'-hydroxyl of a nucleotide in the conserved core to its adjacent phosphodiester bond, and generates a 2', 3'-cyclic phosphate and a free 5'-hydroxyl end.[85]

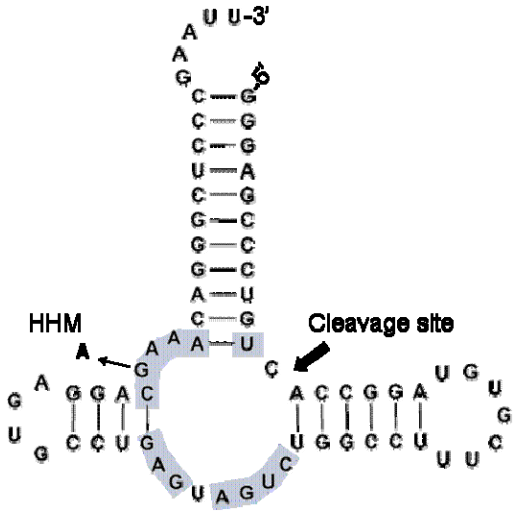

Figure 2.2. Secondary structure of wild type hammerhead ribozyme derived from the satellite RNA of tobacco ringspot virus. Conserved bases are labeled in grey

West Nile virus (WNV) terminal stem-loop (SL)

The genome of WNV is a single stranded positive RNA strand (sense strand).[86-87] There were stem-loop (SL) structures in the 5' noncoding region of WNV genome (SL(+)) (Figure 2.3.B). The studies suggested that the

complementary negative strand of this region, which also formed a SL structure (SL(-)) (Figure 2.3.A), could serve as a promoter for replication of the positive strand. The existence of the terminal secondary structure in the complementary negative strand was confirmed by RNase digestion experiment. [88] These SL structures are probably cell protein binding sites. Analysis of the sequence and structure of the WNV genome can allow potential applications in the treatment and diagnosis of West Nile Virus in humans and animals.

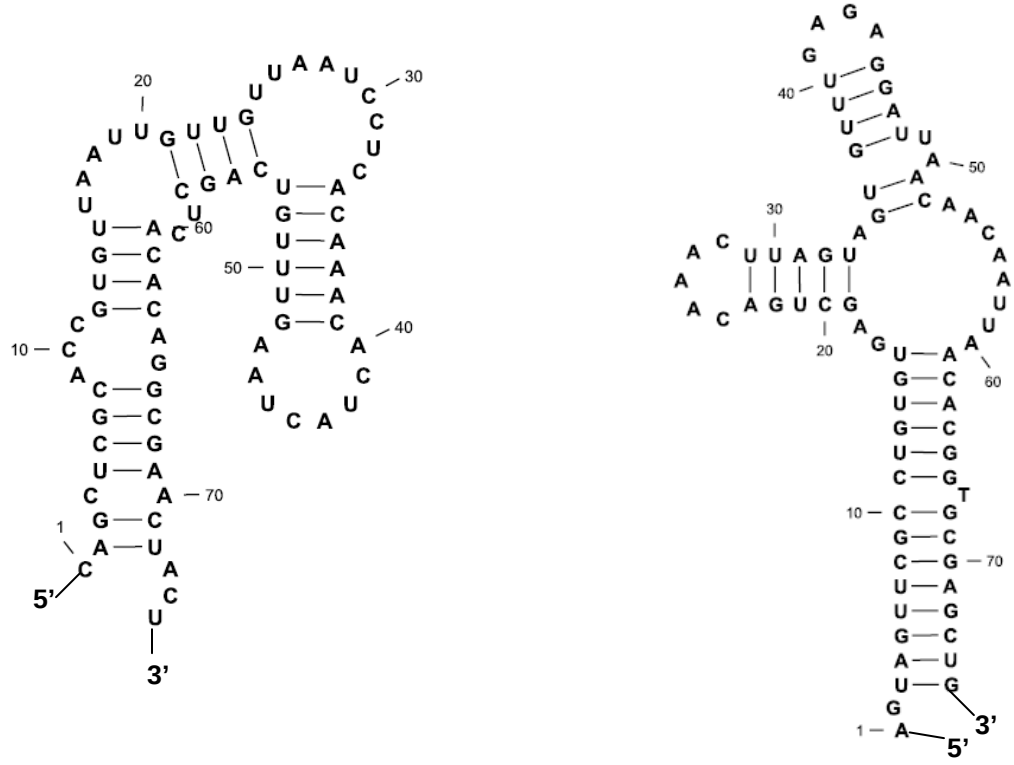

A. WNV 3' SL(-) B. WNV 5' SL (+)

Figure 2.3. Predicted secondary structure of WNV terminal stem-loop SL (-) and SL (+)

P4-P6 domain of group I intron

The group I intron (400 nt) from *Tetrahymena thermophila* was the first described catalytic RNA, which can self-splice itself from a ribosomal RNA transcript. The group I intron has nine paired regions, named from P1 to P9, which are folded into two domains - the P4-P6 domain (formed by the P5, P4, P6 and P6a helices) and the P3-P9 domain (formed by the P8, P3, P7 and P9 helices). [89] P4-P6 domain (160 nt) is an essential part of the group I intron from *Tetrahymena thermophila.*[8] Without the P4-P6 domain, the intron is not active. The P4-P6 domain is not only part of the catalytic core but also stabilizes the intron and helps to bring the intron's folding pathway together.[90] The folding P4-P6 domain is independent from the rest of the intron. A secondary structure of P4-P6 domain is shown in Figure 2.4. The crystal structure of a wild type P4-P6 domain was solved in 1996, by which the principle of folding of large ribozyme into compact, globular structure through long-range tertiary interaction was first revealed. A single site mutant (ΔC209) of P4-P6 domain has been reported to be more stable and easy to crystallize,[91] and makes it a good model molecule to demonstrate the principle of selenium RNA derivatization for X-ray crystallography.

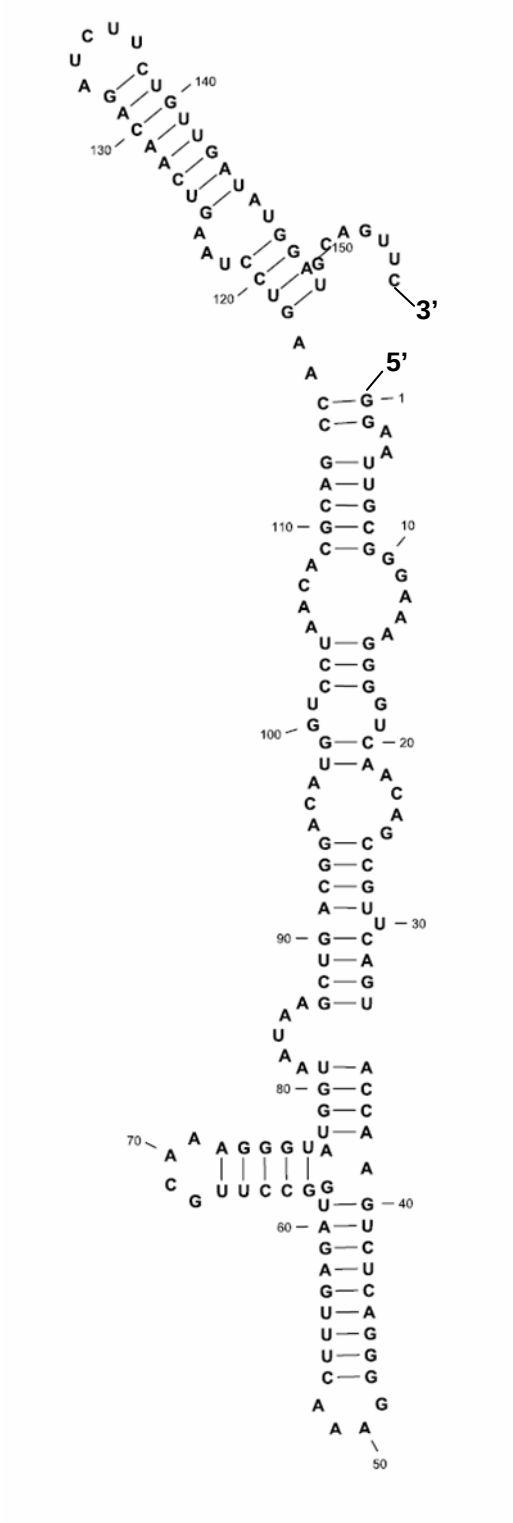

Figure 2.4. Secondary structure of P4-P6 domain of group I intron

Table 2.1. RNA sequences

Name	Sequences
HHM	5’-GGGAGCCCUGUCACCGGAUGUGCUUUCCGGUCUGA UGAGUCCGUGAGGAC**A**AAACAGGGCUCCCGAAUU-3’
HHN	5’-GGGAGCCCUGUCACCGGAUGUGCUUUCCGGUCUGA UGAGUCCGUGAGGACGAAACAGGGCUCCCGAAUU-3’
SL(-)	5’-CAGCUCGCACCGUGUUAAUUGUUGUUAAUCCUCACA AACACUACUAAGUUUGUCAGCUCACACAGGCGAACUACU -3’
SL(+)	5’- AGUAGUUCGCCUGUGUGAGCUGACAAACUUAGUAGU GUUUGAGAGGAUUAACAACAAUUAACACGGTGCGAGCU G -3’
89.24	5’-GGGAGCCCUGUCACCGGAUGUGCUUUCCGGUCUGA UGAGUCCGUGAGGAC**A**AAACAGGGCUCCCGAAUU-3’
55.27	5’-GGCAACCUGAUGAGGCCGAAAGGCCGAAACGUACA-3’
44.1	5’-G GCA ACCGGAUGAGGCCGA AAGGC-3’
P4-P6	5’GGAAUUGCGGGAAAGGGGUCAACAGCCGUUCAGUACC AAGUCUCAGGGGAAACUUUGAGAUGGCCUUGCAAAGGG UAUGGUAAUAAGCUGACGGACAUGGUCCUAACACGCAG CCAAGUCCUAAGUCAACAGAUCUUCUGUUGAUAUGGAU GCAGUUC-3’

2.2 Materials and methods

2.2.1 Synthesis, characterization and purification of nucleosides 5’-(alpha-P-seleno) triphosphates

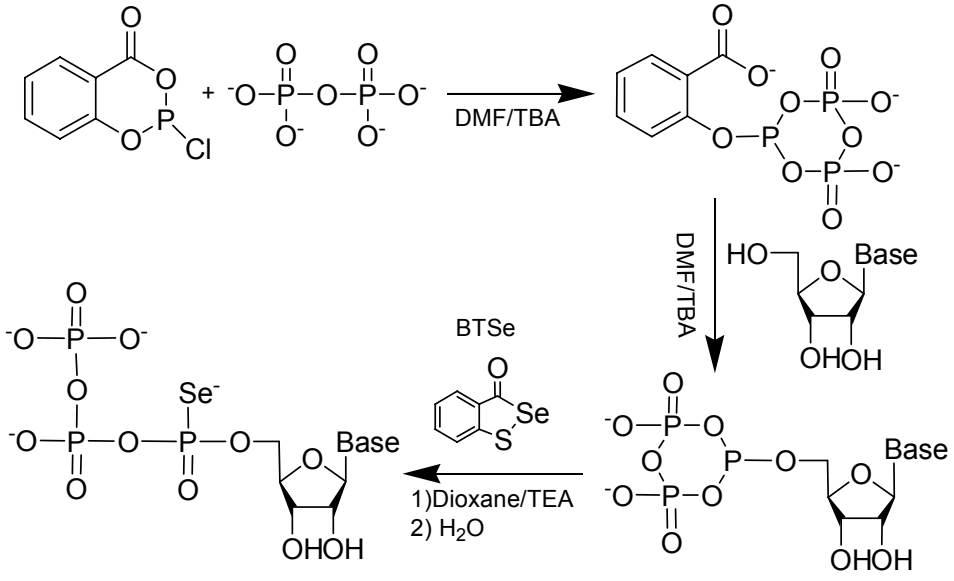

Figure 2.5. Synthesis route of NTPαSe.

2.2.1.1 Synthesis of NTPαSe

The following procedure was performed under argon gas with stirring and all liquids were dried and purged with argon before use:

Tributylammonium pyrophosphate (426 mg, 0.9 mmol, 2 eq., flask 1), individual nucleoside (varied mass, 0.45 mmol, 1 eq., flask 2), and 3H-1, 2-benzothaselenol-3-one (BTSe, flask 3) (195 mg, 0.9 mmol, 2 eq., flask 3),[92-93] were dried in separate flasks at high vacuum for 1 h. The tributylammonium pyrophosphate (flask 1) was dissolved by DMF (0.6 mL) and TBA (1.2 mL). 2-chloro-4H-1,3,2-benzodioxaphosphorin-4-one (182 mg, 0.9 mmol, 2 eq., flask 4) was dried for 15 min, dissolved in 1.2 mL DMF and then injected into pyrophosphate flask (flask 1). The reaction mixture was stirred under argon at room temperature for 30 min. After that, the nucleoside (flask 2), was dissolved in DMF (0.45 mL) (special note: adenosine was dissolved by 0.32 mL DMF and 0.13 mL DMSO, and guanosine was dissolved by 0.225 mL DMF and 0.225 mL DMSO). The reaction mixture (flask 1) of tributylammonium pyrophosphate and 2-chloro-4H-1,3,2-benzodioxaphosphorin-4-one was added to the dissolved nucleoside (flask 2). After nucleoside reaction mixture (flask 2) was stirred under argon at room temperature for 1 h, the 3H-1,2-benzothaselenol-3-one (BTSe, flask 3), was dissolved in dioxane (1.5 ml) and added to the nucleoside reaction mixture (flask 2). The mixture was stirred for a further hour and then water (10.2 ml, twice the reaction solution volume) was added to for hydrolyzation. Two hours after hydrolyzation, an ethanol precipitation was performed with additional fresh DTT (20 mM) at condition of 0.3 mM NaCl and three volumes of ethanol, -80 ^{o}C

30 min then 14k rpm 30 min at 4 ^{o}C. The pellet was redissolved in small amount of water and the concentration was checked by UV at 260 nm.

2.2.1.2 HPLC purification of nucleosides 5'-(alpha-P- seleno) triphosphates:

The synthesized NTPαSes were purified by reverse phase HPLC (RP-HPLC). NTPαSe was eluted using a combination of two solvents at varying proportions: buffer A (20mM TEAAc in water) and buffer B (20mM TEAAc, 50% water, 50% acetonitrile). Analytic HPLC program for ATPαSe, CTPαSe and GTPαSe was 20 min 12.5% acetonitrile with 20 mM TEA·Ac buffer (pH7) at 1 mL/min. Analytic HPLC program for UTPαSe was 20 min 20% ethanol with 20 mM TEA·Ac buffer (pH7) at 1 mL/min. Each diastereomer was collected seperately. Fractions were lyophylizated and one additional ethanol precipitation (as described in *2.2.1.1) was* performed for desalting before NMR data collection or transcription.

2.2.1.3 Boronate column chromatography of nucleosides 5'-(alpha-P-seleno) triphosphates

Wash buffer: 1 M TEABC buffer was prepared by bubbling CO_2 through a solution with 28.2 ml triethylamine in 140 ml H_2O at 4 ^{o}C until pH drops to 9.5 and then bring the solution volume up to 200 ml. The pH was tested each time before the buffer was used. The prepared TEABC buffer was stored at 4 ^{o}C.

Elution buffer: 22.5 mL water and 14 µl of 80% acetic acid were mixed well, and the pH value observed was 4.5, which is considered ideal for the elution

buffer.

Procedure: 0.2 g of boronate affigel (Biorad) was hydrated in 5 mL of TE buffer (10 mM Tris HCl pH 8.0, 1 mM EDTA) and packed in 1 X 4 cm column. The column was equilibrated using 5 mL of 1 M TEABC pH 9.5 at 4 ^{o}C. An ethanol precipitation was done to 200 µL NTPαSe (20 mM) sample using 600 µL ethanol, 20 µL 3 M NaCl and 20 µL 1M DTT before the NTPαSe was loaded on column . The NTPαSe was then redissolved in 1 mL, 1M TEABC buffer, applied to the column and incubated for 15 mins at 4 ^{o}C. Afterwards, washing buffer (1 M TEABC, pH 9.5, 4 ^{o}C) was added. Flow through was collected by 0.5 mL per tube. Fractions were collected until the maximum absorbance value dropped below 0.01 as determined by UV. Maximum absorbance values are as follows: ATPαSe-259nm, UTPαSe-262 nm, GTPαSe-252 nm, CTPαSe-271 nm. Elution was done using the elution buffer (0.05% acetic acid pH 4.5) and fractions were collected by 0.5 mL per tube. The tubes were labelled as E1, E2, and so on depending on the fraction collected. All working buffers were kept on ice during the procedure. DNA quantification was done by UV spectrometer and the absorbance values noted and concentrations calculated. Analytical HPLC analysis was performed to determine the quality of purified NTPαSe.

After the purified NTPαSes were eluted from the column, they were neutralized with 10 µL of TEABC buffer and NaCl/ethanol precipitated. The sample volume was around 500 µL. 10 µL of 1 M DTT, 50 µL of 3 M NaCl, and 1500 µL of ethanol were added and stored at -80 °C for 30 mins followed by centrifugation at 14k RPM for 10 mins. The concentration of all NTPαSes was

adjusted to 20 mM, which was used as 10X solution in transcription reactions.

The HPLC programs for analyzing NTPαSe eluted from the boronate column: NTPαSe was eluted using a combination of two solvents at varying proportions: buffer A (20 mM TEAAc in water) and buffer B (20 mM TEAAc, 50% water, 50% ethanol). The HPLC program for UTPαSe: 20 min 12.5% acetonitrile with 20 mM TEA·Ac buffer (pH 7) eluted at 1 mL/min. HPLC program for ATPαSe, and GTPαSe: 20 min 22.5% ethanol with 20 mM TEA·Ac buffer (pH 7) eluted at 1 mL/min. CTPαSe was 20 min 20% ethanol with 20 mM TEA·Ac buffer (pH 7) eluted at 1 mL/min.

2.2.2 DNA template preparation for RNA transcription

To transcribe RNA, beside the preparation of NTPαSe substrates, the DNA template must be prepared. Three types of DNA templates, plasmid, PCR and synthetic DNA templates were used to test for NTPαSe transcription. Based on the target RNA requirement, different DNA templates can be chosen for transcription.

For the plasmid template (Figure 2.6 A), the RNA gene was inserted into pUC19 plasmid with T7 RNA polymerase promoter sequence. Because there is no special mark to make T7 RNA polymerase stop at certain point during transcription, a restriction site (like EcoR I) has to be inserted at the end of the RNA gene. After the plasmid was purified from *E.coli*, the plasmid has to be linearized by restriction endonuclease before it can be used as RNA transcription template.

For the PCR dsDNA template (Figure 2.6B) preparation, the template for PCR could be plasmid, or synthetic DNA. Advantages of PCR dsDNA template for RNA transcription are that there is neither a specific sequence requirement nor length limit for the target RNA molecule. After the PCR reaction and spin column purification, the PCR product can be directly used for RNA transcription.

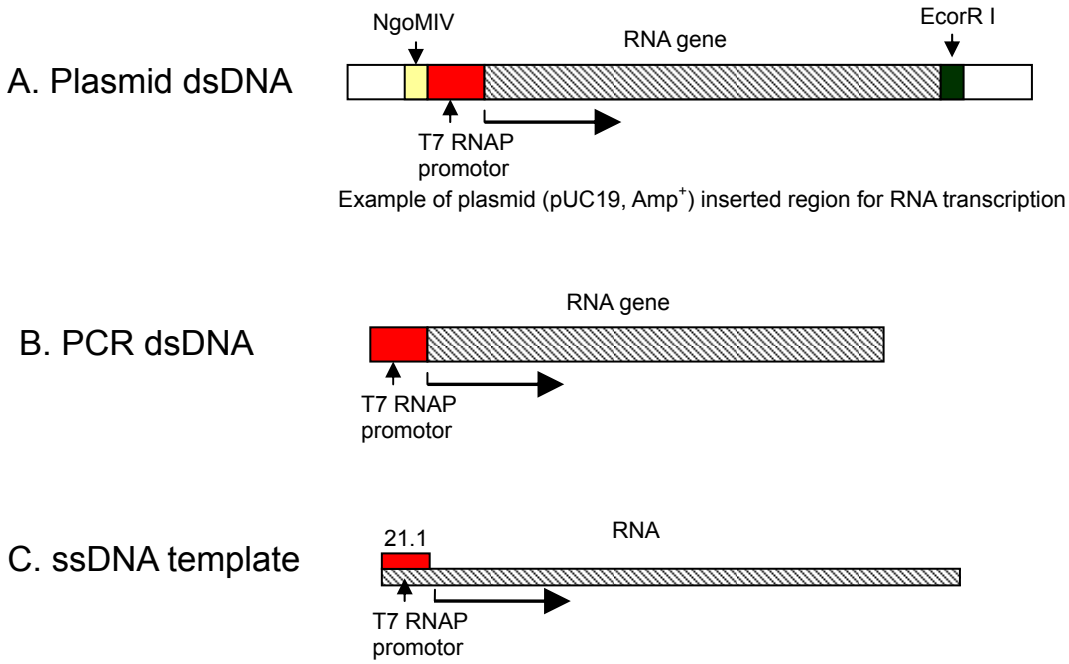

Figure 2.6. Illustration of DNA templates. A: plasmid (pUC19, Amp^+) inserted region for RNA transcription; B: PCR dsDNA template; C: synthetic ssDNA template.

Another choice for DNA template is synthetic template (Figure 2.6C). In general, although T7 RNA polymerase works better on dsDNA template, considering the expense and preparation time, ssDNA is a good option if it is possible. The ssDNA template is usually prepared as illustrated in Figure 2.6C, a full length ssDNA template strand and a 21mer promoter strand. There is no

sequence requirement for the template but there is length limit for synthetic template (<100 nt). Due to the length limit, synthetic ssDNA template can not be used directly for these long RNAs. However, synthetic ssDNA template is a very convenient and economical way for template preparation of short RNAs, like siRNA.

2.2.2.1. Purification of ssDNA template synthesized by solid phase DNA synthesizer

DNA single stranded template, prepared by DNA synthesizer, was deprotected by concentrated ammonium hydroxide at 55 ^{o}C over night. DNA in the supernatant was precipitated by nine volume of n-butanol, redissolved in water and purified through the appropriate percentage of denature PAGE. The DNA band on gel, visualized by UV shadowing, was cut and crushed. Gel debris was soaked with two volumes of water overnight at RT on tube rotator. Next day, the soaking solution was centrifuged at 3K rpm for 15 min to separate the gel debris and liquid supernatant. The supernatant was transferred to a clean tube and the gel debris was washed by one more volume of water (three times) plus centrifugation for separation each time. All of the supernatant collected after centrifugation was combined in a fresh tube and filtered by 0.2 μm nylon syringe filter (Pall). An NaCl/ethanol precipitation was performed on the filtered supernatant (-80 ^{o}C for 30 min then centrifuge at 14k rpm for 30 min). The DNA pellet was redissolved in small amount of water and the concentration was determined by UV at 260 nm. All of the ssDNA template and PCR primers used

in this dissertation were also purified by this method.

Table 2.2 Sequences of DNA templates prepared by solid phase DNA synthesizer.

Name	Sequence
21.1	5'-GCGTAATACGACTCACTATAG-3'
55.27	3'-CGCATTATGCTGAGTGATATCCGTTGGACTACTCCGGC TTTCCGGCTTTGCATGT-5'
89.24	3'-CGCATTATGCTGAGTGATATCCCTCGGGACAGTGGCCT ACACGAAAGGCCAGACTACTCAGGCACTCCTG**T**TTTGTCCCGAGGGC TTAA-5'

2.2.2.2 Plasmid construction for RNA transcription template

a. PCR of inserted fragment (New England Biolabs PCR Kit):

Characteristic PCR reactions (100 μL) were carried out using 1 μL plasmid template - pWNV (80 ng/mL) or 8 μL ssDNA (10 nM) from solid phase synthesizer, 10 μL each of forward and reverse primers (10 μM), 10 μL 10 X PCR standard buffer with Mg^{2+}, 0.4 μL Taq DNA polymerase (5 u/μL), 2 μL 10 mM dNTP, and the proper amount of water to make a final volume of 100 μL. PCR started at 94 ^{o}C for 2 min, then repeated for 35 following cycles 94 ^{o}C (30 sec), 55 ^{o}C (30 sec, temperature varied for different sequences. Basically, it was 5 ^{o}C below *Tm* of primers) and 72 ^{o}C (30 sec) and the final extension at 72 ^{o}C for 2 min. The PCR product was purified by Qiagen MinElute PCR purification kit using the manufacturer's suggested protocol. The product was eluted with 20 μL of water and checked on a 2% agarose gel.

b. Restriction endonuclease digestion of PCR product:

A typical 20 μL double digestion reaction was performed as follows: 6 μL PCR purified product, 1 μL EcoR I (20 u/ μL) 1 μL NgoMIV(10u/μL), 2 μL 10x

NEB4 buffer (New England Biolabs restriction endonuclease Buffer 4) and desired amount of water to make final volume 20 µL. The reaction mixture was kept at 37 °C for 2 hours. The product was purified by Qiagen MinElute PCR purification kit using the manufacturer suggested protocol. The product was eluted with 20 µL of water and checked on a 2% agarose gel.

Table 2.3. PCR template sequences and primer sequences for plasmid construction

Name		Sequence
HHM	Template	3'-CGCATTATGCTGAGTGATATCCCTCGGGACAGTGGC CTACACGAAAGGCCAGACTACTCAGGCACTCCTG**T**TTT GTCCCGAGGGCTTAA-5'
	PCR Primers	PF:5'CGACGCCGGCGCGTAATACGACTCACTATAG-3' (31nt) PR:3'ACTCCTG**T**TTTGTCCCGAGGGCTTAAGTACT-5' (31nt)
HHN	Template	3'-CGCATTATGCTGAGTGATATCCCTCGGGACAGTGGC CTACACGAAAGGCCAGACTACTCAGGCACTCCTG**C**TTT GTCCCGAGGGCTTAA-5'
	PCR Primers	PF:5'-CGACGCCGGCGCGTAATACGACTCACTATAG-3' (31nt) PR:3'-ACTCCTG**C**TTTGTCCGAGGGCTTAAGTACT-5'(31nt)
SL(-)	Template	3'-CGGCCGCGCATTATGCTGAGTGATATCGTCGAGCG TGGCACAATTAACAACAATTAGGAGTGTTTGTGATGATT CAAACAGTCGAGTGTGTCCGCTTGATGANCTCTGCTTA AG -5'
	PCR Primers	PF: 5'-CGACGCCGGCGCGTAATACGACTCACTATAGCA GCTCGCACCGTGTTAATT -3' (51nt) PR:3'-CGAGTGTGTCCGCTTGATGANCTCTGCTTAAGTG CAC -5' (37 nt)
SL(+)	Template	3'-CGGCCGCGCATTATGCTGAGTGATATCTCATCAAGC GGACACACTCGACTGTTTGAATCATCACAAACACTCCT AATTGTTGTTAATTGTGCCACGCTCGACCATGGCTTAAG -5'
	PCR Primers	PF:5'CGACGCCGGCGCGTAATACGACTCACTATAGAGTA GTTCGCCTGTGTGAGC -3' (51nt) PR:3'-TTAATTGTGCCACGCTCGACCATGGCTTAAGTG CAC -5' (36nt)

c. Plasmid restriction endonuclease digestion and purification:

The obtained pUC19 based plasmids (pSAM) were double digested by EcoR I and NgoMIV as follows: 7 µL purified pSAM (1.4 µg/µL), 1 µL EcoR I (20 u/ µL) and 1 µL NgoMIV(10 u/µL), 2 µL 10x NEB4 (New England Biolabs restriction endonuclease Buffer 4) and proper amount of water to make a final volume 20 µL. The reaction mixture was kept at 37 °C, 2 h and purified on a 0.6% Agarose gel. Linear plasmid bands, visualized by UV photo illuminator were cut and purified by Qiagen gel extraction kit using the manufacturer suggested protocol. The product was eluted by 20 µL of water.

d. Ligation:

Purified, restriction endonuclease digested PCR product and linearized pHHM were ligated with T4 DNA ligase under the following conditions: 1 µL 10X T4 DNA ligase buffer, 1 µL T4 DNA ligase, 2 µL linearized pHHM, 2 µL PCR product and 2 µL water were mixed and kept in 16 ^{o}C for 1 hours. The reaction was stopped by inactivating T4 ligase with heating to 65 ^{o}C for 10 min.

e. Transformation (Invitrogen Top10 cell):

Transformation of ligated plasmid was carried out using Invitrogen One Shot® TOP10 chemically competent *E. coli* using manufacturer's suggested protocol. Ten overnight clones on plate were selected for small scale plasmid preparation using Qiagen Plasmid Mini kit and sent for sequencing.

f. Large scale plasmid purification and digestion for RNA transcription

The clone with correctly sequenced plasmid was used for large scale plasmid purification by Qiagen Plasmid Maxi kit. Before transcription, the plasmid was linearized by EcoR I as follows: 25 μL plasmid (1.5 μg/μL), 3 μL EcoR I (20 u/ μL), 10 μL NEB buffer 4 and proper amount of water to make final volume 100 μL. The reaction mixture was kept at 37 °C 4 h, and then 65 °C for 20 min to inactivate EcoR I. The product was checked on a 0.6% Agarose gel. The linear plasmid was isolated by NaCl/ethanol precipitation from digestion buffer. 20 μL of water was added to redissolve the plasmid. The plasmid solution was further desalted by 3K Nanosep centrifugal devices (Pall) at 10K rpm for 10 min. The desalting procedure was repeated once by adding 20 μL more water and centrifuging again. Then the plasmid was recovered by 20 μL of RNase free water

2.2.2.3 dsDNA Template prepared by PCR

a. Klenow extension for making full length long DNA template:

Due to the size limit for the oligonucleotide that could be obtained from solid phase synthesizer, two fragments of P4-P6 DNA template (a 98mer and a 99mer) were synthesized by solid phase DNA synthesizer for Klenow DNA polymerization to get full length template.

A 5 μL Klenow extension reaction was performed as following: 0.5 μL denature PAGE purified 98mer and 99mer (10 μM), 0.2 μL of dNTPs with a

concentration of 10mM, 0.5 µL of 10X Klenow buffer, 0.2 µL of Klenow DNA Polymerase (5 U/ µL) and desired amount of water to make a final volume of 5 µL. This reaction was incubated at 37 ^{o}C for an hour and checked via Agarose gel electrophoresis. The Klenow extended full length double stranded product was purified by 12% denature PAGE.

Table 2.4. Polymerization primer sequences for P4-P6

Name	Sequence
P4-P6 Polymerization primer 1 (99 nt)	5'-GCGTAATACGACTCACTATAGGGAATTGCGGGA AAGGGGTCAACAGCCGTTCAGTACCAAGTCTCAG GGGAAACTTTGAGA**TGGCCTTGCAAAGGGTAT**-3'
Polymerization primer 2 (98 nt)	5'-GAACTGCATCCATATCAACAGAAGATCTGTTGAC TTAGGACTTGGCTGCGTGTTAGGACCATGTCCGT CAGCTTATTACC**ATACCCTTTGCAAGGCCA**-3'

b. PCR (New England Biolabs PCR Kit):

Characteristic PCR reactions (100 µL) were carried out using 1 µL plasmid template - pWNV (80 ng/mL) or 8 µL ssDNA (10 nM) from solid phase synthesizer, 10 µL each of forward and reverse primers (10 µM), 10 µL 10 X PCR standard buffer with Mg^{2+}, 0.4 µL Taq DNA polymerase (5 u/µL), 2 µL 10 mM dNTP, and desired amount of water to make a final volume of 100 µL. PCR started at 94 ^{o}C for 2 min, then repeated 35 following cycles 94 ^{o}C (30 sec), 55 ^{o}C (30 sec, temperature varied for different sequences). Basically, it was 5 ^{o}C below *Tm* of primers) and 72 ^{o}C (30 sec) and the final extension at 72 ^{o}C for 2 min. The PCR product was purified by 3K Nanosep centrifugal devices (Pall) at 10K rpm for 10 min before transcription. It was reported that with 2'-O-methyl

modification at the last two nucleotides of 5' of DNA increased the fidelity of RNA transcription.[94] Therefore, two types of primers were tested. One set was just a commonly used native primers; the other set has one primer with 2'-O-methyl modification at the last two nucleotides of 5', which was the end of transcription.

Table 2.5. PCR template sequences and primer sequences

Name		Sequence
SL(-)	Template	3'-GCGCATTATGCTGAGTGATATCGTCGAGCGTGGC ACAATTAACAACAATTAGGAGTGTTTGTGATGATTCA AACAGTCGAGTGTGTCCGCTTGATGA -5'
	PCR Primers	P2: 3'CGAGTGTGTCCGCTTGATGmAm5' (21nt) 21.15'-GCGTAATACGACTCACTATAG-3' (21nt)
SL(+)	Template	3'-GCGCATTATGCTGAGTGATATCTCATCAAGCGGAC ACACTCGACTGTTTGAATCATCACAAACACTCCTAAT TGTTGTTAATTGTGCCACGCTCGAC -5'
	PCR Primers	P2: 3'TTAATTGTGCCACGCTCGAmCm5' (21nt) 21.15'-GCGTAATACGACTCACTATAG-3' (21nt)
P4-P6 Template		3'-CGCATTATGCTGAGTGATATCCCTTAACGCCCTTT CCCCAGTTGTCGGCAAGTCATGGTTCAGAGTCCCCT TTGAAACTCT**ACCGGAACGTTTCCCATA**CCATTATTC GACTGCCTGTACCAGGATTGTGCGTCGGTTCAGGAT TCAGTTGTCTAGAAGACAACTATACCTACGTCAAG-5'
P4-P6 PCR Primers		P2: 5'-GmAmACTGCATCCATATCA ACAG-3' (21nt) 21.15'-GCGTAATACGACTCACTATAG-3' (21nt)

2.2.3 Phosphoroselenoate modified RNA (PSe-RNA) transcription with radioactive label

RNA transcribed with radioactive labeling was performed according to the protocol from the manufacturer (Epicentre T7 RNA polymerase, T7905K) for

1 h at 37 ^{o}C. Each time one type of 10 mM NTPαSe was used to substitute one type of normal 10 mM NTP solution in protocol (for example, to ATPαSe I tube, ATPαSe I, CTP, GTP and UTP were added). NTP sample was labeled both by ATP [α-^{32}P] and CTP [α-^{32}P]. Different types of templates were tested in the transcription reaction. A typical 10 μL reaction was performed under the final condition of 1 μM ssDNA template and top promoter strand or 50 ng/μL plasmid or 6 ng/μL dsDNA PCR template, 0.5 mM NTP or NTPαSe, 10 mM DTT, 1 μL of 10 X Epicentre T7 RNA transcription buffer, 1 μL of Epicentre T7 RNA polymerase and desired amount of RNase-free water to add volume up to 10 μL. ATPαSe and GTPαSe samples were labeled by CTP[α-^{32}P], and CTPαSe and UTPαSe samples were labeled by ATP[α-^{32}P]. The transcription reaction was quenched by adding equal volume of loading dye containing EDTA (100 mM). The transcription result was determined by 15% denature PAGE gel by exposure to film.

2.2.4 PSe-RNA transcription for large scale RNA preparation

Hammerhead ribozyme as an example:

Mutant hammerhead ribozyme (HHM) transcripts (500 μL) were prepared according to the protocol of the manufacturer (Epicentre T7 flash transcription kit). The reaction was also includeing 0.1 u/μL phosphatase and 2 mM $MnCl_2$ and the reaction was incubated for 2 h at 37 ^{o}C. 100 mM NTPαSe was used to substitute normal 100 mM NTP from the kit each time. A typical 10 μL reaction was performed under the final condition of 1.5 μM ssDNA template

and top promoter strand, or 150 ng/μL plasmid, or 50 ng/μL dsDNA PCR template, 9 mM ATP, 9 mM CTP, 9 mM GTP and 9 mM UTP (when one type of NTPαSe was used, the corresponding NTP was not added to the transcription mixture), 10 mM DTT, 0.008 unit pyrophosphatase, 2 mM $MnCl_2$, 1 μL of 10 X Epicentre T7 RNA transcription buffer, 1 μL of Epicentre T7 RNA polymerase and proper amount of RNase-free water to add volume up to 10 μL. After transcription incubation, 10 μL (10 u) Epicentre DNase I was added at 37 ^{o}C for 15 min to remove DNA template. After 37 ^{o}C incubation was finished, an NaCl/ethanol precipitation was performed (14K RPM, 10 min) to remove enzymes, short RNA fragments and NTP. RNA pellet was redissolved in 200 μL water.

2.2.5 Purification of PSe-RNA

2.2.5.1 Gel purification of PSe-RNA

PSe-RNA was purified by denaturing polyacrylamide gel electrophoresis (PAGE). RNA from transcription was mixed with gel loading dye (1:1 ratio) that contained 8 M urea. The percentage of denaturing PAGE used for RNA purification was P4-P6 (9%), hammerhead ribozyme (12%), SL RNA (12%) and siRNA (19%). After the gel was finished, one glass plate was lifted and a plastic wrap was placed on PAGE gel. Then a TLC plate was placed on the top of the plastic wrap. The whole plates and gel set were flipped over with the glass plate on the top. The PAGE gel was carefully separated from the glass plate with a spatula. The RNA band on gel was visualized by UV shadowing. The RNA

band was cut from the gel, transferred to a clean tube and crushed by a RNase-free spatula (All of the solutions used after this step, including RNase-free water, ethanol, 3M NaCl and so on, were filtered by 0.2 μm nylon membrane filter. For PSe-RNA purification, 20 mM DTT was added to all RNase-free water used in the purification steps to dissolve the PSe-RNA). RNase-free water (2 gel volume) was added to the crushed gel placed in a clean tube for soaking. After soaking for 4 h at 4 ^{o}C with rotation, the gel soaking solution was centrifuged (3K rpm, 10 min, at 4 ^{o}C) to remove gel fragments. The supernatant was transferred to a fresh tube and RNase-free water (one more gel volume) was added to the gel for washing. The solution was centrifuged again (3K rpm, 10 min, at 4 ^{o}C) and the supernatant was combined with the previous supernatant. This washing step was repeated two more times. All of the supernatant was collected and filtered through 0.2 μm nylon syringe filter to a high speed centrifuge tube. NaCl/ethanol precipitation was then performed to pellet the RNA out of the solution. A typical ethanol precipitation started with adding 1/10 volume of 3 M NaCl, 3 volume of ethanol and 10 mM DTT and mixed well. The mixture was left in -80 ^{o}C for 30 min and centrifuged at 14K rpm (4 ^{o}C) for 30 min. The RNA pellet was redissolved in water and desalted by 10K Nanosep centrifugal device (Pall) at 8K rpm for 10 min.

2.2.5.2 FPLC purification of PSe-RNA

RNA pellet from transcription was redissolved in 100 μL water. PSe-RNA was further purified by GE AKTA FPLC system using HiTrap Q anion

exchange column applying a salt gradient from 0.3 M NaCl to 1 M NaCl. Ethanol precipitation was then performed to pellet the RNA out of the solution. A typical NaCl/ethanol precipitation started with adding 1/10 volume of 3 M NaCl, 3 volume of ethanol and 10 mM DTT and mixed well. The mixture was left in -80 ^{o}C for 30 min and centrifuged at 14K rpm (4 ^{o}C) for 30 min. The RNA pellet was redissolved in water and desalted by 10K Nanosep centrifugal devices (Pall) at 8K rpm for 10 min.

2.2.6 Stability studies of PSe-RNA.

ATPαSe and dTSeT were loaded on the gel with the same protocol as the large scale RNA purification and recovered from 12.5% denaturing polyacrylamide gel. ATPαSe and dTSeT bands were visualized by UV shadowing. The ATPαSe and dTSeT bands cut from the gel were soaked in water overnight then the solution was centrifuged to remove gel fragments. The supernatant was collected and filtered with 0.2 μm syringe filter. The filtered solutions were analyzed in reverse phase HPLC for components by comparing with standard samples.

2.2.7 Crystallization of PSe-RNA

Hammerhead ribozyme:

RNA was annealed in the following condition: 1 mM RNA was heated to 95 ^{o}C for 2 min with 10 mM Na-cacodylate pH 6.5 and 1mM spermine, and cool down to room temperature on heating block.

Crystallization of hammerhead ribozyme was tested using hanging drop method in a buffer containing 0.5 mM RNA, 28 mM $MgCl_2$, 18.9 mM spermine HCl, 35 mM Na-cacodylate pH 6.5, and 6% polyethylene 400. Reservoir solution is 0.08 M $MgCl_2$, 18 mM spermine HCl, 0.1 M Na-cacodylate pH 6.5, and 18% polyethylene 400 [95]. More HHM crystallization conditions were screened by nucleic acid sparse matrix (Natrix, Hampton) using hanging drop method.

P4-P6 domain of group I intron:

RNA was annealed in the following condition: 3.5 mg/mL RNA was heated 50 ^{o}C for 5 min with 5 mM $MgCl_2$, 10 mM NaCl, 5 mM HEPES, pH 6.5. The solution was cooled to RT on the heating block and $MgCl_2$ concentration was adjusted to 25 mM after that. [91]

Crystallization was tried for P4-P6 RNA by mixing the annealed RNA solution with reservoir solution (21% MPD, 50 mM sodium cacodylic acid, pH 6.5, 0.37 mM Spermine) at 2:1, 1:1 and 1:2 ratios using hanging drop method. [91]

2.3 Results

2.3.1 Synthesis, characterization and purification of nucleosides 5'-(alpha-P-seleno) triphosphates

NTPαSes were successfully synthesized without any protective group on nucleoside and purified by reverse phase HPLC (RP-HPLC). This synthesis was developed from Ludwig's and Stawinski's methods.[92-93] For the first time, all

eight types of NTPαSe diastereomers were fully characterized by mass spectrometry, reverse phase HPLC, ^{1}H, ^{13}C and ^{31}P NMR (Table 2.6-2.9 and Figure 2.7).

The RP-HPLC profiles of crude products indicated a dominant preference for 5' triphosphates products (results not shown). Based on previous research results,[96] NTPαSe peak 1 (NTPαSe I) from HPLC profile (Figure 2.7) was assigned as *Sp* and NTPαSe peak 2 (NTPαSe II) was assigned as *Rp*. The conformation needs to be further confirmed.

The NTPαSe purified by boronate column was a diastereomer mixture (Figure 2.8-2.11). The UV profiles of all washing and elution fragments of NTPαSes from boronate column were checked with chromatography as shown in (Figure 2.8-2.11. left figures). The fragments with high absorption at Max wavelength of individual nucleotides were collected, combined and ethanol precipitated. The purified diastereomer mixtures were re-injected into HPLC to compare with standard samples. The collected fragments were confirmed to contain two NTPαSe diastereomers without significant oxidation to native NTPs (Figure 2.8-2.11. right figures). The RNA transcription with NTPαSe diastereomers mixture was successful (Figure 2.15). The hammerhead ribozyme mutant (HHM) was transcribed with all four types of NTPαSe diastereomer mixtures.

2.3.1.1 Synthesis yield, MS and NMR of nucleosides 5'-(alpha-P- seleno) triphosphates

Table 2.6 NTPαSe ESI-MS and yield

NTPαSe	Molecular Formula	calcd. $[M]^-$	observed $[M]^-$	%yield[a]
ATPαSe I ATPαSe II	$C_9H_{15}N_2O_{14}P_3Se$	546.8901	546.8848 546.8818	32
CTPαSe I CTPαSe II	$C_9H_{16}N_3O_{13}P_3Se$	545.8983	545.8989 545.8972	46
GTPαSe I GTPαSe II	$C_{10}H_{16}N_5O_{12}P_3Se$	569.9174	569.9082 569.9077	44
UTPαSe I UTPαSe II	$C_{10}H_{16}N_5O_{13}P_3Se$	585.9044	585.9043 585.9052	67

[a]Yield calculated in percentage by UV

Table 2.7. ^{1}H-NMR (400 MHz) Chemical Shifts (ppm) of NTPαSe in D_2O

NTPαSe	H8	H2	H6	H5	H1'	H2'	H3'	H4'	H5'
ATPαSe I	8.64	8.16			6.06	4.71	4.56	4.33	4.28-4.18
ATPαSe II	8.55	8.16			6.06	4.66	4.56	4.36	4.27-4.19
CTPαSe I			8.01	6.08	5.91	4.75	4.66	4.32	4.25-4.22
CTPαSe II			7.96	6.07	5.91	4.75	4.66	4.33	4.26-4.21
GTPαSe I	8.12				5.85	4.74	4.65	4.55	4.31-4.20
GTPαSe II	8.19				5.85	4.75	4.65	4.51	4.30-4.21
UTPαSe I			8.05	6.01	5.89	4.75	4.65	4.39	4.34-4.24
UTPαSe II			7.96	5.93	5.88	4.75	4.65	4.40	4.35-4.23

Table 2.8.^{13}C-NMR (100 MHz) Chemical Shifts (ppm) of NTPαSe in D_2O

NTPαSe	C4	C2	C6	C8	C5	C4'	C1'	C3'	C2'	C5'
ATPαSe I	149.14	152.79	155.57	140.39	118.57	86.70	83.80	74.28	70.40	65.05
ATPαSe II	149.12	152.78	155.57	140.14	118.50	86.72	83.79	74.33	70.45	65.78
CTPαSe I	166.17	157.80	142.03		96.78	89.02	82.51	74.20	69.40	64.43
CTPαSe II	165.99	157.33	141.77		96.63	88.92	82.53	73.90	69.30	65.13
GTPαSe I	151.82	153.96	158.91	138.04	116.10	86.69	83.76	73.66	70.69	65.39
GTPαSe II	151.71	153.93	158.68	137.69	115.83	86.66	83.66	73.77	70.57	65.76
UTPαSe I	166.31	151.92	142.13		102.70	88.13	83.10	73.69	69.63	64.64
UTPαSe II	166.33	151.92	142.98		102.77	88.15	83.21	73.75	69.58	65.46

Table 2.9.^{31}P-NMR (161.97 MHz) Chemical Shifts (ppm) of NTPαSe in D_2O

NTPαSe	αP	γP	ßP	$J_{α,ß(Hz)}$	$J_{ß,\ γ(Hz)}$
ATPαSe I	34.04	-6.89	-22.77	32.34	19.44
ATPαSe II	33.82	-6.16	-22.65	34.01	19.44
CTPαSe I	33.59	-9.14	-23.97	34.01	19.44
CTPαSe II	33.17	-7.11	-23.39	30.77	19.44
GTPαSe I	33.77	-9.54	-23.96	32.39	19.44
GTPαSe II	33.09	-6.26	-23.12	32.39	21.06
UTPαSe I	32.82	-6.50	-23.21	29.96	19.40
UTPαSe II	33.68	-5.63	-22.48	34.02	19.44

2.3.1.2 HPLC profiles of nucleosides 5'-(alpha-P- seleno) triphosphates

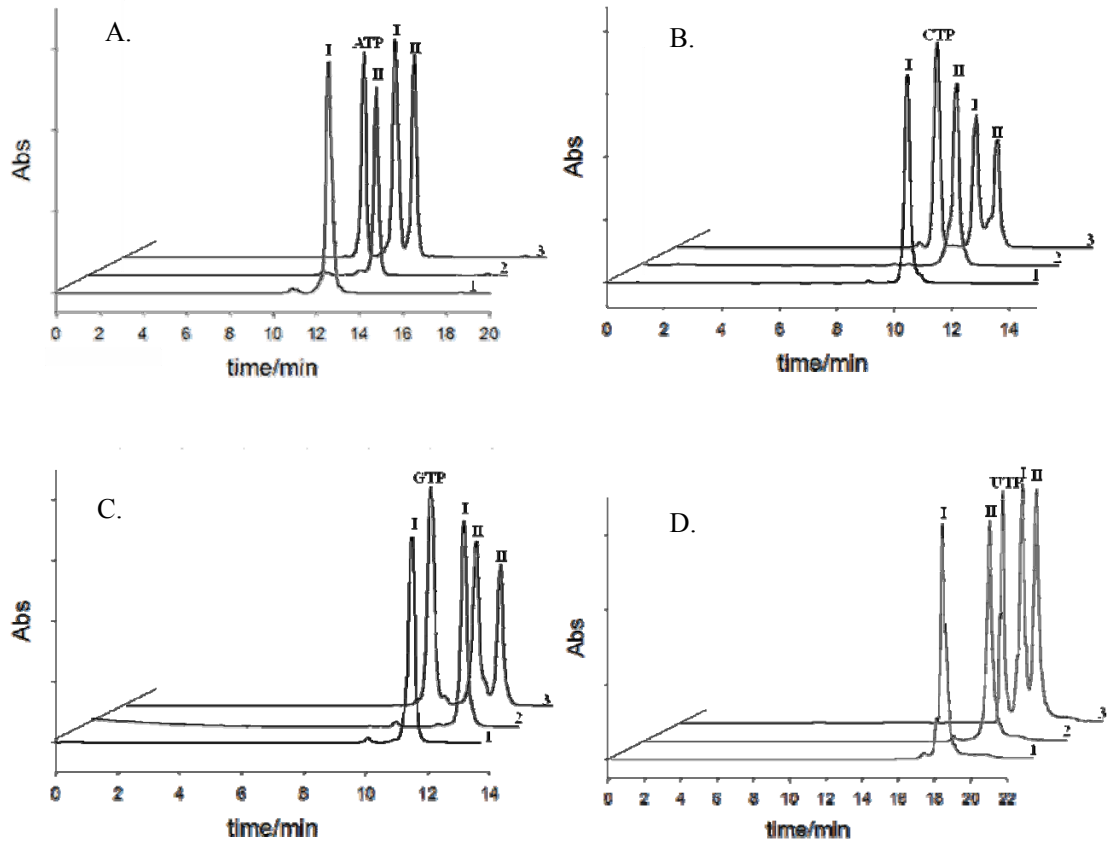

Figure 2.7. Analytic HPLC profiles of NTP, NTPαSe diastereomer I and diastereomer II.

A1. ATPαSe I (I, 17.4 min); A2. ATPαSe II (II, 18.0 min); A3. Conjection of ATP (16.4 min), ATPαSe I (I, 17.4 min) and ATPαSe II (II, 17.8 min).

B1. CTPαSe I (I, 10.5 min); B2. CTPαSe II (II, 11.2 min); B3. Conjection of CTP (9.1 min), CTPαSe I (I, 10.5 min) and CTPαSe II (II, 11.2 min).

C1. GTPαSe I (I, 11.5 min); C2. GTPαSe II (II, 12.1 min); C3. Conjection of GTP (10.0 min), GTPαSe I (I, 11.5 min) and GTPαSe II (II, 12.2 min).

D1. UTPαSe I (I, 17.4 min); D2. UTPαSe II (II, 18.0 min); D3. Conjection of UTP (16.4 min), UTPαSe I (I, 17.4 min) and UTPαSe II (II, 18.0 min)

2.3.1.3 boronate column purification of nucleosides 5'-(alpha-P- seleno) triphosphate

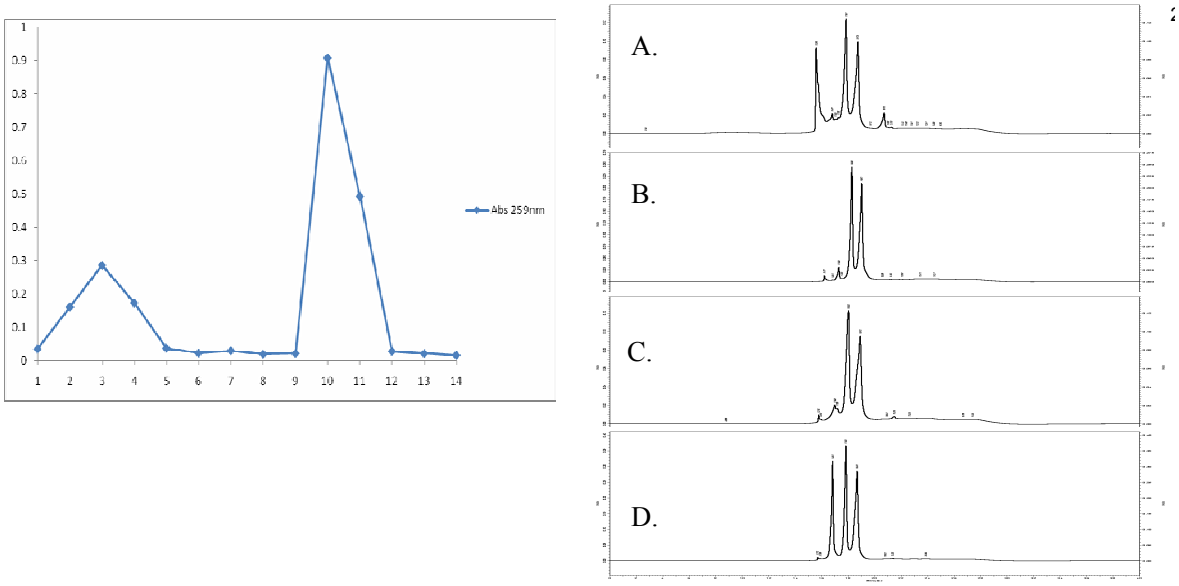

Figure 2.8.

Left: ATPαSe Boronate column purification. Abs at 259 nm

Tube 1-7 were washed by TEABC buffer, pH 9.5

Tube 8-14 were eluted by 0.05 % acetic acid buffer, pH 4.5

Right: HPLC profiles of ATPαSe from boronate column purification.

A. unpurified.

B. after B-column E3

C. after B-column E4

D co-injection of ATP and ATPαSe purified by boronate column (E3)

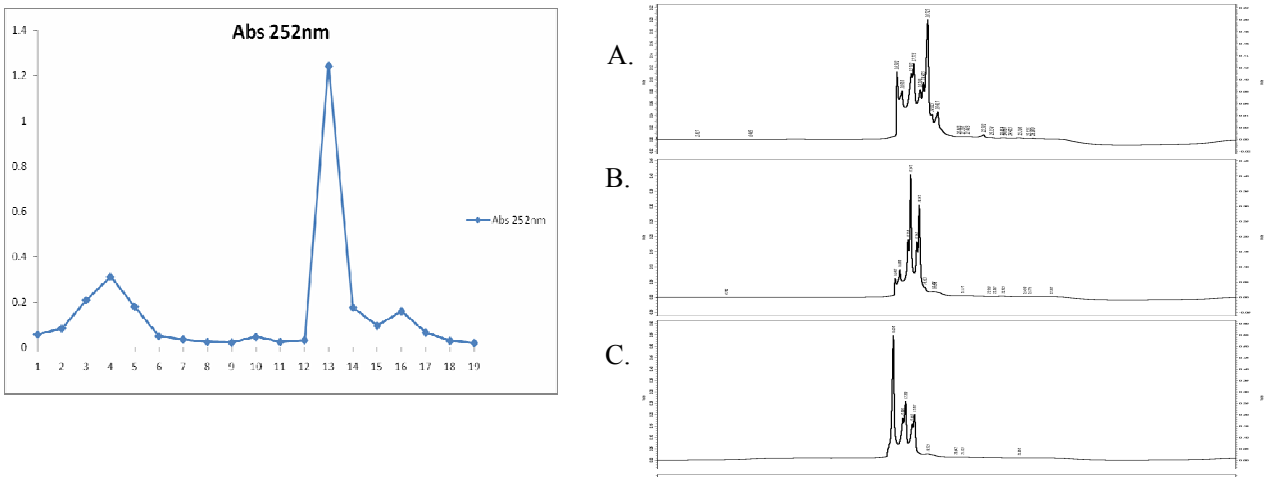

Figure 2.9.

Left: GTPαSe boronate column purification. Abs at 252 nm (0.5 mL per tube)

Tube 1-9 were washed by TEABC buffer, pH 9.5

Tube 10-19 were eluted by 0.05 % acetic acid buffer, pH 4.5

Right: HPLC profiles of GTPαSe from boronate column purification (20 min 45% ethanol)

A. unpurified.

B. after B-column E4

C. co-injection of ATP and ATPαSe purified by boronate column (E3)

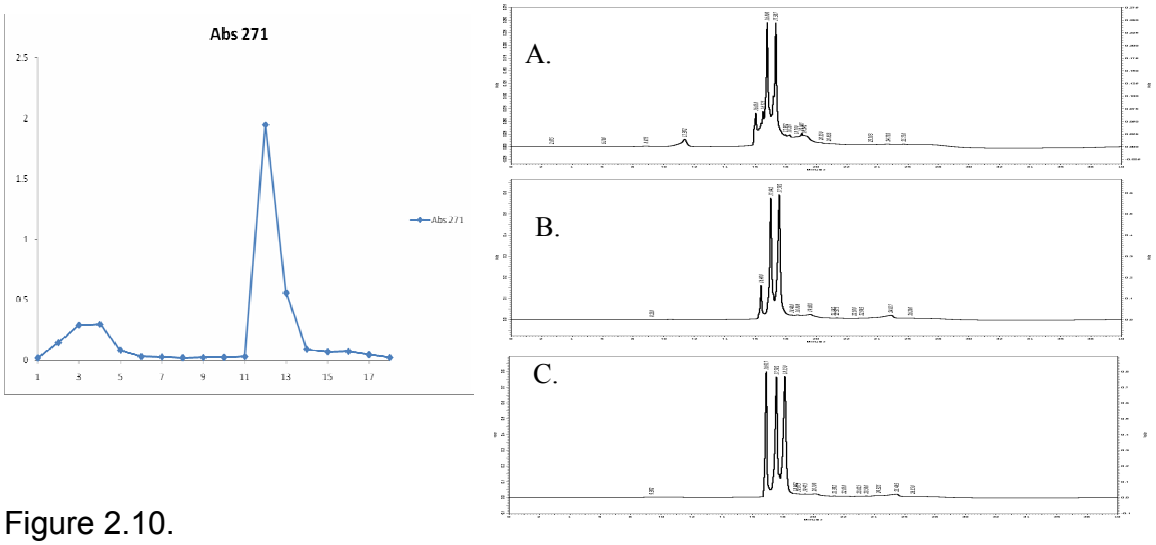

Figure 2.10.

Left: CTPαSe boronate column purification. Abs at 271 nm

Tube 1-9 were washed by TEABC buffer, pH 9.5

Tube 10-18 were eluted by 0.05 % acetic acid buffer, pH 4.5

Right: HPLC profiles of CTPαSe from boronate column purification.

A. unpurified.

B. after B-column E3

C. co-injection of CTP and CTPαSe purified by boronate column (E3)

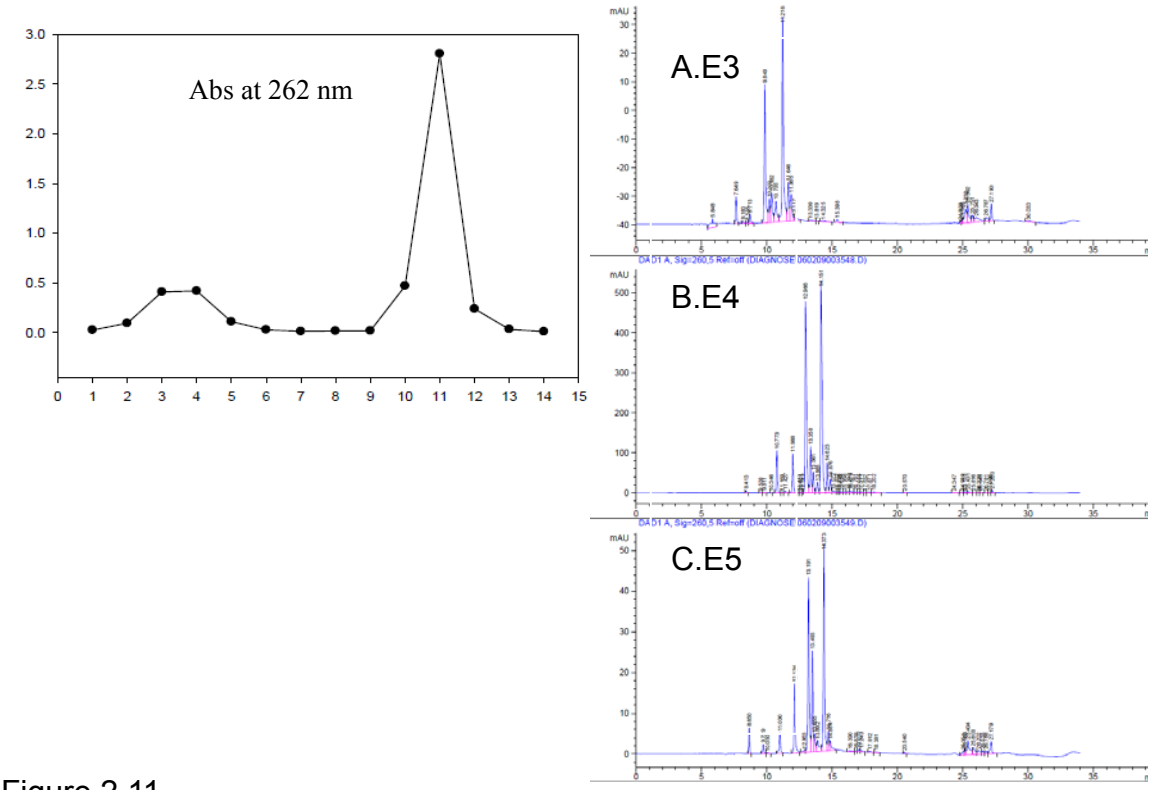

Figure 2.11.

Left: UTPαSe boronate column purification. Abs at 262 nm

Tube 1-7 were washed by TEABC buffer, pH 9.5

Tube 8-14 were eluted by 0.05 % acetic acid buffer, pH 4.5

Right: HPLC profiles of UTPαSe from boronate column purification.

A. after B-column E3

B. after B-column E4

C. after B-column E5

2.3.2 Phosphoroselenoate modified RNA (PSe-RNA) transcription with radioactive label

2.3.2.1 NTPαSe purified by HPLC for PSe-RNA transcription with radioactive label

Both NTPαSe diastereomers were tested for RNA incorporation through plasmid template, PCR template and ssDNA template (Figure 2.12, 2.13 and 2.14). Only NTPαSe I was recognized by T7 RNA polymerase (Figure 2.12, 2.13 and 2.14). The generation of PSe-RNA (HHM, 69mer RNA) with 15 UTPαSe I incorporation was confirmed by MALDI-TOF (Figure 2.21).

Two types of hammerhead ribozymes were tested for the incorporation of NTPαSe (Table 2.1 and Figure 2.2). The wild type hammerhead ribozyme (HHN), transcribed by native NTPs, could cleave itself under transcription condition right after it has been transcribed (Figure 2.15, NTP, lane N); while with single nucleotide mutation G→A (Table 2.1 and Figure 2.2), major RNA transcripts from mutant hammerhead ribozyme (HHM), were full length product (Figure 2.15, NTP, lane M). Due to the presence of phosphoroselenoate between C and A at the cleavage site (Figure 2.2), HHN transcribed by ATPαSe I showed no self-cleavage activity (Figure 2.14, ATPαSe I, lane N); while substitution of other NTPαSe I (except ATPαSe I) in HHN did not result in any inhibition on the self-cleavage activity (Figure 2.15). Consistent with our previous results,[38] the selectively selenium derivatized ribozymes were still active, and suggested that selenium modifications on non-essential phosphate did not cause major structural perturbation that would significantly affected the ribozyme activity.

The inhibited hammerhead ribozyme self-cleavage activity due to ATPαSe I incorporation (Figure 2.15, ATPαSe, lane N), also supported that the full length RNA bands in Figure 2.12 were not oxidized native RNA products.

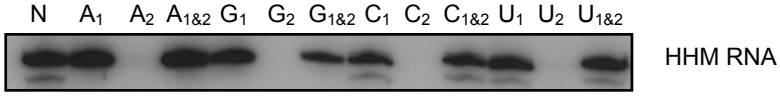

Figure 2.12. Enzymatic incorporation of NTPαSe I and II into HHM RNA using plasmid template. As described in the method 2.2.3, RNA was labeled by ATP [α-^{32}P] and CTP [α-^{32}P].

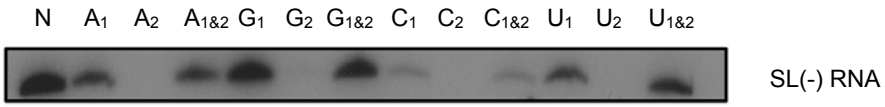

Figure 2.13. Enzymatic incorporation of NTPαSe I and II into SL(-) RNA using double strands DNA templates prepared from PCR. As described in method 2.2.3, RNA was labeled by ATP [α-^{32}P] and CTP [α-^{32}P].

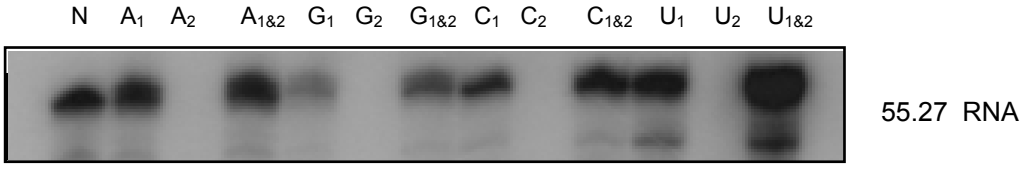

Figure 2.14. Enzymatic incorporation of NTPαSe I and II into 55.27 RNA using ssDNA templates prepared from solid phase synthesizer. As described in method 2.2.3, RNA was labeled by ATP [α-^{32}P] and CTP [α-^{32}P].

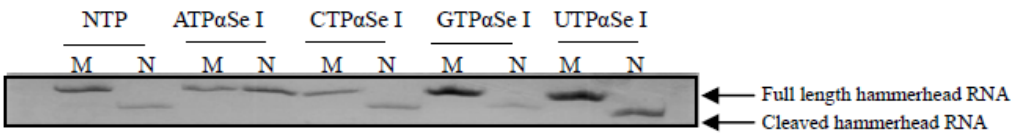

Figure 2.15. Transcription of a hammerhead ribozyme mutant (HHM RNA is represented as M) and wild type (HHN RNA is represented as N) using NTP or NTPαSe I.

2.3.2.2 Transcription of NTPαSe purified by boronate column for PSe-RNA transcription with radioactive label

NTPαSe diastereomers purified by boronate column were tested for transcription of HHM (Figure 2.16). Full length RNA products were obtained for all four types of NTPαSe diastereomers. The results proved that the boronate column was able to remove the impurities from NTPαSe synthesis and mixture of NTPαSe diastereomers could be used for transcription directly. The boronate column method could be a convenient way for large scale NTPαSe purification.

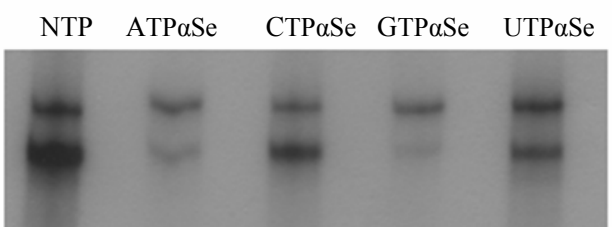

Figure 2.16. Transcription of NTPαSe purified by boronate column (12% PAGE). All RNA transcripts were labeled by CTP [α-^{32}P].

2.3.3 Phosphoroselenoate modified RNA (PSe-RNA) transcription for large scale RNA preparation

For the modified nucleotides incorporation by T7 RNA polymerase, the transcription condition needs to be tested and optimized to yield maximum PSe-RNA. Considering that Mn^{2+} could give T7 RNA polymerase more flexibility and Mn^{2+} has higher affinity to selenium than Mg^{2+}, additional Mn^{2+} was added to Epicentre T7 RNA transcription buffer. The appropriate Mn^{2+} concentration and transcription time were tested and result is shown in Figure 2.17. With plasmid template, 2 h transcription and 2 mM additional Mn^{2+} was the best condition for UTPαSe incorporation.

The transcriptional yields for hammerhead ribozyme mutant from two batches of UTPαSe (seU1 and seU2), with half amount of plasmid (1/2 HHM) are shown in Figure 2.18. There was no difference between two batches of UTPαSe I (seU1 and seU2, Figure 2.18). Reduced plasmid quantity resulted in significant decrease in product yield during a 2 h transcription. The best transcription condition, from the results of optimization experiment is stated in method 2.2.4 PSe-RNA transcription for large scale RNA preparation.

The effect of 2'-O-methyl modification (2'Me) at the last two nucleotides of 5' on DNA template was tested in P4-P6 RNA transcription (Figure 2.19). 2'Me modification of the template increased the yield of RNA transcription in both NTP and UTPαSe1 transcription for about 2.5 fold (Figure 2.19. Right). The proper concentration of 2'Me PCR template for large scale RNA transcription was tested using a protocol for large scale RNA preparation (Figure 2.20). For 2'-O-

Me PCR template 500 ng/μL working solution was used for large scale RNA transcription.

The generation of PSe-RNA (HHM, 69mer RNA) with 15 UTPαSe I incorporation was confirmed by MALDI-TOF (Figure 2.21). The mass native HHM RNA is shown in Figure 2.22.

2.3.3.1. Optimization for PSe-RNA transcription

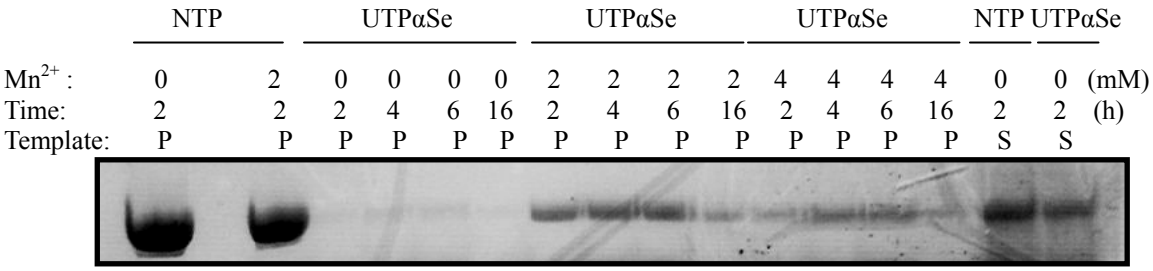

Figure 2.17. Optimization of large scale UTPαSe RNA transcription conditions using T7 RNA polymerase in 2-16 hours (RNA bands were shown by UV shadowing). RNA transcript is hammerhead ribozyme mutant (HHM). P: plasmid template. S: synthetic template.

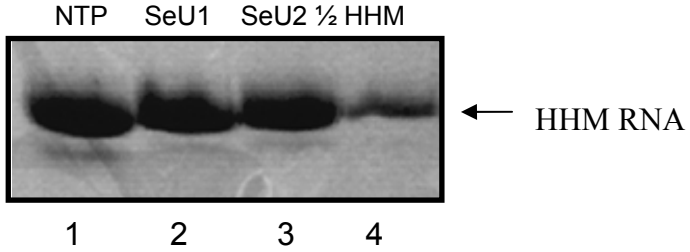

Figure 2.18. Plasmid template concentration optimization for HHM transcription condition (RNA bands were showed by UV shadowing). Lane 1-3: final 160 ng/μL. Lane 4: final 80 ng/μL.

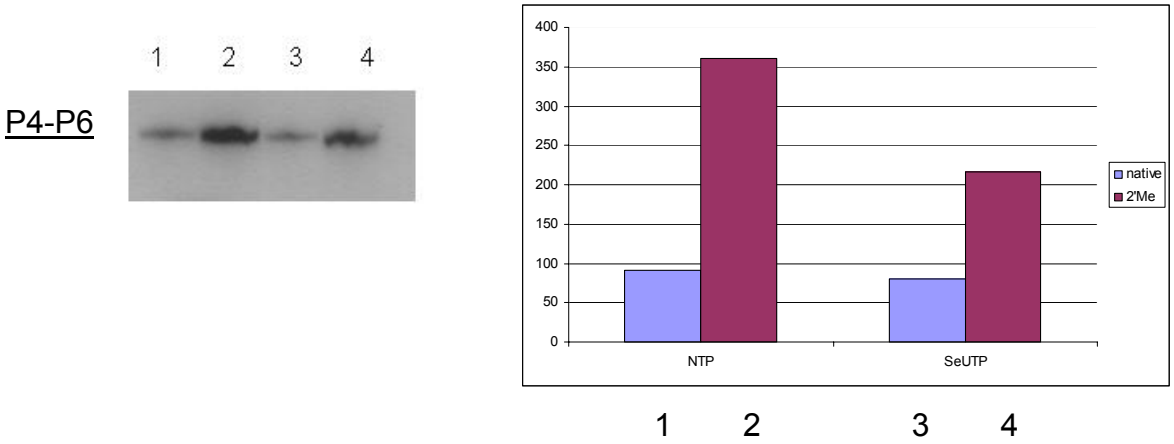

Figure 2.19. Comparison of normal PCR template and 2'-O-methyl modified PCR template for P4-P6 RNA transcription by NTP and UTPαSeI.

Left: GeI image. All RNA transcripts were labeled by ATP [α-^{32}P]. Lane 1: NTP with normal PCR DNA template; Lane 2: NTP with 2'-O-methyl modification PCR DNA template; Lane 3: UTPαSe1 substitution with normal PCR DNA template; Lane 4: UTPαSe1 substitution with 2'-O-methyl modification PCR DNA template. Right: quantified data of gel image (Left).

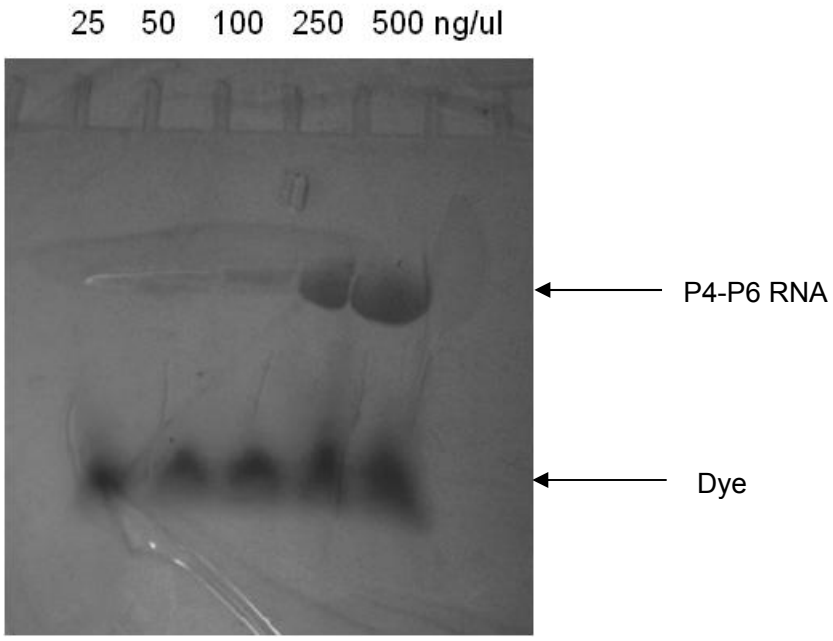

Figure 2.20. Concentration test for P4-P6 2'-O-methyl modification PCR DNA template. The top concentration label is 10 X working solution of P4-P6 2'-O-methyl modified PCR DNA template. RNA bands from 5 µL transcription were showed by UV shadowing.

2.3.3.2. MALDI-TOF of PSe-RNA

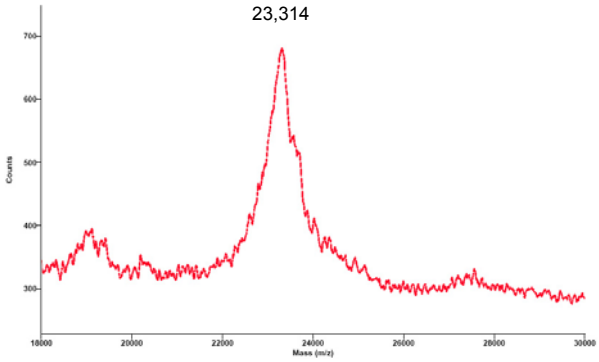

Figure 2.21. MALDI-TOF of PSe-U hammerhead ribozyme (HHM) ($C_{657}H_{814}N_{264}O_{465}P_{68}Se_{15}$) Cald. [M] 23,144, [M+THAP] 23,312. Observed [M+THAP] 23,314. THAP, standing for 2′,4′,6′-Trihydroxyacetophenone ($C_8H_8O_4$,

mass 168.04), is a type of MALDI matrix.

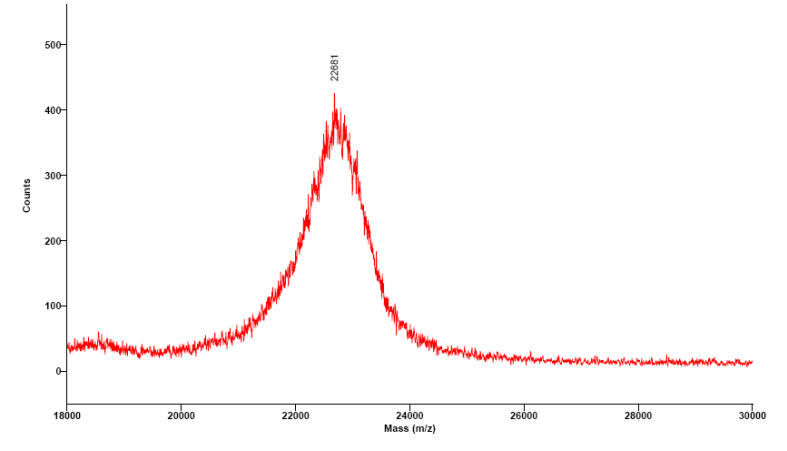

Figure 2.22. MALDI-TOF of native hammerhead ribozyme (HHM) calc. [M] =22,456; observed [M+Na^++Spermine] =22,681

2.3.4 Purification of PSe-RNA

The full length PSe-RNA could be purified by denaturing PAGE or FPLC. Figure 2.23 and 2.24 showed the RNA bands on denaturing PAGE. These RNA bands were visualized by UV shadowing. Figure 2.23 compared RNA SL(-) (plasmid template) transcription yield from all native NTP condition and with UTPαSe I substitution. Figure 2.24 showed the transcription yield of hammerhead ribozyme from synthetic stranded template (89.24) and plasmid template (HHM and (HHN). The sequence of RNA from 89.24 was the same as HHM (Table 2.1), while HHN RNA was the wild type self-cleaved hammerhead ribozyme.

The FPLC profile for purifying PSe-RNA is shown in Figure 2.25. NTP (Figure 2.25, peak at 1.08 min) was removed in the washing steps of the anion

exchange column. PSe-RNA eluted at 10.89 min. The RNA after anion exchange column was desalted by size exclusion column and concentrated by spin column. The RNA purified under these denature conditions was annealed later to the proper conformation.

2.3.4.1 Gel purification of PSe-RNA

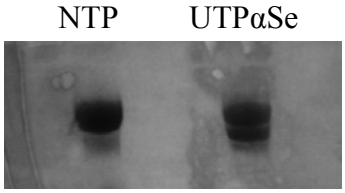

Figure 2.23. RNA band of WNV ribosome entry site SL(-) (plasmid template) from NTP and UTPαSe on denature PAGE.

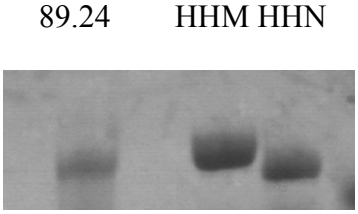

Figure 2.24. RNA transcribed from single stranded 89.27 ssDNA template and plasmid DNA template HHM (hammerhead ribozyme mutant) and HHN (native hammerhead ribozyme) on denature PAGE.

2.3.4.2 FPLC purification of PSe-RNA

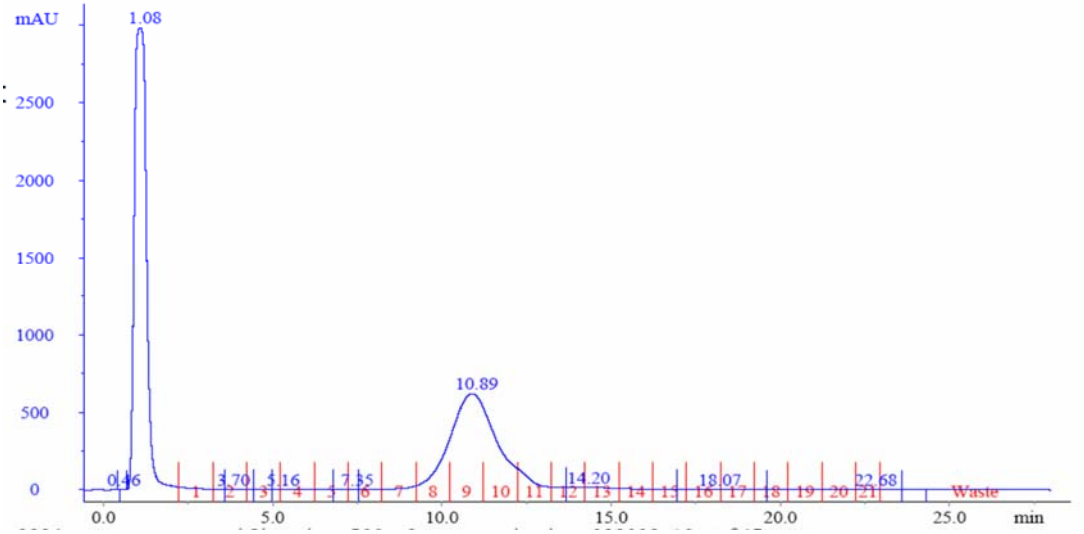

Figure 2.25. FPLC anion exchange column purification of PSe-U hammerhead ribozyme (10.89 min)

2.3.5 Stability studies of PSe-RNA

The stability of PSe-RNA during gel purification process was tested by a dT-PSe-T dimer. The data from RP-HPLC analysis (Figure 2.26) showed that ATPαSe, as well as dT-PSe-T, were quite stable in polyacrylamide gel. Only less than 5% dT-PSe-T dimer converted to native dTT dimer. This suggested that RNA with selenium incorporation could be purified by ordinary polyacrylamide gel, and is a quite convenient way for selenium containing RNA purification.

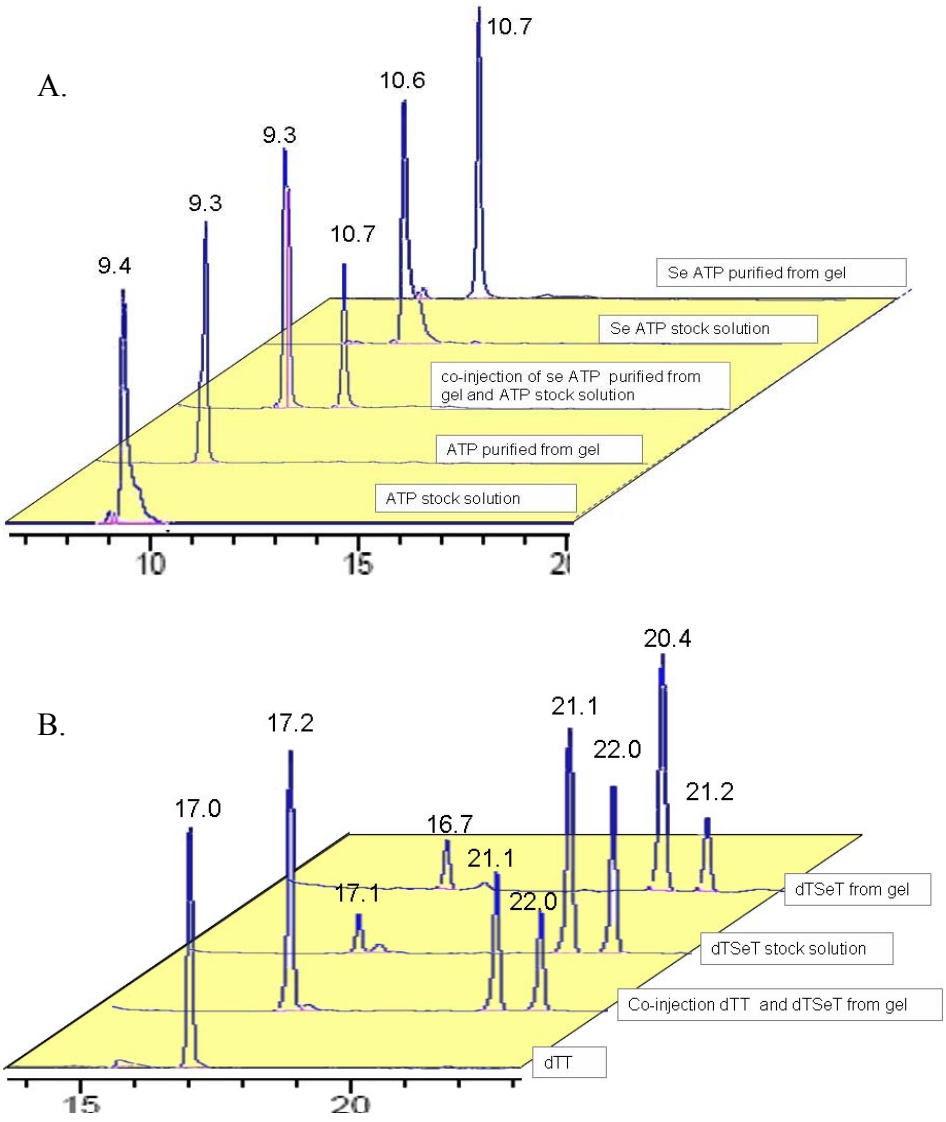

Figure 2.26. Stability studies of PSe-RNA (A). HPLC profiles of ATP stock solution, ATP purified from gel, co-injection of ATPαSe purified from gel and ATPαSe stock solution, ATPαSe stock solution and ATPαSe purified from gel. (B). HPLC profiles of dTT, co-injection dTT and dTSeT from gel, dTSeT stock solution and dTSeT from gel.

2.3.6 Crystallization of PSe-RNA

The hammerhead ribozyme and P4-P6 RNA was tested for crystallization. The experiment has not been finished.

2.4 Discussion

Nucleotide triphosphates are common biological molecules in all life forms, and their analogues could have wide scientific and therapeutic applications. Phosphorothioate analogues have been used for enzymatic mechanism, antisense and RNAi studies,[97] which are also potential applications for phosphoroselenoate analogues. Our new facile synthesis route, separation method for NTPαSe diastereomers and preparation protocol for PSe-RNA enabled preparation of PSe-RNA for X-ray crystallography.

The template tests showed that only NTPαSe I could be incorporated into RNA by T7 RNA polymerase through both ssDNA and dsDNA. Then the transcribed PSe-RNA was diastereomerically pure, which was different from PSe-DNA generated from solid phase synthesis method reported by Egli and co-workers [27].

An ideal nucleic acid heavy atom derivative should be stable during the X-ray crystallography experimental process, not cause significant structure perturbation and be site-specifically incorporated into nucleic acid. The selenium modification at the alpha phosphate position was relatively stable during the RNA purification step with DTT added as reducing agent. Whether the PSe-RNA is still stable during crystallization conditions and X-ray radiation condition and

whether the additional reducing agent can change the crystallization conditions needs to be further investigated. Another concern is whether there is structure perturbation on PSe-RNA. Although the short double stranded PSe-DNA did not show significant structure perturbation, [27] the final answer about PSe-RNA requires crystal structures of PSe-RNA, which are not available now. A few questions can be addressed here through the hammerhead cleavage experiment (Figure 2.15). The selenium substitution of oxygen at the non-bridging site between C and A at the cleavage site (Figure 2.15) inhibited hammerhead ribozyme cleavage reaction, which could be caused by lower selenium affinity to Mg^{2+} compared with oxygen, as happened with the phosphorothioate ribozyme.[44] On the other hand, selenium substitutions of other non-bridging sites of the hammerhead ribozyme, like in the cases of CTPαSe I, GTPαSe I and UTPαSe I (Figure 2.15), did not inhibit the ribozyme cleavage activity. This indicated that the hammerhead ribozyme could still fold into the active conformation with selenium substitutions. The inihibition effect may only come from the atomic change in active site. For the concern about affecting RNA global folding due to altered metal affinity, phosphate modification site could be selected and tested, since all four types of NTPαSe are ready to be chosen. This concern also leads to the discussion of the difficulty in site-specificity for enzymatic incorporation. Unlike the low natural abundance of methionine in proteins (2.2%),[98] there are only four types of nucleic acids. Replacement of any one of the nucleic acid substrate with selenium modified substrate in transcription reaciton will result in around 25% nucleic acid substitution, which is much more

than what is needed for solving the phase problem and may result in unwanted structure perturbations and difficulties in locating these selenium atoms. To help solve these problems, a substrate mixture of NTP and NTPαSe can be used to reduce the amount of selenium incorporation. For even higher requirements on site specific incorporation, a combination with the T4 RNA ligase method can be an option. [75]

In summary, we have synthesized and characterized all eight types of NTPαSe diastereomers. The method described here is a very efficient way for the synthesis of 5'-(alpha-P-seleno)triphosphates, which does not require any protective groups on nucleosides and no multiple steps of purification. The generation of 5'-(alpha-P-seleno)triphosphates was confirmed by MS, ^{1}H, ^{13}C and ^{31}P NMR, and T7 RNA transcription. These NTPαSes were purified through either RP-HPLC or boronate column method. All RP-HPLC purified NTPαSe I are good substrates for T7 RNA polymerase, while NTPαSe II are neither inhibitor nor substrates for T7 RNA polymerase. NTPαSe diastereomers mixture purified by boronate column could be directly used for RNA transcription (Figure 2.16). The transcription conditions for large scale preparation of PSe-RNA has been optimized with additional Mn^{2+} in transcription buffer. Full length PSe-RNA with multiple selenium modifications was generated, purified by gel or FPLC and confirmed by mass spectrum. The PSe-RNA was relatively stable under gel purification conditions. The information in this dissertation would definitely help to advance studies on ribozyme catalytic mechanism, RNA X-ray crystal structure and function, and RNA interference

3. PHOSPHOROSELENOATE RNA FOR RNA INTERFERENCE STUDIES

3.1 Introduction

RNA interference (RNAi), the post transcriptional gene silencing (PTGS) induced by double-stranded (dsRNA), is a powerful tool for directed inhibition of gene expression in scientific research and it also has great potential for therapeutic applications. [99] RNAi can be induced by short (21-23 nt) dsRNA, known as small interference RNA (siRNA), which will be further processed by RNA-induced silencing complex (RISC) in cytoplasm.[100] The antisense strand (guide strand) in siRNA is complementary to the sequence of target mRNA molecule. After siRNA has assembled with RISC, RISC unwinds the duplex and only the antisense strand is loaded in activated RISC. The activated RISC with antisense strand siRNA will degrade the target mRNA or inhibit the translation of target mRNA.[101]

There are still several major problems in the application of RNAi for therapeutic purpose. [100] First is target identification; RNA interference works with mismatches, therefore, one siRNA may have more than one substrate.[102] Target specificity has to be considered in siRNA design to avoid side effect. Second, the effective delivery of oligonucleotides to the cell is also a problem.[103-104] Third, the stability of siRNA against nuclease degradation has to be improved.[105] In primitive organism and plants, siRNA is quite effective. Long dsRNA can be converted to many 21-23 nt siRNA with some degree of amplification. [106] However, in mammalian cells, long dsRNA could trigger the interferon reaction[107] and there are lots of nucleases in the serum. Increasing

the RNase resistance of siRNA is a practical way to elongate the siRNA lifetime and thus enhance RNAi activity.

A good chemical modification on RNA should increase the RNase resistance of siRNA without reducing the RNAi effect and being toxic for cells [108]. Thermodynamic stability of modified siRNA has to be checked since that could also affect target affinity and specificity.[109] Nucleases basically cut the phosphodiester bond of RNA. Modification of certain phosphodiester linkage on siRNA is considered to be able to increase the half-life of siRNA in vivo. Phosphothioate (PS) linkage modification was previous used on antisense technology to increase the resistance to RNase and also proved able to increase the siRNA stability.[37, 108] Phosphoselenoate (PSe) linkage has similar characteristics as phosphothioate linkage and has also shown RNase resistance; while due to unavailability of the material; this type of modification has never been tested for RNAi activity yet.[38]

SiRNA could be prepared through enzymatic and synthetic methods. [110] For enzymatic modification, the nucleoside triphosphate with modification has to be accepted by RNA polymerase. Our lab developed the method for enzymatic synthesis of PSe-siRNA using NTPαSe. To test the RNA interference activity of these PSe-siRNAs, target protein selected was pyruvate kinase type M2 (PKM2), a nonorganspecific tumor marker and a key regulator in tumor metabolome.[111] Inhibition of PKM2 in the cell experiment by commercial siRNA was not efficient due to rapid RNase degradation. SiRNA with more RNase resistance was desired by study on PKM2. PSe-RNA had previously

demonstrated strong RNA resistance,[38] as a result, PSe-siRNA against PKM2 was designed for RNAi activity test. It was reported that siRNA synthesized by the most commonly used bacteriophage T7 RNA polymerase with 5' triphosphate induced interferon reaction in mammalian cells. [110] Therefore, we also tested the whether 5' triphosphate of siRNA would induce cell apoptosis.

3.2 Materials and methods

UTPαSe used for siRNA transcription was purified by HPLC. The detailed synthesis and purification method were stated in chapter one.

Table 3.1. siRNA sequences

Name	Sequence
Antisense(N)	5'-GGUCGCUGGUAAUGGGCGCCUU-3'
Sense (N)	5'-GGCGCCCAUUACCAGCGACCUU-3'
Antisense (Se)	5'-GGseUCGCseUGGseUAAseUGGGCGCCseUseU-3'
Sense (Se)	5'-GGCGCCCAseUseUACCAGCGACCseUseU-3'

3.2.1 siRNA transcription

SiRNA transcription (100 μL) was performed according to manufacturer protocol (Epicentre T7 flash transcription kit) with extra pyrophosphatase in reaction buffer for 2 h. 100 mM UTPαSe I (purified by RP-HPLC) was used to substitute normal 100 mM UTP from the kit. A typical 100 μL reaction was performed under the final condition of 1.5 μM ssDNA template and top promoter strand, 9 mM NTP or NTPαSe I, 10 mM DTT, 0.08 u pyrophosphatase, 10 μL of 10 X Epicentre T7 RNA transcription buffer, 10 μL of Epicentre T7 RNA polymerase and proper amount of RNase-free water to add volume up to 100 μL.

After transcription, 20 μL (20 u) DNase I was added at 37 ^{o}C for 15 min to remove DNA template. The product was purified by 19% denature PAGE gel with same protocol for large scale RNA purification as stated in *2.2.5.1.* Ethanol precipitation was then performed to recover RNA from gel soaking solution. Pellet was redissolved in 50 μL RNase-free water. The gel purified siRNA was desalted by 3K centrifugal membrane filter (Pall).

To investigate the 5' triphosphate effects on RNAi, a set of siRNA was prepared with additional alkaline phosphatase to remove 5' phosphate before gel purification. The alkaline phosphatase reaction was performed as following: siRNA strand transcribed from 100 μL reaction after ethanol precipitation was re-dissolved by 1X alkaline phosphatase buffer with 50 u alkaline phosphatase. The mixture was left in 37 ^{o}C water bath for 1 h and the reaction was stopped by adding equal volume of gel loading dye. This set of siRNA without 5' triphosphate was labeled as siRNA 1 to 4. The other set of siRNA with 5' triphosphate was labeled as siRNA A to D.

The siRNA sample purified by gel and desalted by 3K centrifugal membrane filter, was performed one more ammonium salt ethanol precipitation for MALDI-TOF analysis. The siRNA sample was sent to Scripps Center for Mass Spectrometry for MALDI-TOF.

3.2.2 siRNA duplex preparation

Two complementary strands of PSe-siRNA (50 μM each) were annealed in 800 μL 2.5 X PBS buffer (10X phosphate buffered saline, pH 7.4, 10

mM KH_2PO_4, 1550 mM NaCl, 30 mM Na_2HPO_4). The siRNA samples for Melting temperature (*Tm*) studies was annealed with additional 20 mM borane in tetrahydrofuran (THF, Sigma 176192). The siRNA samples for RNAi activity study was annealed with additional 100 mM DTT in annealing buffer. Annealing of RNA was performed on a heating block by holding at 95 ^{o}C for 5 min then slowly cooled down to room temperature in 2 h. The annealed siRNA duplex was purified by 10K membrane centrifugal filter and redissolved in 20 µL water.

There are eight types of annealed siRNA. The set without 5' triphosphate was labeled as siRNA 1 to 4. The other set of siRNA with 5' triphosphate was labeled as siRNA A to D. The PSe-siRNA 1 represents for antisense(N)+sense(N) duplex; PSe-siRNA 2 represents for antisense(N)+sense(Se) duplex; PSe-siRNA 3 presents for antisense(Se)+sense (N) duplex; PSe-siRNA 4 represents for antisense(Se)+sense(Se) duplex. The PSe-siRNA A represents for antisense(N-3P)+sense(N-3p) duplex; PSe-siRNA B represents for antisense(N-3P)+sense(Se-3p) duplex; PSe-siRNA C represents for antisense(Se-3P)+sense(N-3p) duplex; PSe-siRNA D represents for antisense(Se-3P)+sense(Se-3p) duplex.

3.2.3 siRNA duplex *Tm* study

The melting temperature (*Tm*) sample was prepared by mixing 20 µL annealed siRNA duplex solution with 780 µL *Tm* buffer (pH 7.0, 0.1 M diammonium citrate). Sample was overlaid with 20 µL light mineral oil to prevent evaporation at higher temperature. The *Tm* of PSe-siRNA was performed by

measuring the change in absorbance at 260 nm using Cary 300 Bio UV/Vis spectrophotometer thermal software from 14 ^{o}C to 98 ^{o}C and from 98 ^{o}C to 14 ^{o}C in 2 ^{o}C increments with an equilibration time of 0.2 min at each temperature.

3.2.4 siRNA RNAi activity study

Cell Culture

SW480 cells were grown in L-15 medium (Leibovitz) supplemented with 10% fetal bovine serum at 37°C in a CO_2-free incubator. Cells were sub-cultured in a ratio of 1:4 or 1:6 twice weekly.

siRNA transfection and cell viability assay

SW480 cells were grown in a density of 30% confluence in 6-well plates and transiently transfected with 200 pmole small interfering RNA (siRNA) using Lipofectamine™ RNAiMAX (Invitrogen). The viability of transfected cells was analyzed by Trypan Blue (Sigma) staining method 48 h after siRNA transfection. By the time of viability assay, the cells were suspended using trypsin-EDTA (Invitrogen). The cells were then washed and re-suspended by ice-cold PBS buffer. The suspended cells were mixed with 0.4% Trypan Blue in a ratio of 1:1 (50 µl+ 50 µl). After 5 min incubation, the cells were counted using hemocytometer under light microscope. The transparent cells were taken as the live cells and the dark blue cells were the dead cells. The non-targeted siRNA and wild type PKM2 siRNA were used in this experiment as a control.

Western Blot

Protein samples were loaded and separated in a SDS polyacrylamide gel. The electrophoresed proteins in gel were transferred onto a nitrocellulose membrane (Millipore) and the membrane was incubated in blocking solution (5% BSA/TBST (20mM Tris-HCl pH7.4, 150mM NaCl, 0.1% Tween-20)) for 1 hour at room temperature. The membrane was washed with washing buffer (TBST) for 3 times, 5 min for each and then incubated with rabbit anti-human PKM2 antibodies which were diluted 1:1000 in blocking buffer for 2 hours at room temperature. The probed membrane was washed 3 times with washing buffer, 5 min for each, at room temperature and incubated with an appropriate secondary reagent such as goat anti-rabbit IgG-HRP at 1:5000 dilution in blocking buffer for 1 hour at room temperature. The membrane was then washed and the signal was detected with chemiluminescence reagents

3.3 Results

3.3.1 Characterization of PSe-siRNA

3.3.1.1 MALDI-TOF of siRNA transcript

The mass of native siRNA and PSe-siRNA are showed in Figure 3.1 (A. antisense and B. Sense) and Table 3.2. These results confirmed the generation of full length RNA transcripts with six selenium atoms in antisense strand and four selenium atoms in sense strand.

Table 3.2. Summary of siRNA MALDI-TOF MS.

Name	Composition	calc.[M]	obs.[M]
Antisense (N)	$A_2C_5G_9U_6$	[M]=7305	[M]=7305
Antisense (Se)	$A_2C_5G_9Use_6$	$[M+H^+]$=7684	$[M+H^+]$=7687
Sense (N)	$A_4C_9G_5U_4$	$[M+H^+]$=7189	$[M+H^+]$=7191
Sense (Se)	$A_4C_9G_5Use_4$	$[M+H^+]$=7445 $[M+H^++Na^++K^+]$=7506	$[M+H^+]$=7447 $[M+H^++Na^++K^+]$=7508

3.3.1.2 PSe-siRNA Tm study

The experiment on siRNA duplex indicated that the selenium modification on phosphate did not interrupt RNA duplex base-pairing. There was no significant difference on the melting temperature (*Tm*) (Table 3.3) of native siRNA (Figure 3.2. A), siRNA with single strand selenium modification (Figure 3.2. B and C), and siRNA with double strands selenium modification (Figure 3.2.D)

Table 3.3.Summary of siRNA Tm result.

siRNA duplex	Tm result
Antisense (N)+Sense(N)	88.25±0.48 ^oC
Antisense (N)+Sense(Se)	87.26±0.51 ^oC
Antisense (Se)+Sense(N)	89.27±0.45 ^oC
Antisense (Se)+Sense(Se)	89.39±0.60 ^oC

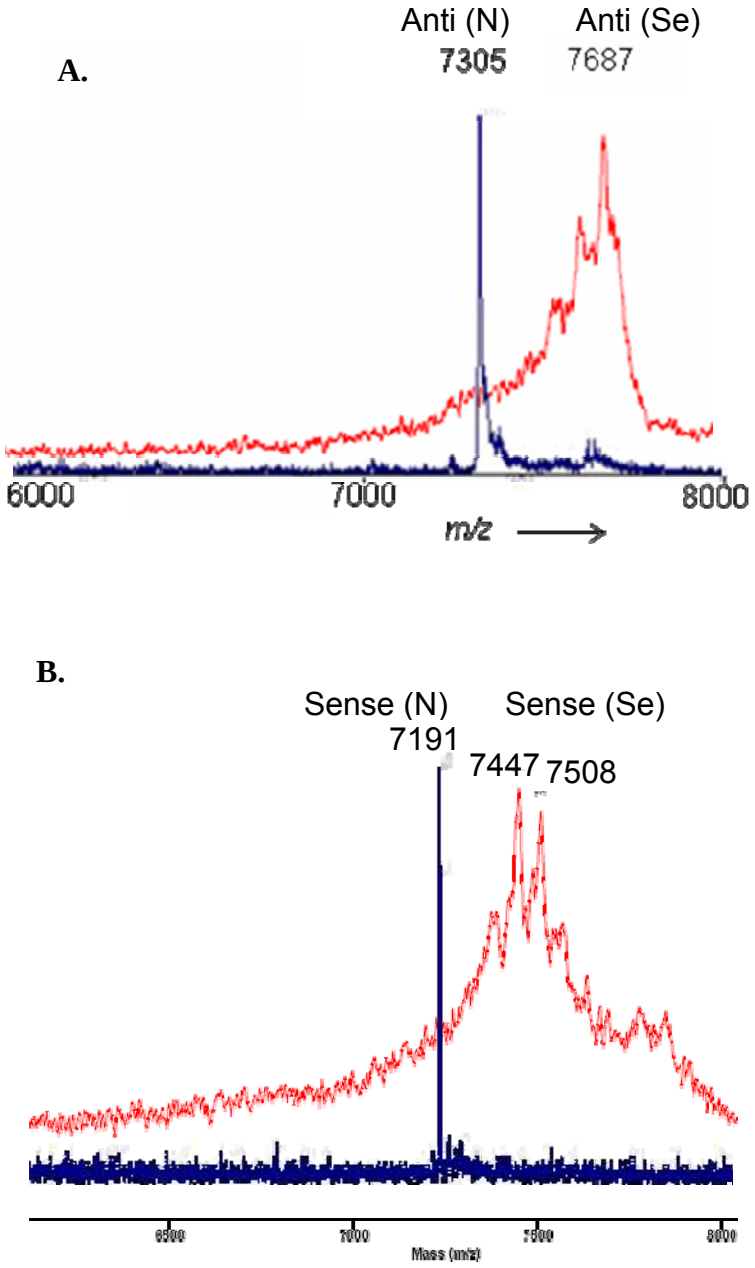

Figure 3.1.MALDI-TOF Mass-spectrum of siRNA antisense strand (A) and sense strand (B)

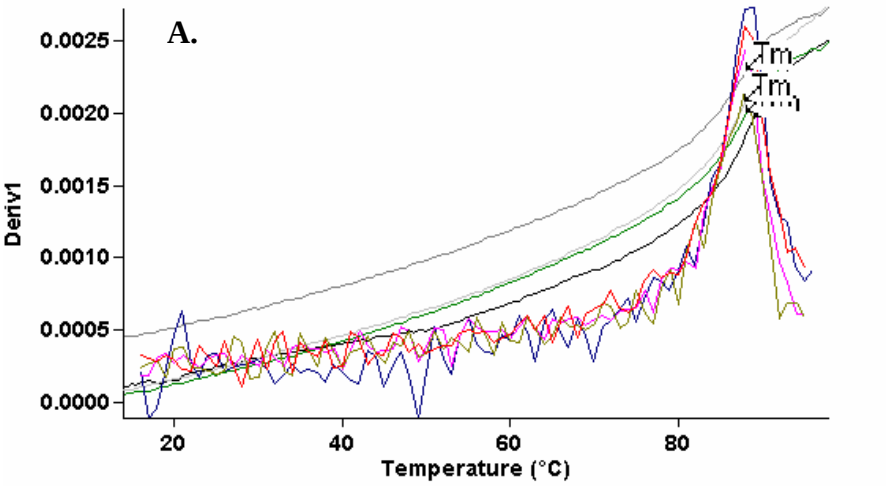
A.
Deriv1
0.0025
0.0020
0.0015
0.0010
0.0005
0.0000
20
40
60
80
Temperature (°C)
Tm
Tm1

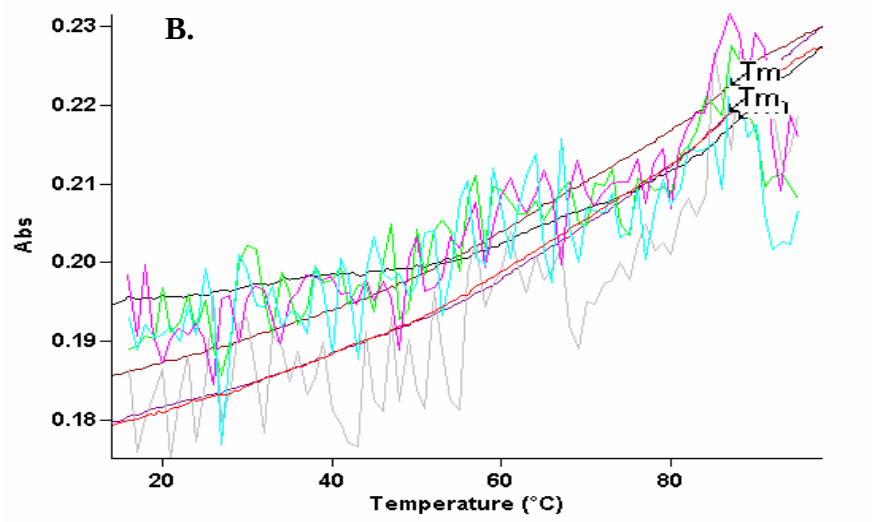
B.
Abs
0.23
0.22
0.21
0.20
0.19
0.18
20
40
60
80
Temperature (°C)
Tm
Tm1

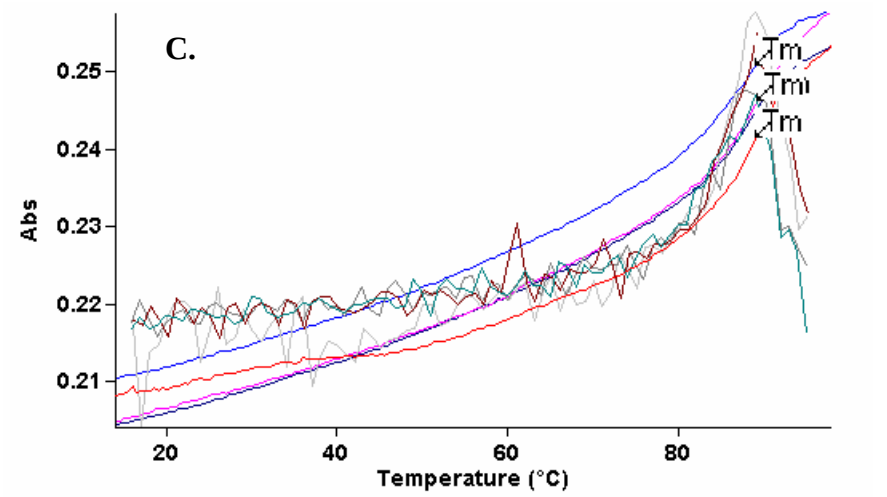
C.
Abs
0.25
0.24
0.23
0.22
0.21
20
40
60
80
Temperature (°C)
Tm
Tm1
Tm

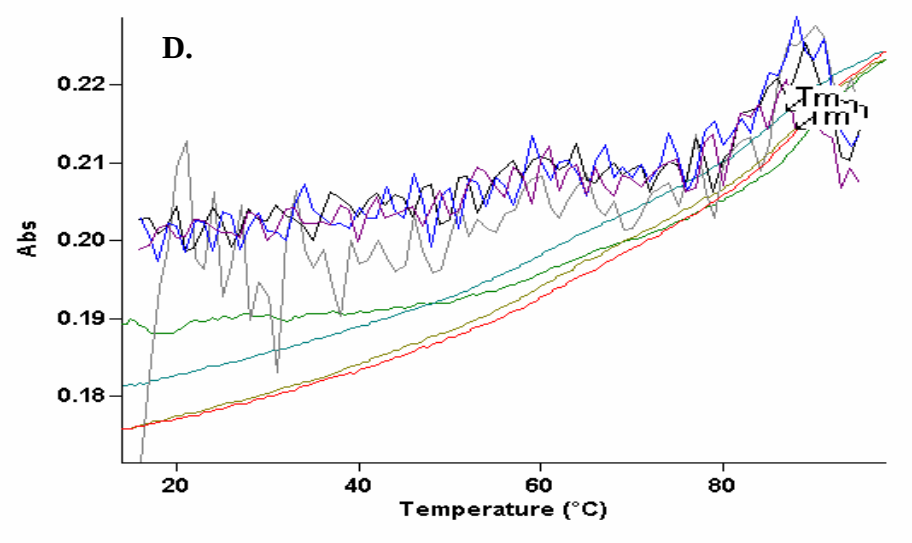

Figure 3.2. PSe-siRNA *Tm* study. A. Antisense (N)+Sense(N);B. Antisense (N)+Sense(Se); C. Antisense (Se)+Sense(N); D. Antisense (Se)+Sense(Se)

3.3.2 PSe-siRNA interference activity

3.3.2.1 siRNA interference activity and cell growth of siRNAs with triphosphate on 5'annealed with borane in tetrahydrofuran.

The first RNAi test was done with siRNAs with triphosphate on 5' and these siRNA was annealed with borane in tetrahydrofuran. siRNA with double strand selenium modifications (Figure 3.3. Lane 3) showed highest RNAi effect. The siRNA with antisense selenium modification (Figure 3.3. Lane 2) had higher activity than no selenium modification (Figure 3.3. Lane 1). The results of native siRNA A and commercial PKM2 siRNA was comparable (Figure 3.3. Lane 1 and 4). siRNA with double strand selenium modifications showed higher cell death number compared with other single strand modification and native siRNA (Figure 3.4 A and B). It was suspected either the 5' triphosphate of siRNA duplex, selenium or the borane used for annealing played a role on the increased cell

growth inhibition.

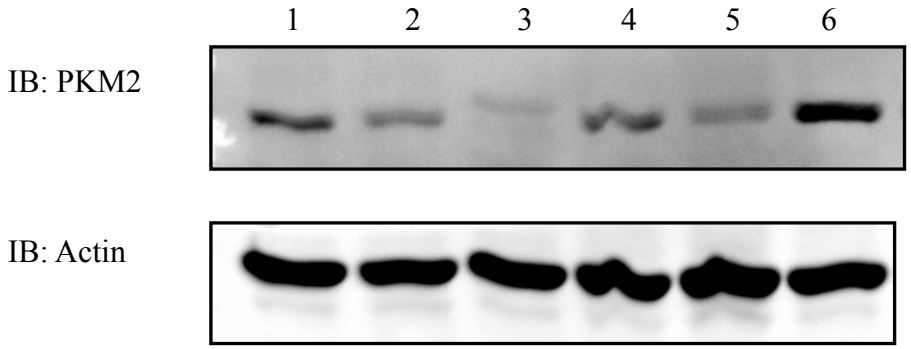

Figure 3.3. PSe-siRNA RNA knocked down PKM2 (48h). PKM2 (pyruvate kinase type M2). The siRNAs were annealed with borane in tetrahydrofuran. These siRNAs have triphosphate on 5'. 1. PSe-siRNA A; 2. PSe-siRNA C 3. PSe-siRNA D; 4. Commercial native siRNA; 5. Smart top: mix of siRNA targeting PKM2; 6. no siRNA control

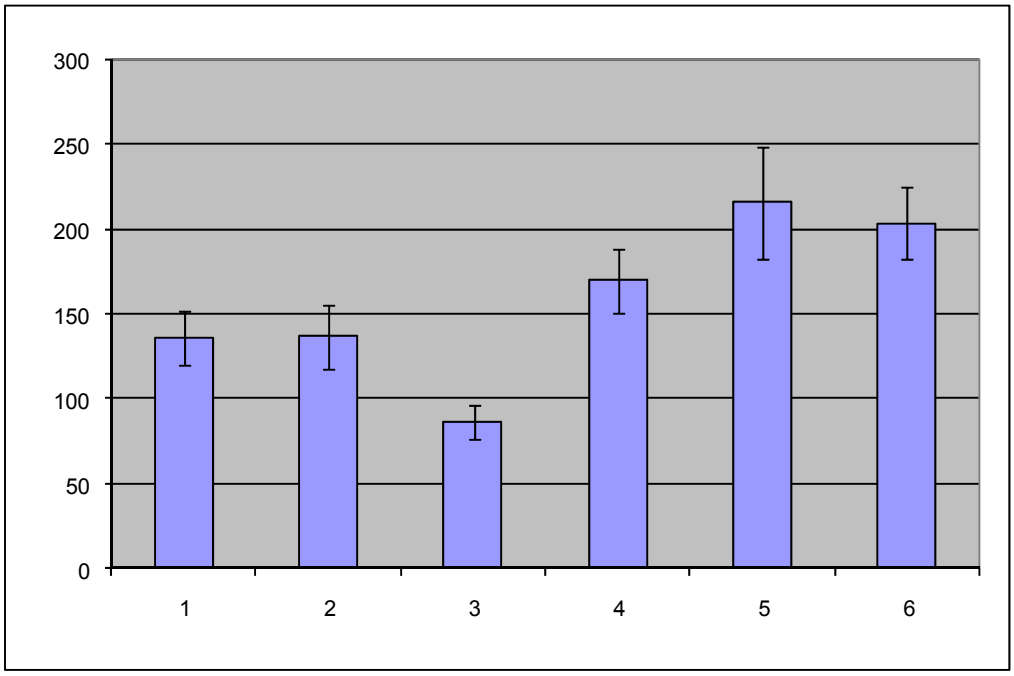

Figure 3.4.A. Se-RNA treatment inhibits cell growth (24h). PKM2 (pyruvate

kinase type M2). The siRNAs were annealed with borane in tetrahydrofuran with triphosphate on 5'. 1: PSe-siRNA A 2: PSe-siRNA C; 3: PSe-siRNA 4; Commercial siRNA; 5: Commercial siRNA with difference sequence targeting same protein. 6: no siRNA control.

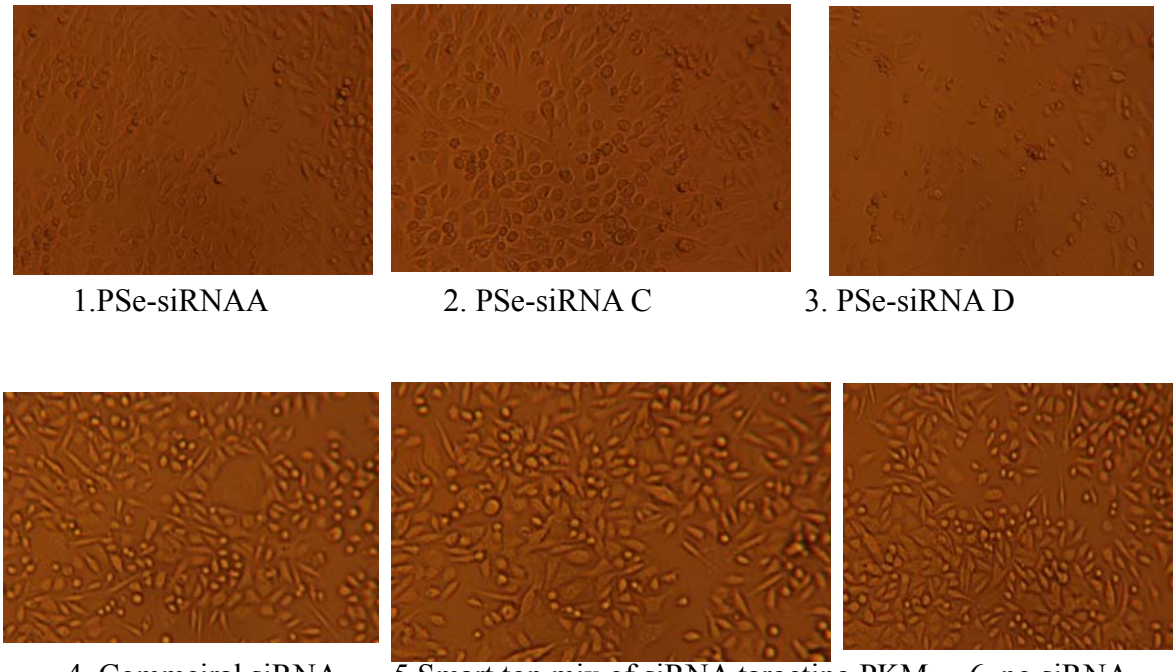

Figure 3.4.B. Se-RNA treatment inhibits cell growth (48h). PKM2 (pyruvate kinase type M2). The siRNAs were annealed with borane in tetrahydrofuran. These siRNAs have triphosphate on 5'.

3.3.3.2: siRNA interference activity and cell growth of siRNAs without triphosphate on 5'.annealed by 100 mM DTT.

Considering the borane and tetrahydrofuran leftover in annealing solution may affect the cell growth, another type of reducing agent DTT was used

in later annealing processes. RNAi activity from siRNA without 5' triphosphate was showed in Figure 3.5. Native siRNA 1, single strand modified siRNA 2 and 3 had similar RNAi effect as commercial siRNA (Figure 3.5. Lane 6). PKM2 expression was strongly inhibited by double strand selenium modified siRNA 4 (Figure 3.5. Lane 4). There was no significant difference on cell growth for all samples (Figure 3.6). The double strand selenium modified siRNA 4 had best RNAi effect and was not toxic to cell (Figure 3.5. Lane 4 and Figure 3.6. Lane 4).

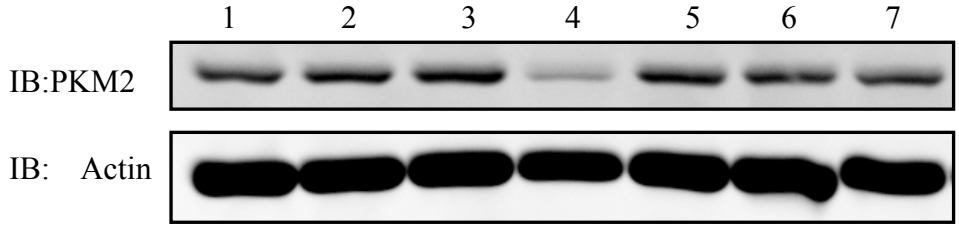

Figure 3.5. PSe-siRNA RNA knocked down PKM2 (48h). PKM2 (pyruvate kinase type M2). The siRNAs were annealed with 100 mM DTT. These siRNAs do not have triphosphate on 5'. 1. siRNA 1; 2. siRNA 2; 3. siRNA 3; 4. siRNA 4; 5. no siRNA control ; 6. Commercial normal siRNA; 7. Smart top: mix of siRNA targeting PKM2

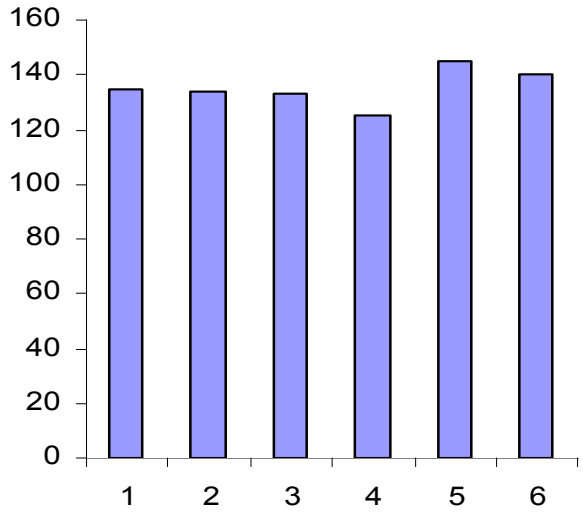

Figure 3.6. Se-RNA treatment does not inhibit cell growth (48h). PKM2 (pyruvate kinase type M2). The siRNAs were annealed with 100 mM DTT. These siRNAs do not have triphosphate on 5'. 1. siRNA 1; 2. siRNA 2; 3. siRNA 3; 4. siRNA 4; 5. No siRNA control; 6. Commercial normal siRNA;

3.3.3.3: siRNA interference activity and cell growth of siRNAs with triphosphate on 5'.annealed with DTT.

This RNAi test was done with siRNAs with triphosphate on 5' and these siRNA was annealed with 100 mM additional DTT in buffer. Double strand modified siRNA (Figure 3.7. Lane 6) showed higher RNAi effect. The siRNA with antisense strand selenium modification (Figure 3.7. Lane 5) had higher activity than sense strand selenium modification (Figure 3.7. Lane 4). The result of native siRNA A and commercial PKM2 siRNA was comparable (Figure 3.7. Lane 3 and 2). siRNA with double strand selenium modifications showed higher cell death number compared with other single strand modification and no modification

(Figure 3.9). siRNA A (Figure 3.9. Lane 3) did not show significant difference on cell death rate compared with commercial siRNA (Figure 3.9. Lane 2).

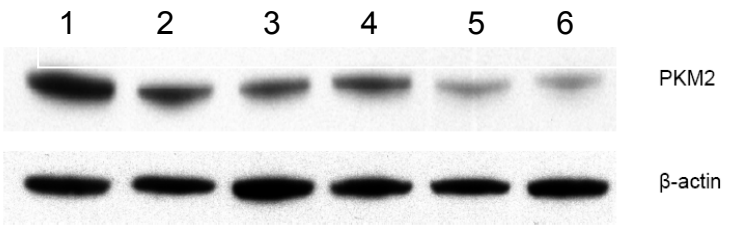

Figure 3.7. Western blot analysis of siRNA (A-D) knockdown of PKM2 in SW620 cells. The siRNAs were annealed with DTT. These siRNAs have triphosphate on 5'. 1. No siRNA control; 2. Commercial normal siRNA; 3. siRNA A; 4. siRNA B; 5. siRNA C; 6. siRNA D;

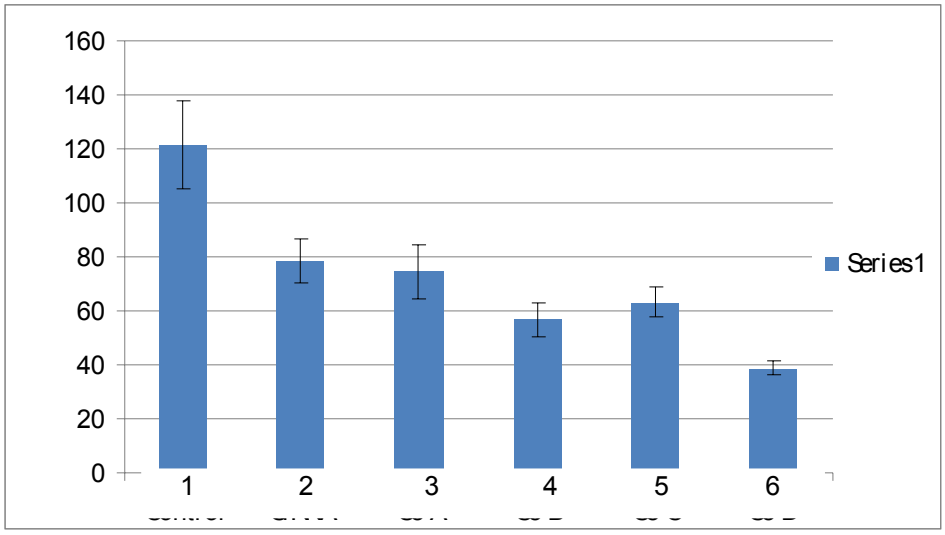

Figure 3.8. PKM2 inhibition by siRNA (A-D) showed as column. 1. No siRNA control; 2. Commercial normal siRNA; 3. siRNA A; 4. siRNA B; 5. siRNA C; 6. siRNA D.

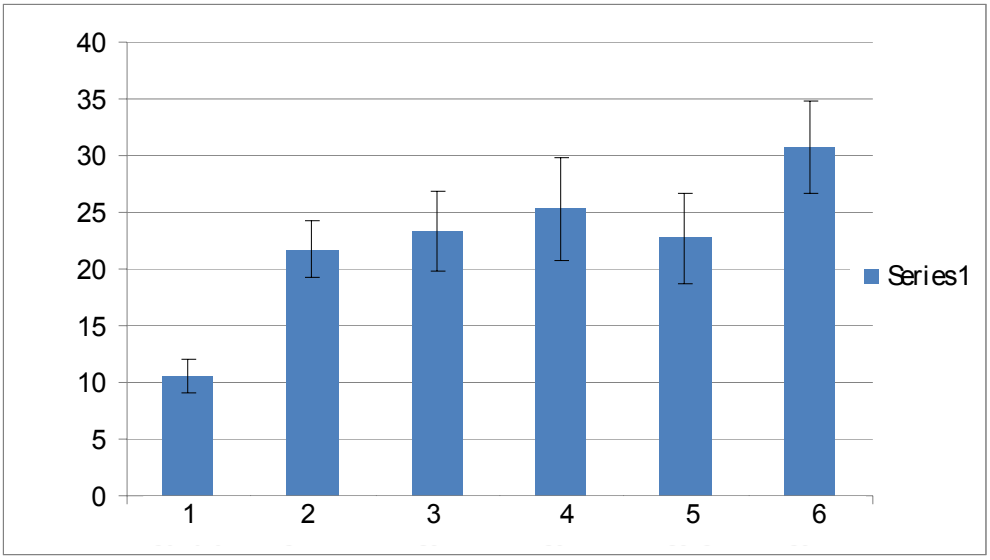

Figure 3.9. The number of dead cells in siRNA (A-D) knockdown of PKM2 in SW620 cells. 1. No siRNA control; 2. Commercial normal siRNA; 3. siRNA A; 4. siRNA B; 5. siRNA C; 6. siRNA D.

3.3.3.4 siRNA interference activity and cell growth of all eight types of siRNA duplex annealed with DTT.

To investigate the effect of 5' triphosphate on RNAi, eight types of siRNA were prepared and tested simultaneously. The siRNA 1-4 showed higher RNAi activity than siRNA A-D (Figure 3.10). The loading control of these results was not consistent; therefore the results were not conclusive. There was no significant difference on the average living cell numbers between the two groups (Figure 3.11). An additional experiment was repeated with the same groups of siRNA and conditions for cell viability (Figure 3.12). There was no significant difference between the group siRNA A-D (with 5' triphosphate) and siRNA 1-4 (without 5' triphosphate).

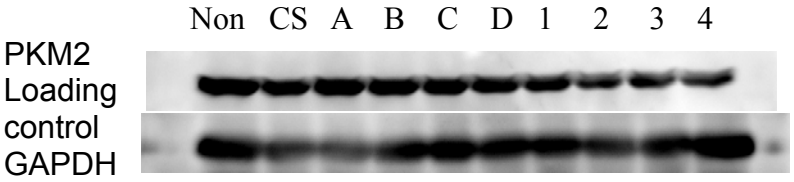

Figure 3.10. PKM2 inhibition with eight types of siRNAs. Non: no siRNA control; CS: Commercial siRNA; A: PSe-siRNA A; B: PSe-siRNA B; C: PSe-siRNA C; D: PSe-siRNA D; 1: PSe-siRNA 1; 2: PSe-siRNA 2; 3: PSe-siRNA 3; 4: PSe-siRNA 4.

Figure 3.11. The numbers live cells in eight types of siRNA treatment. nt: no siRNA control; PKM2: Commercial siRNA; A: PSe-siRNA A; B: PSe-siRNA B; C: PSe-siRNA C; D: PSe-siRNA D; 1: PSe-siRNA 1; 2: PSe-siRNA 2; 3: PSe-siRNA 3; 4: PSe-siRNA 4.

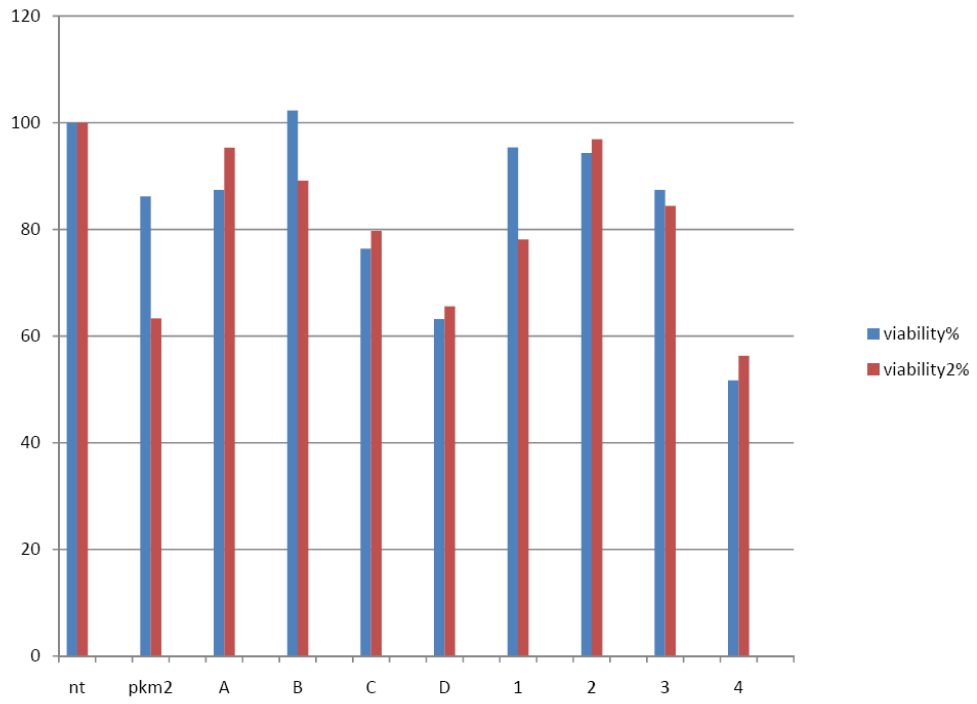

Figure 3.12. SW240 cell viability in eight types of siRNA treatment. nt: no siRNA control; PKM2: Commercial siRNA; A: PSe-siRNA A; B: PSe-siRNA B; C: PSe-siRNA C; D: PSe-siRNA D; 1: PSe-siRNA 1; 2: PSe-siRNA 2; 3: PSe-siRNA 3; 4: PSe-siRNA 4. Two repeats experiment were done. Test 1 in blue. Test 2 in red.

3.4 Discussion

Since the discovery of triggering of RNA interference activity by small interfering RNA (siRNA) in mammalian cells, researchers have been trying to push the RNA interference technique into clinical applications.[112] Certain chemical modifications could help to solve some issues faced in the use of siRNA as a therapeutic reagent, such as serum stability, biodistribution, immune response and pharmacokinetic properties of the siRNA. [113]

We have prepared different types of selenium modifications on nucleic

acids for X-ray crystallography purpose. However, none of the selenium modifications have been tested for siRNA activities. In contrast, all kinds of thiol modifications have been tested for siRNA activities to improve nuclease stability and selectivity. Therefore, we prepared PSe-siRNA and evaluated their RNAi effect in cells. Based on the experimental results above, the RNAi activity from PSe-siRNA, especially from double stranded modified siRNA, was stronger than others. This was probably due to the longer life time for double stranded modified siRNA. The cell death rate from double strand modified siRNA was also the highest. Except in the experiment result 3.3.3.2, siRNA 4 did not show significant cell growth inhibition. The reason for the cause of the higher cell death rate from modified siRNA has not yet been conclusive. It is likely that the triphosphate at 5' end of siRNA did not play a role in affecting the cell death rate. The remaining borane in tetrahydrofuran from the annealing solution in experiment 3.3.2.1 could be the reason for a higher cell death rate for all four types of homemade siRNA, while compared to commercial siRNA. After switching to DTT as the reducing agent in the annealing buffer, cell death rate of home-made non-modified siRNA was similar to that of commercially available siRNA. Experiment 3.3.3.3 (Figure 3.9) and Figure 3.12 indicated that double strand selenium modification has a higher cell death rate. The effect of selenium on cell death has to be further investigated.

4. SYNTHESIS OF 4-SE-URIDINE 5'-TRIPHOSPHATE AND ITS INCORPORATION INTO RNA

4.1 Introduction

Natural modifications on RNA molecules have been known for a long time and over 100 special natural modifications on RNA have been found to date. [114] Although the functionalities of many modifications are still unclear, the characterized modifications are usually located in important functional regions of RNA, such as the pseudouridine and 2'-O-methylation on rRNA,[115] and anticodon loop of tRNA.[114] Besides studies on natural RNA modifications, development of unnatural RNA modifications also has great significance on improving biotechnology for RNA-based research tools and therapeutic methods [116]. Modified nucleotides can be used for research like probing the functional groups of ribozyme [117] and investigating the base-pairing fidelity of replication.[118] Chemical modifications have also been applied to increase siRNA serum stability and RNAi activity. [37]

It is not well-known that selenium also naturally occurs in bases of tRNA, usually in the wobble base position, which may have some special functions. Detailed studies about the natural Se-derivatized RNAs are rather limited.[61, 119] Our group previously reported derivatization of DNA at 4-position of thymidine (4-Se-T) through solid phase synthesis and enzymatic incorporation.[79-80] In the crystal structure of the solid phase synthesized short DNA duplex containing 4-Se-thymidine, selenium formed a hydrogen bond with 6-amino group of A on the complimentary strand.[80] It is very interesting that this

selenium modification at 4 position of thymidine gave DNA a visible bright yellow color. The synthesis method for 4-Se-uridine 5'-triphosphate (4-Se-UTP) and its enzymatic incorporation was described in this dissertation to continue development of selenium building blocks for RNA crystallography and make potential RNA visualization tool for RNA detection.

Unlike deoxyribose modification, in the synthesis of unnatural ribose modification, choosing the right ribose 5' and 2' protecting groups is important. [114] A good 2'-hydroxyl group should be easy to introduce, stable under the particular reaction condition and easily removed afterwards. For the synthesis of 4-Se-UTP, the selenium at 4 position also needs to be protected from the aggressive reaction conditions that are used for generating triphosphate. The lack of a methyl group at 5 position on uridine compared with thymidine also changes the chemical property of 4-Se-urindine and makes new challenges for its synthesis and incorporation. In this chapter, the synthesis method for 4-Se-UTP has been described in detail and the incorporation of 4-Se-UTP into RNA was also reported with supporting kinetics data.

4.2 Materials and methods

4.2.1 Simple synthetic route for 4-Se-UTP

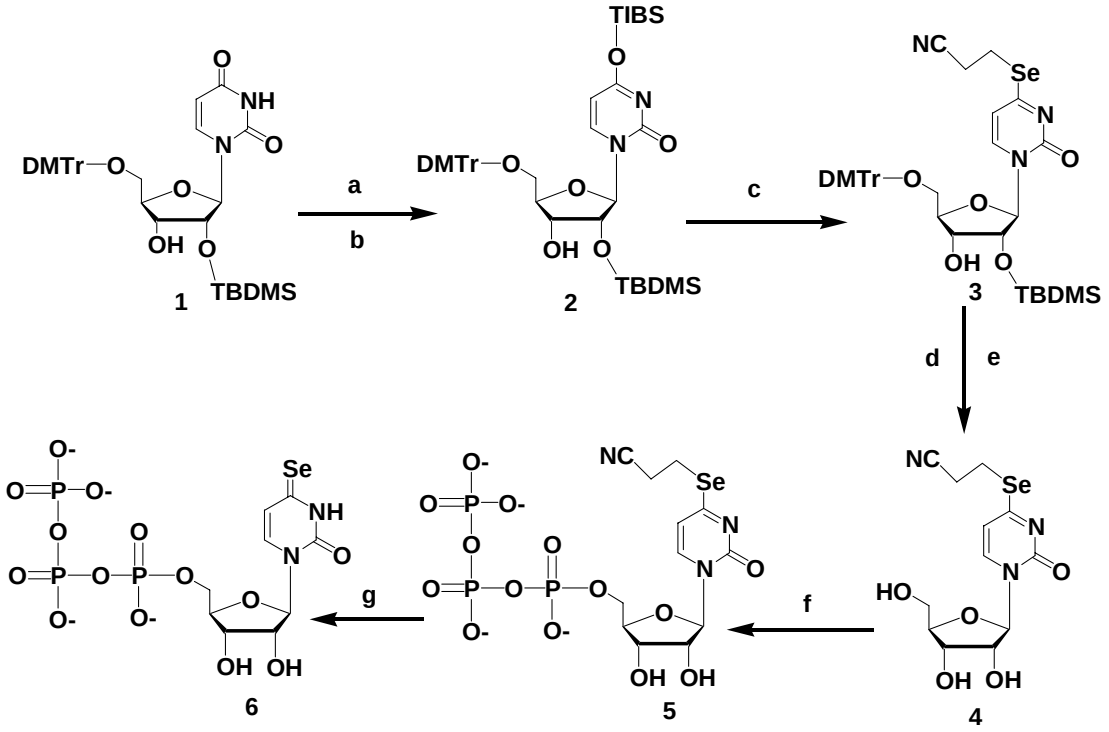

Figure 4.1. Synthetic route of 4-Se-UTP

Reagents and conditions: (a) TIBSCl, DMAP, CH_2Cl_2, RT; (b)$(NCCH_2CH_2Se)_2/NaBH_4$, EtOH, RT; (c) triethylamine, THF, 45 ^oC, 1h ; (d) 80% acetic acid, RT, 30min; (e) Phosphorus oxychloride, proton sponge, TMP, 0 ^oC, 1 h; (f) tributylammonium pyrophosphate, DMF, 0 ^oC, 1 min, followed by 0.25 M triethylamine carbonate, RT, 2 h; (g) 0.1 M K_2CO_3 in methanol and water (3:1), RT. TIBSCl: 2,4,6-(Triisopropylbenzene)sulfonyl chloride; DMAP: 4,4'-dimethylamino-pyridine; THF: trihydroflouride; TMP: trimethyl phosphate.

As showed in Figure 4.1, the synthesis started from the partially protected 2'-TBDMS-5'-trityl-uridine (compound 1). Considering the presence of

bulky TBDMS group at the 2' position, the synthesis route was simplified by using a relatively more chemoselective TIBS (2,4,6-Triisopropylbenzenesulfonyl) group to activate position 4, instead of the previous trizaole group, thus avoided the protection and deprotection steps for the 3'-hydroxyl group. Without purifying this activated intermediate (compound 2), the selenium functionality was introduced directly by the substitution of TIBS group at position 4 with sodium 2-cyanoethylselenide in good yield, which was generated by the reduction of di-(2-cyanoethyl) diselenide with $NaBH_4$ in ethanol. The details for synthesis of compound 3 is as following: dichloromethane solution of 2,4,6-Trisopropyl-Benzenessulfonyl chloride was drop wisely added to a dry dichloromethane solution of the starting material compound 1 and 4,4'-dimethylamino-pyridine (DMAP) under argon, followed by several drops of triethyl amine. The system was stirred for one hour before this reaction was finished (monitor by TLC, 5% methanol in dichloromethane). At the same time, the $NaBH_4$ suspension (250 mg $NaBH_4$ in 5 mL of EtOH) was injected into a flask containing di(2-cyanoethyl) diselenide [$(NCCH_2CH_2Se)_2$, 0.45 mL, d= 1.8 g/mL, 3.0 mmol] and ethanol (8 mL) on an ice bath and under argon. The yellow color of the diselenide disappeared in approximately 15 min, giving an almost colorless solution of sodium selenide ($NCCH_2CH_2SeNa$). Then, the solution of compound **1** (1.34 g, 2 mmol) was slowly injected into this solution. The selenium incorporation step was finished in 45 min, which was checked on TLC by 5% MeOH in CH_2Cl_2 (product R_f = 0.68). 100 mL water was then added to the reaction flask. The solution was adjusted to pH 7-8 using CH_3COOH (10%), and was then extracted with ethyl acetate (3 x

100 mL). The organic phases were combined, washed with NaCl (sat., 100 mL), dried over $MgSO_4$ (s) for 30 min, and evaporated to minimum volume under reduced pressure. Then 5 mL methylene chloride was used to dissolve the crude product. The crude product was purified by a silica gel column equilibrated with hexanes/methylene chloride (1:1). The gradient used to elude the compound was methylene chloride (CH_2Cl_2) with 0.5%, 1%, and 2% MeOH (500 mL each gradient). After solvent evaporation and dry on high vacuum, the pure compound 3 was obtained as a slightly yellow foamy product (1.07 g, 81% yield).

The purified compound 3 was treated by triethylamine in THF, at 45 ^oC for 1h to remove TBDMS group and purified by TLC plate. The DMTr group on purified product was removed by 80% acetic acid, at RT for 30min. The acetic acid in solution was eliminated by coevaporation with toluene and ethanol (9:1) mixture three times. Compound 4 was purified by TLC plate once before proceed to the next step.

4-Se-UTP (Figure 4.1. compound 6) was made using a modification of Yoshikawa procedure.[120] Compound 4 (0.025 mmole, 9 mg) was dried in a flask with proton sponge (1.5 eq., 0.0375 mmole, 8 mg) on high vacuum for 1 h. The dried compound 4 and proton sponge were dissolved in 110 µL trimethyl phosphate (TMP). Phosphorus oxide chloride ($POCl_3$) (1.2 eq., 0.03 mmole, 2.75 µL) was added to reaction flask at 0 ^oC. The reaction mixture was stirred for 2 h. Then tributyl ammonium pyrophosphate (2 eq., 0.05 mmole, 22.75 mg) was dissolved in 0.25 mL DMF and injected into reaction flask at 0 ^oC. The reaction was kept at 0 ^oC for 1 min after adding tributyl ammonium pyrophosphate. Then

2.5 mL 0.25 M triethylammonium bicarbonate buffer (pH 8.5) was added to reaction mixture, which was continually stirred for another 2 h. Ethanol precipitation was performed on hydrolyzed triphosphate. The protective group was removed by treating the compound 5 with 3 eq. K_2CO_3 (0.1 M) in methanol and water (3:1) at RT for 2 h. The reaction was followed by UV spectrum scanning until the maximum and the main peak for the absorption of neutralized solution was at 365 nm and original 312 nm peak for compound 5 completely disappeared. After the deprotection reaction finished, several drops of 3 M HCl was added to neutralize the base in solution. The compound 6 was purified by reversed phase HPLC, and it was analyzed and compared with natural TTP by UV and HPLC after purification. The purified product was confirmed by high resolution mass spectrometry.

4.2.2 Optimization of 4-Se-UTP in transcription

4-Se-UTP was enzymatically incorporated into RNA through both synthetic template and plasmid template by Epicentre T7 RNA polymerase (T7950K) with modified protocol. The 10X transcription buffer was Tris (400 mM), spermine (20 mM), DTT (100 mM), $MgCl_2$ (20 mM), pH 7.0. 10 mM 4-Se-UTP was used to substitute normal 10 mM UTP. Typical final reaction was performed under the condition of 1 μM ssDNA template and top promoter strand or 50 ng/μL dsDNA plasmid or 6 ng/μL PCR dsDNA template, and 0.5 mM other NTP and 0.1 u/μL phosphatase. $MnCl_2$ concentration was varied from 0 mM to 5 mM in final transcription reaction for screening. The incorporation result was checked by

^{32}P[α] CTP label.

4.2.3. Stability studies of 4-Se-UTP in transcription buffer

Pure 4-se-UTP has a maximum UV peak at 365 nm and a minor peak at 262 nm. The stability of 4-Se-UTP in transcription buffer is concerned. The 4-Se-UTp was treated with 1X commercial New England Biolabs transcription buffer (pH 7.8) plus 10 mM DTT, 10 mM DTT alone, 40 mM Tris (pH 7.8) alone, 10 mM DTT then 40 mM Tris (pH 7.8), and 1X modified New England Biolabs transcription buffer (pH 6.5) plus 10 mM DTT. UV spectrum was monitored every 10 min at RT.

The stability of 4-Se-UTP in homemade 1X transcription buffer, Tris (40 mM), spermine (2 mM), DTT (10 mM), $MgCl_2$ (2.5 mM), $MnCl_2$ (2 mM), pH 7.0, was tested by mixing the 4-Se-UTP with 1X transcription buffer and monitoring the UV spectrum every 10 min at RT.

4.2.4 Kinetic study of 4-Se-UTP enzymatic incorporation into RNA.

A transcription mixture with condition in 4.2.2 and 2 mM Mn^{2+} was prepared without any UTP, which was separated into two equal proportions to two tubes. Proportional UTP as stated in Method 4.2.2 was added to one tube and equal amount of 4-Se-UTP was added to the other tube. T7 RNA polymerase (Epicentre) was added to two tubes containing either UTP or 4-Se-UTP. From the same time point, these tubes were incubated at 37 ^{o}C. At different time points (0, 5, 15, 30, 60, 90, 120 150 min), 5 μL transcription solution was taken

out and 5 μL loading buffer was added to the mixture to end the transcription. The result was checked by 12% denature PAGE.

4.3 Results

4.3.1 Synthesis and characterization of 4-Se-UTP

4-Se-UTP was successfully synthesized and the compound confirmed by high resolution mass spectrum (Figure 4.2). The color of 4-Se-UTP was bright yellow while native UTP was colorless (Figure 4.3). 4-Se-UTP had two UV absorption peaks. The major peak was at 365 nm (Figure 4.4). The minor one was at 260 nm. The 4-Se-UTP peaks of 365 nm and 260 nm appeared at the same retention time RP-HPLC (Figure 4.5), which proved that pure 4-Se-UTP has two absorption peaks. RP-HPLC program used for analysis was 20min reaching 12.5 % ACN (in 20 mM TEA·Ac buffer, pH7) running at 1 mL/min.

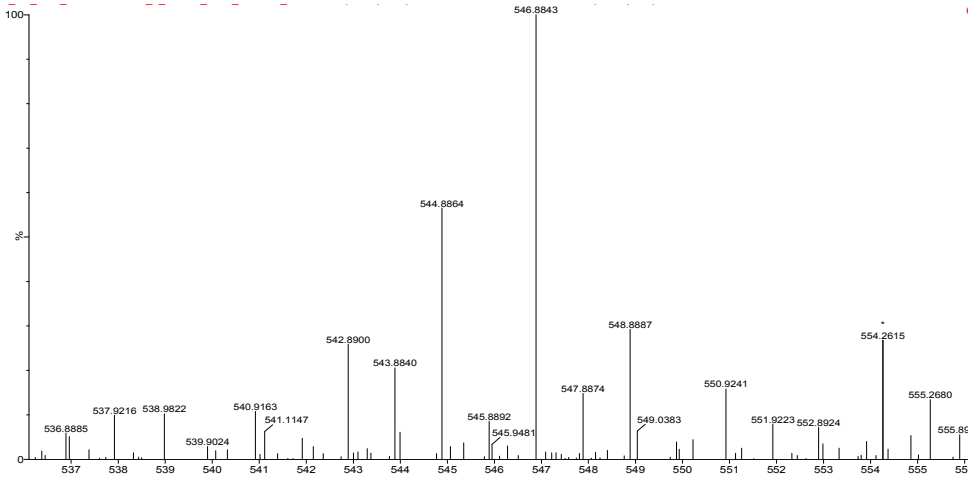

Figure 4.2. High resolution MS (ESI) of 4-Se-UTP. $[M-H]^-$ =546.8843 (calcd 546.8823).

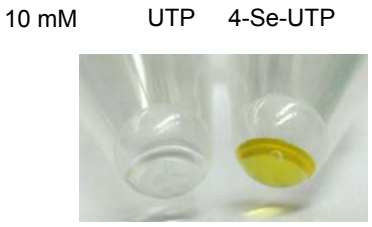

Figure 4.3. Color comparison of 10 mM UTP and 4-Se-UTP. 10 mM UTP was colorless, while 10 mM 4-Se-UTP was yellow.

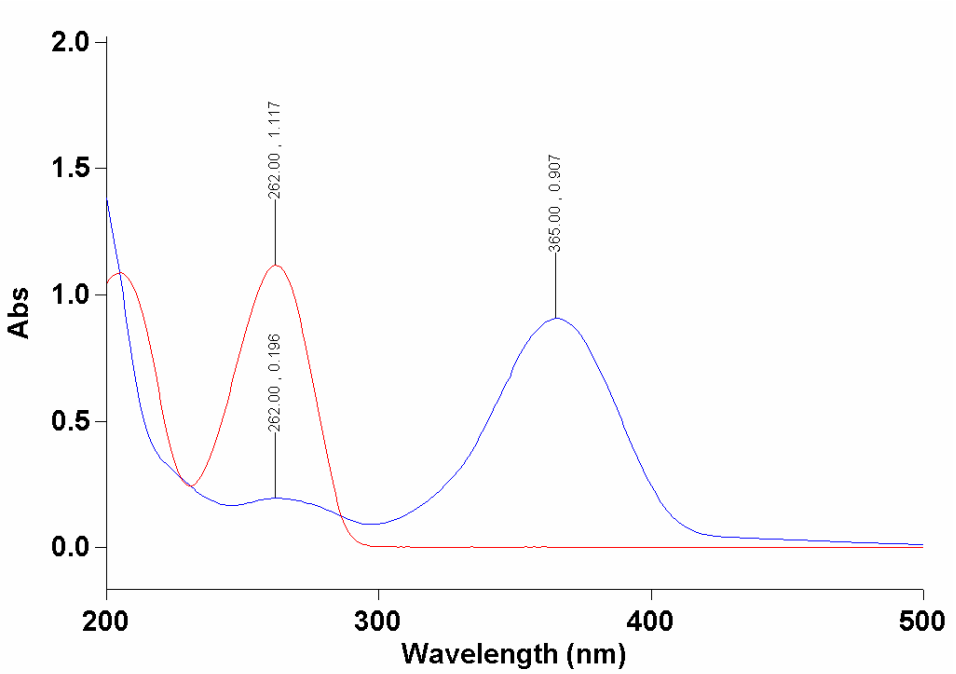

Figure 4.4. 4-Se-UTP UV absorption (blue, 262 nm and 367 nm); UTP UV abs (red, 262 nm)

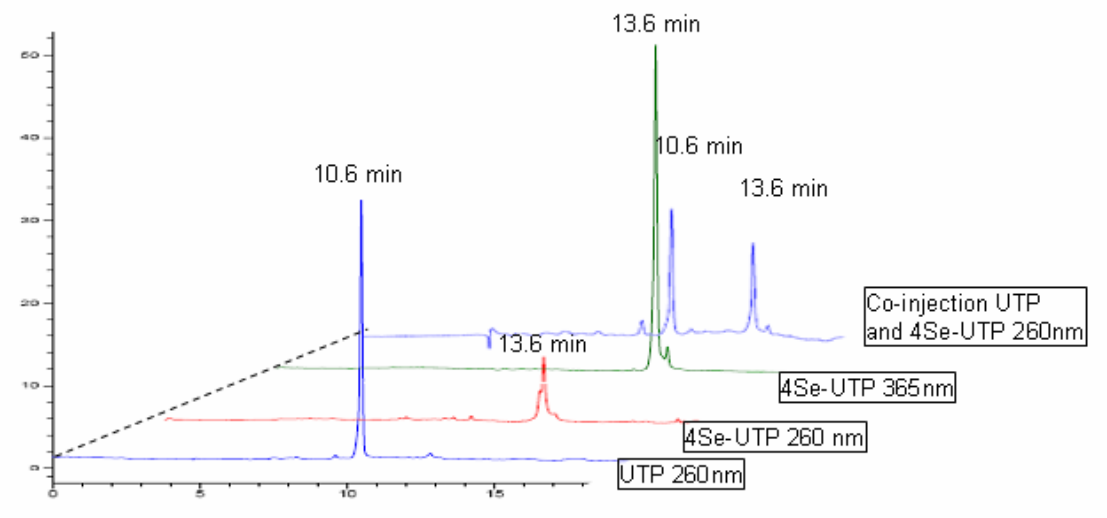

Figure 4.5. 4-Se-UTP and UTP HPLC profiles.

4.3.2 4Se-UTP stability and transcription studies

The stability was inspected in several different buffer conditions. The result suggested that 4-Se-UTP was not very stable in commercial New England Biolabs T7 RNA polymerase buffer (Figure 4.6.A). The effects of DTT alone (Figure 4.6.B), Tris buffer alone (Figure 4.6.C), and DTT plus Tris buffer (Figure 4.6.D) on 4-Se-UTP stability were also checked separately. From these results, it was suspected that DTT would cause deselenization or oxidation under basic conditions. Therefore the transcription condition was adjusted to neutral and slightly acidic conditions. The 4-Se-UTP was relatively stable in pH 6.5 transcription buffer (Figure 4.6.G). 4-Se-UTP in homemade 1X transcription buffer, Tris (40 mM), spermine (2 mM), DTT (10 mM), $MgCl_2$ (2.5 mM), $MnCl_2$ (2 mM), pH 7.0, was also considered to be relatively stable (Figure 4.6.H)

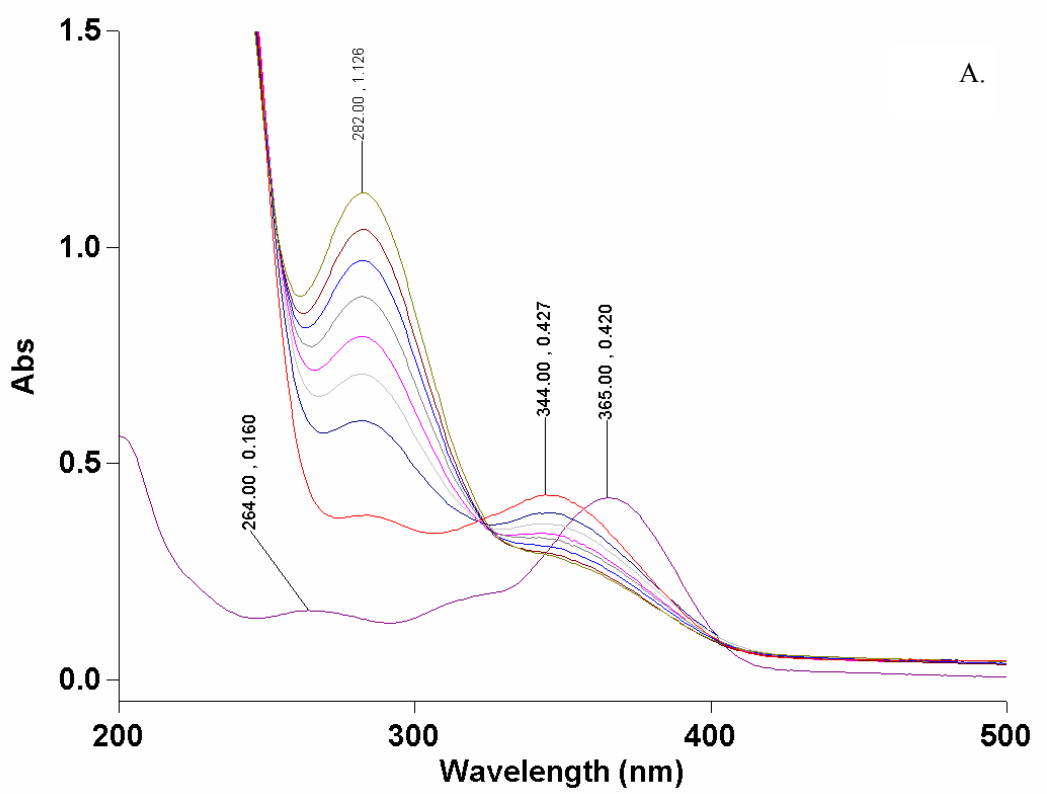

Figure 4.6.A. 4-Se-UTP stability in 1X transcription buffer (pH7.8) +10 mM DTT. UV spectrum was scanned every 10 min for 1 h at RT. The original 365nm peak disappeared and 282 nm oxidized DTT peak kept increasing.

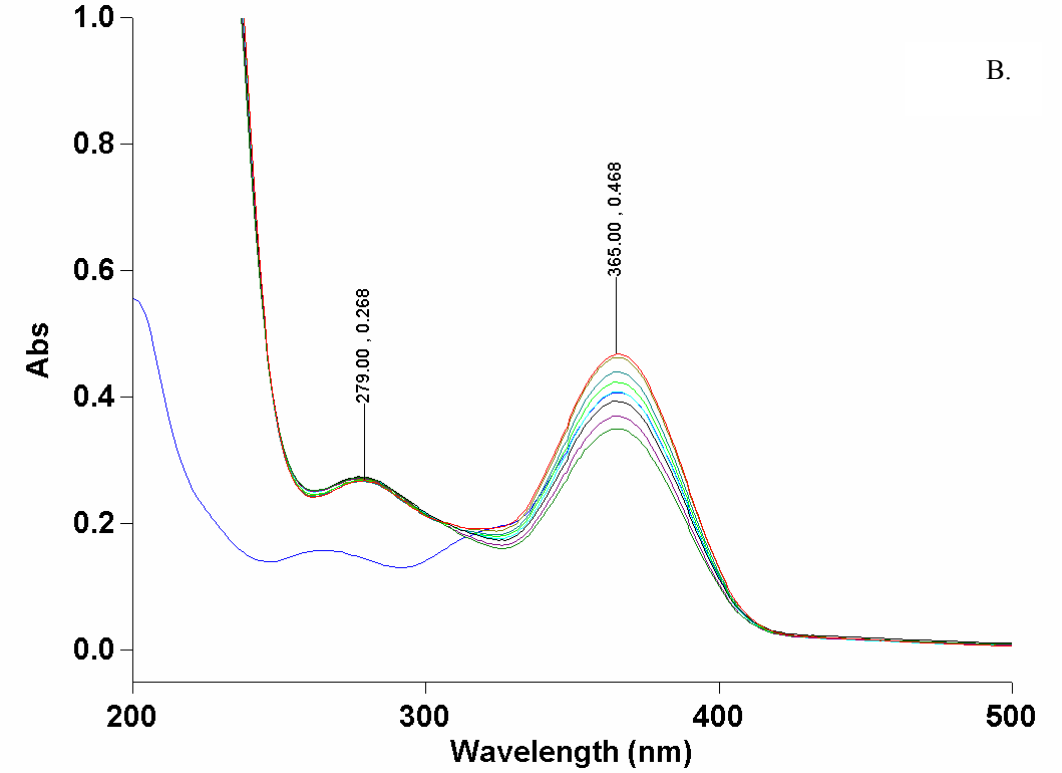

Figure 4.6.B. 4-Se-UTP stability in 10 mM DTT (pH 7). UV spectrum was scanned every 10 min for 1h at RT. The original 365nm peak got lower over the time. The 279 nM DTT peak was stable.

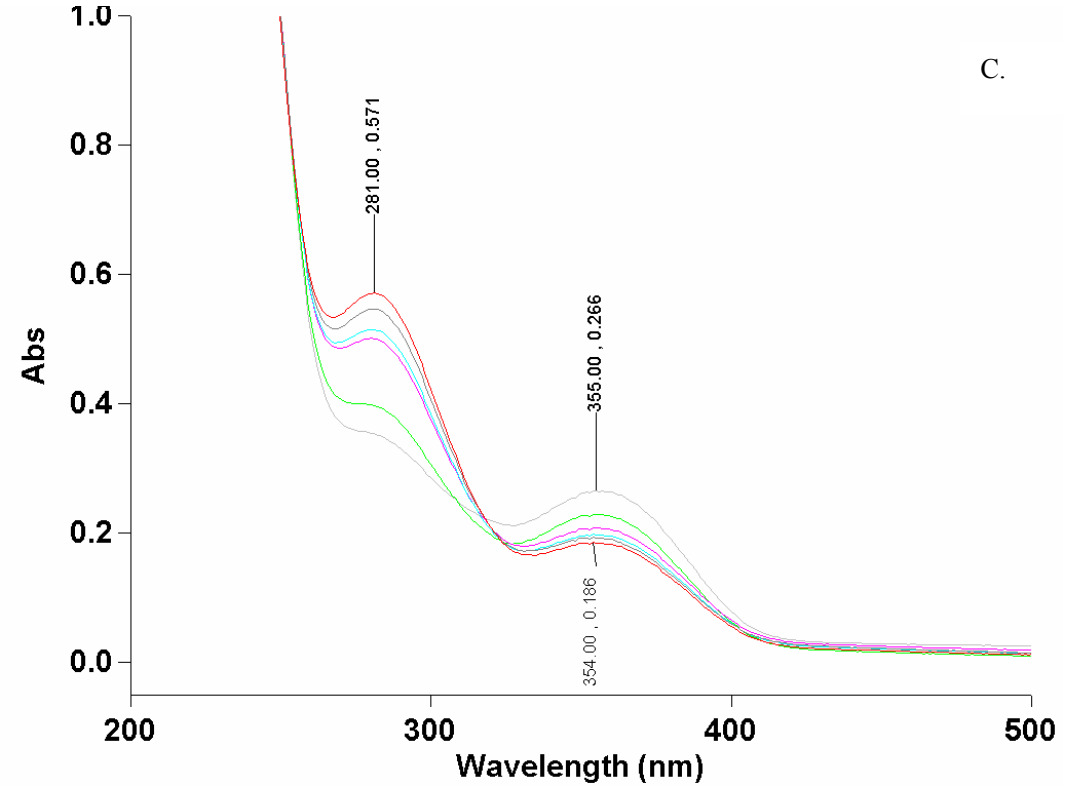

Figure 4.6.C. 4-Se-UTP stability sample after the experiment from figure 4.5.B was added 40 mM Tris pH7.8. UV spectrum was scanned every 10 min for 1h at RT. The 365 nm peak switched to 355 nm and continued get lower over the time and 281 nm oxidized DTT peak kept increasing.

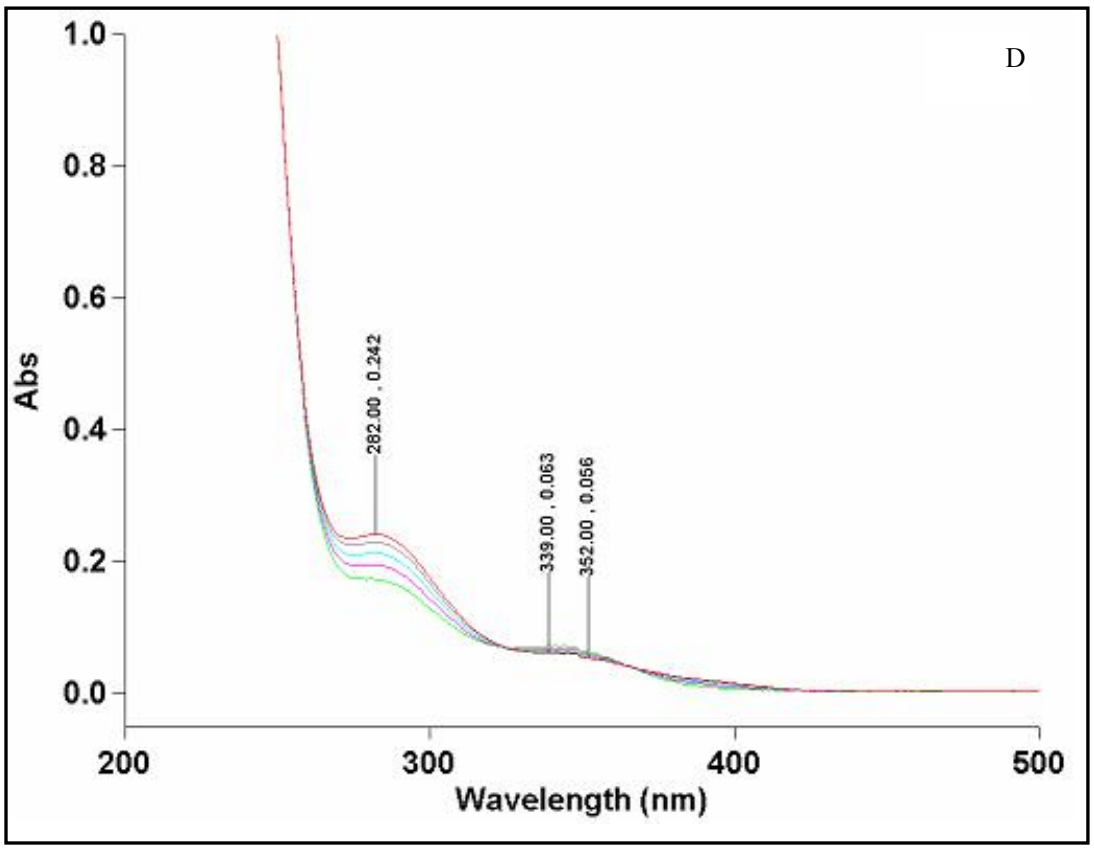

Figure 4.6.D. UV spectrum of 10 mM DTT and 40 mM Tris pH 7.8. UV spectrum was scanned every 10 min for 1h at RT. DTT peak at 282 nm got increased over the time.

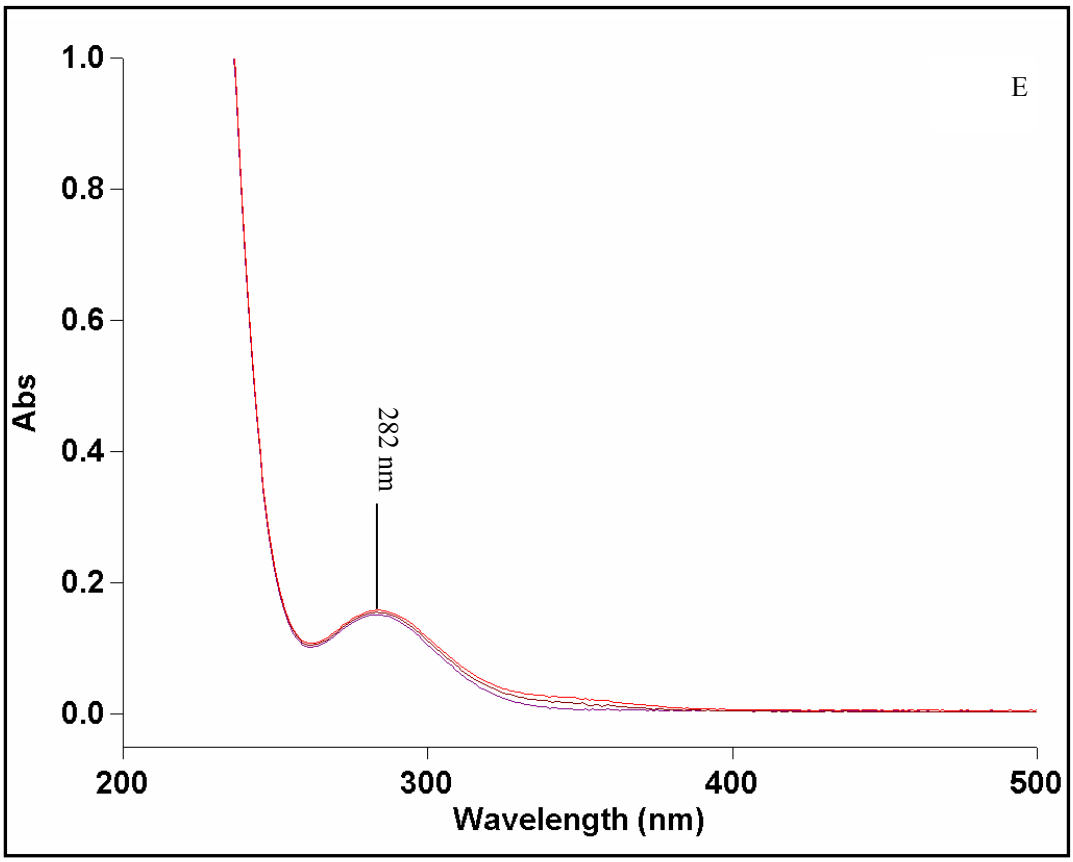

Figure 4.6.E. UV spectrum of 10 mM DTT (pH 7). UV spectrum was scanned every 10 min for 1h at RT.

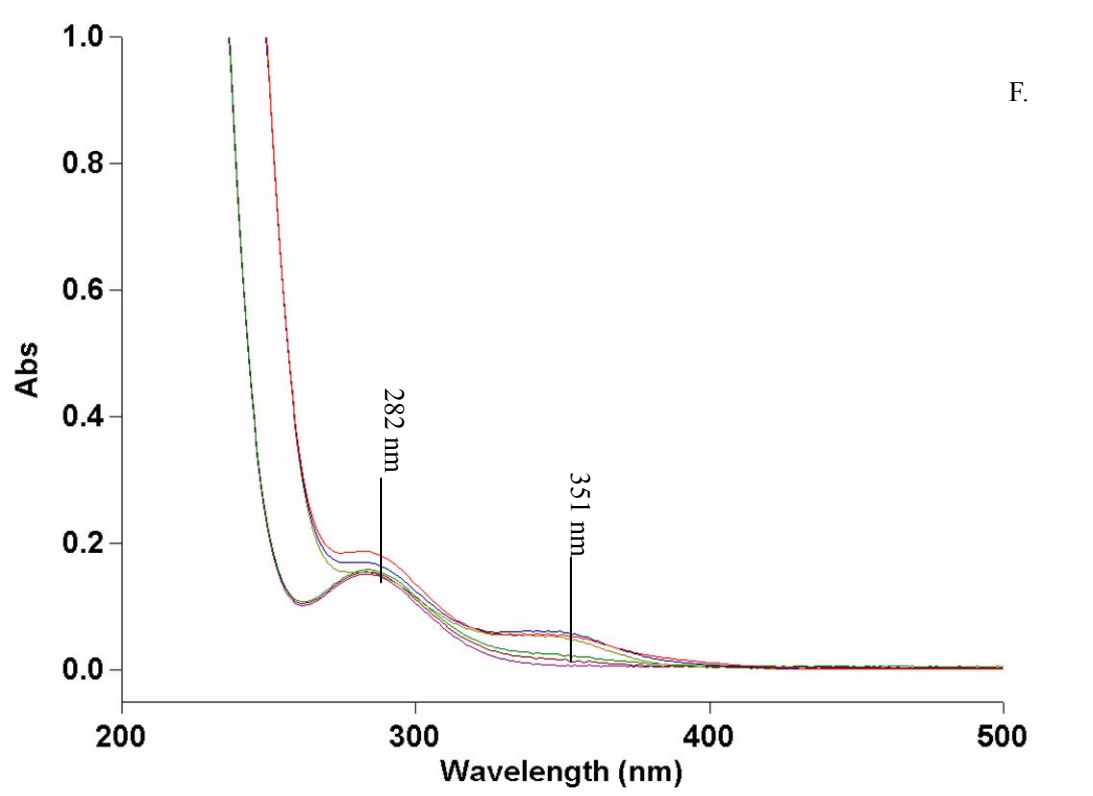

Figure 4.6.F. 10 mM DTT after the experiment from Figure 4.5.E was added 40 mM Tris pH 7.8 UV spectra were scanned every 10 min for 1h at RT. The new lines in Figure 4.5.F compared with 4.5.E. show the DTT spectrum with Tris added.

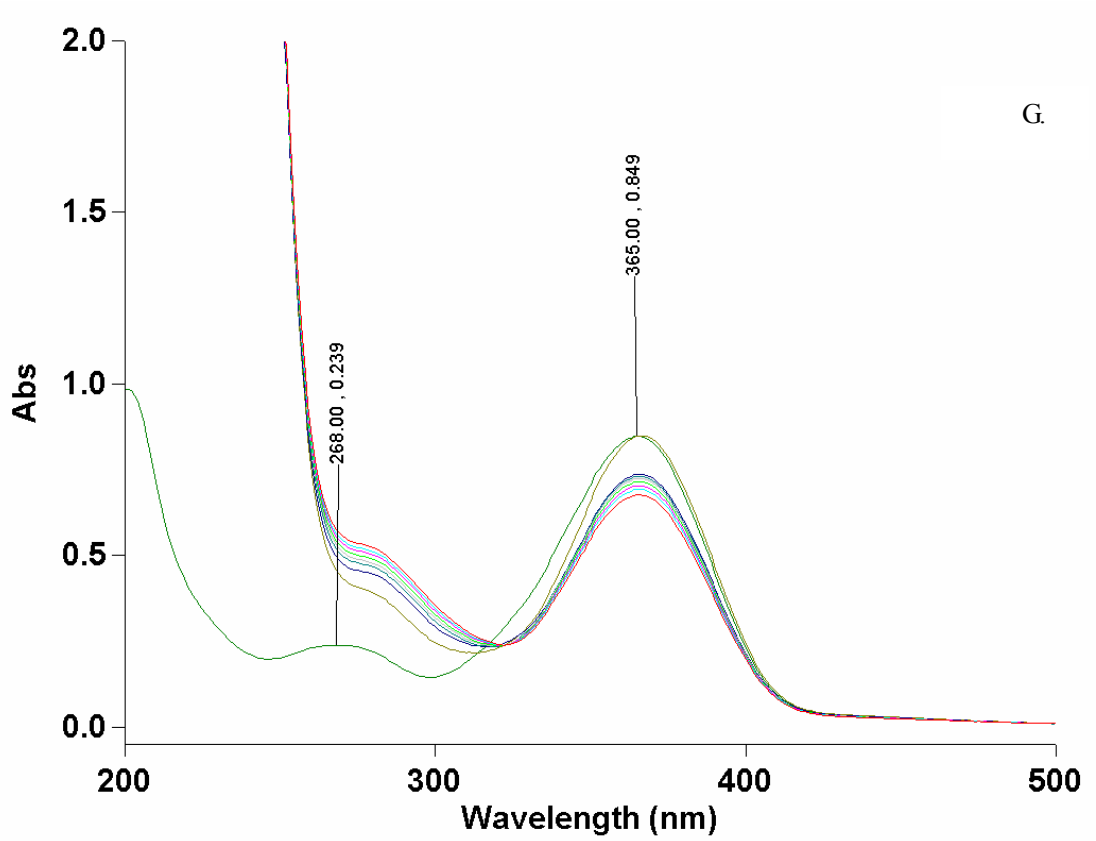

Figure 4.6.G. 4-Se-UTP stability in 1X New England Biolabs transcription buffer (pH 6.5) plus 10 mM DTT. UV spectrum was scanned every 10 min for 1h at RT. The original 4-Se-UTP (green) 365 nm peak got slightly lower after mixed with the buffer and stable over the scanning time.

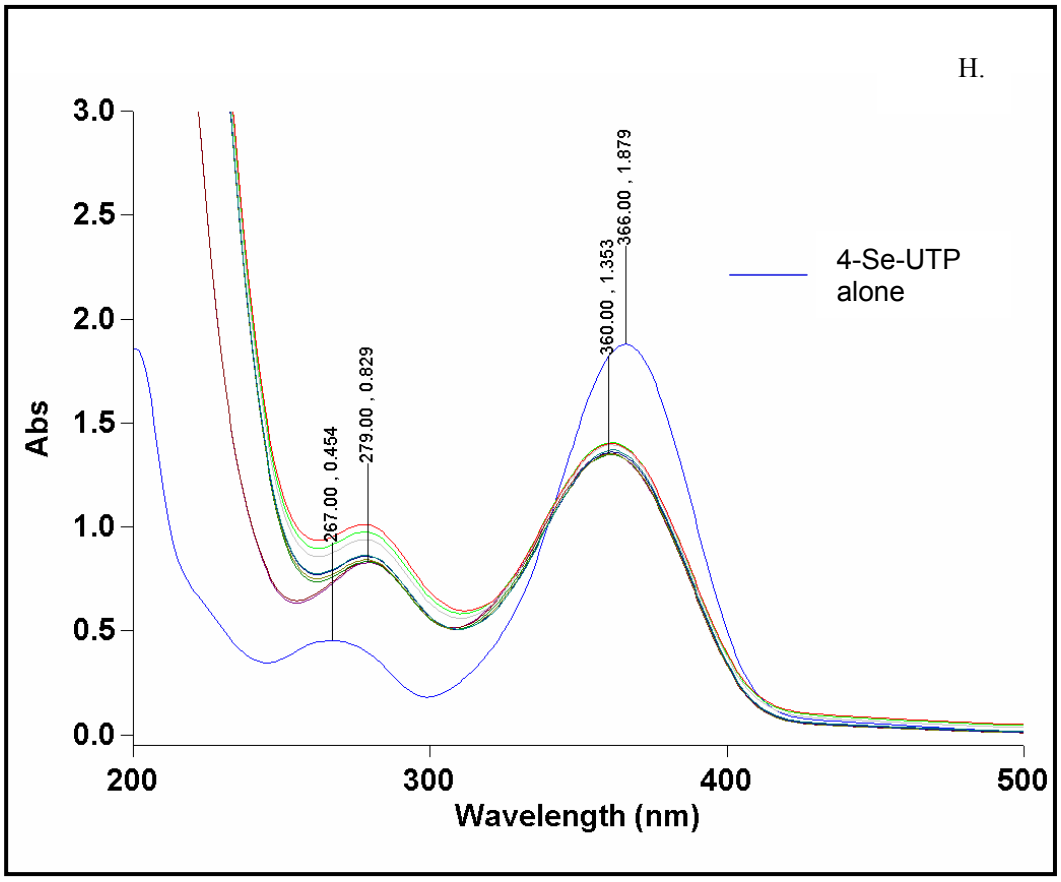

Figure 4.6.H. 4-Se-UTP stability in 1X homemade transcription buffer (pH 7.0), Tris (40 mM), spermine (2 mM). UV spectrum was scanned every 10 min for 1h at RT. The original 4-Se-UTP (Blue) 365 nm peak got slightly lower immediately after mixed with the buffer and relatively stable over the scanning time. The 365 nm peak did not change after adding of $MgCl_2$ (2.5 mM) and $MnCl_2$ (2 mM).

4.3.3 4-Se-UTP RNA incorporation

There were some problems using common T7 RNA polymerization condition to insert 4-Se-UTP into RNA, like stability of 4-Se-UTP in the transcription buffer and low yield of 4-Se-U-RNA. Based on previous UV stability experiment results, the pH of the transcription buffer was adjusted from 7.9 to 7.0

to improve the stability of 4-Se-UTP. Mn^{2+} could give T7 RNA polymerase more flexibility on substrate choice, therefore, Mg^{2+} concentration was decreased to 2.5 mM and the best Mn^{2+} concentration was determined by screening experiment (Figure4.7). The Mn^{2+} enhanced both UTP and 4-Se-UTP RNA transcription. The maximum yield for RNA transcribed by either UTP or 4-Se-UTP was generated in 1.5-2.0 mM Mn^{2+} range. The kinetic curves for 4-Se-UTP incorporation into RNA compared with UTP were done with the best Mn^{2+} concentration (2 mM) (Figure 4.8). The incorporation rate of UTP over 4-Se-UTP by T7 RNA polymerase was 3/1.8 (Figure 4.8.C). UTP was about one fold better than 4-Se-UTP as transcription substrate. The incorporation of 4-Se-UTP into RNA still could not be confirmed by MALDI-TOF, only the oxidized full length product was observed (Figure 4.9. A and B). It was unclear at which step the oxidization happened. The possible reasons are discussed in 4.4 Discussion part.

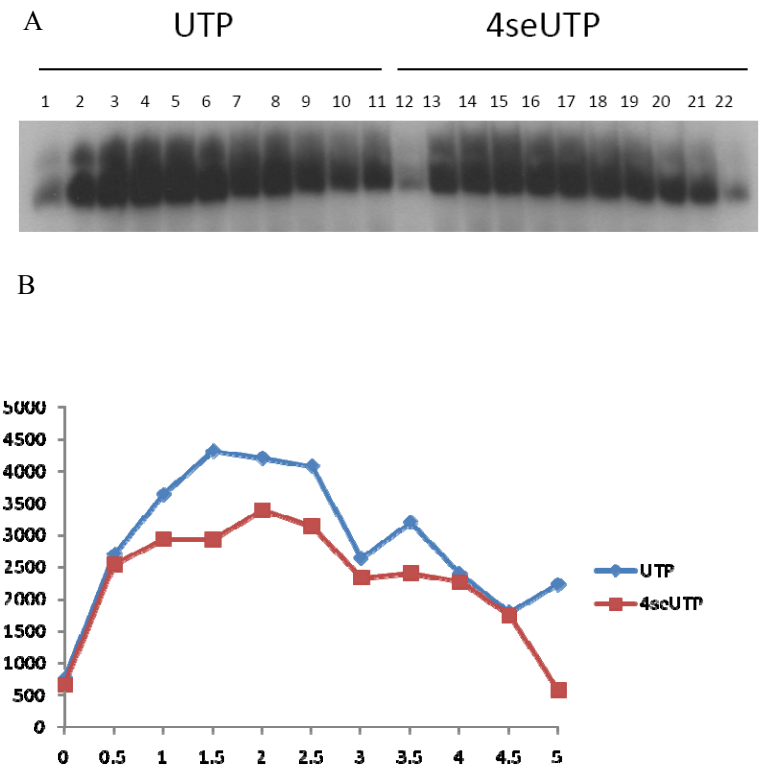

Figure 4.7 . Mn^{2+} concentration screening for the best transcription condition for 4-Se-UTP. Lane 1-11: UTP with Mn^{2+} gradient from 0 mM to 5 mM, increasing by 0.5 mM per tube. Lane 12-22: 1x 4-Se-UTP with Mn^{2+} gradient from 0 mM to 5 mM, increasing by 0.5 mM per tube. A: gel image. B: quantified data shown in curves

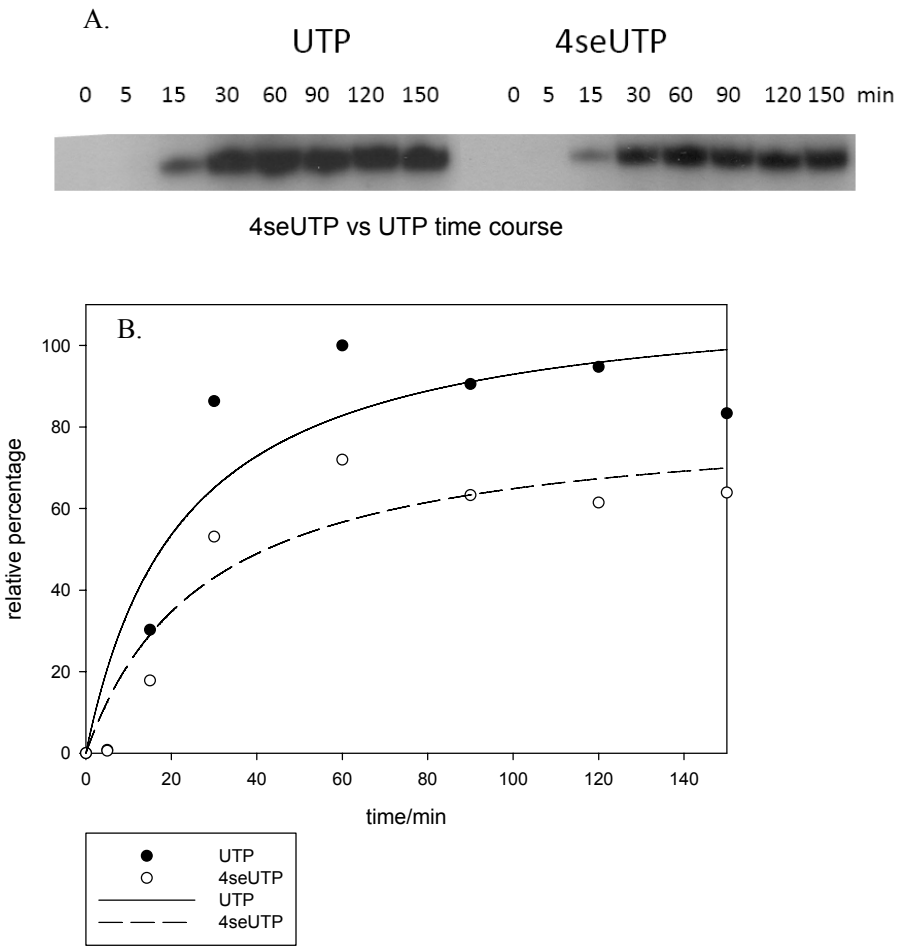

Figure 4.8. Kinetic curves for incorporation of UTP and 4-Se-UTP into RNA using 2 mM Mn^{2+} transcription condition. A: gel image. B: quantified relative intensity with curve. C: slope of the kinetic curve.

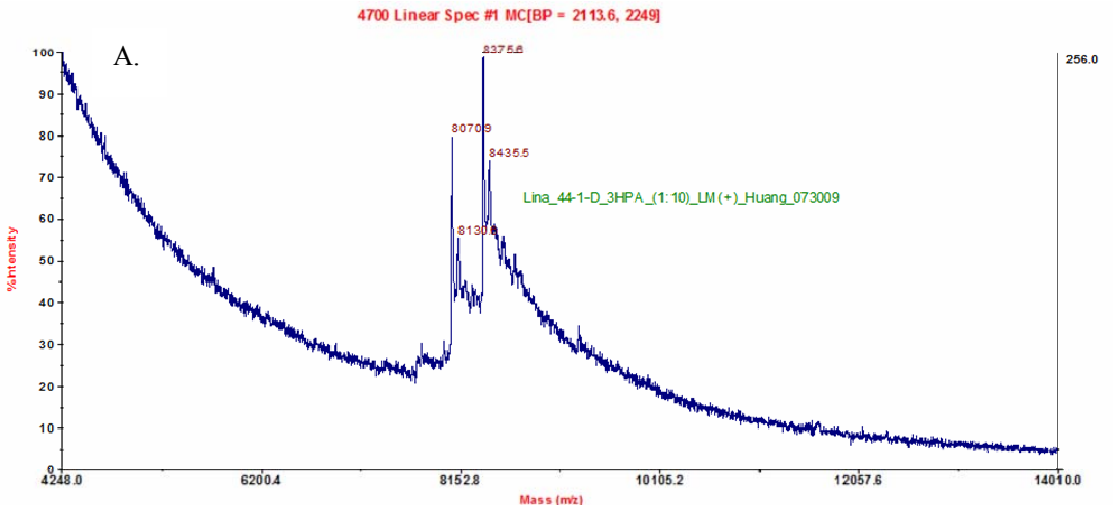

Figure 4.9.A. MALDI-TOF of native 44.1 RNA ($G_{10}A_7C_6U_1$) (calcd. [M] 8067, Observed [M] 8070)

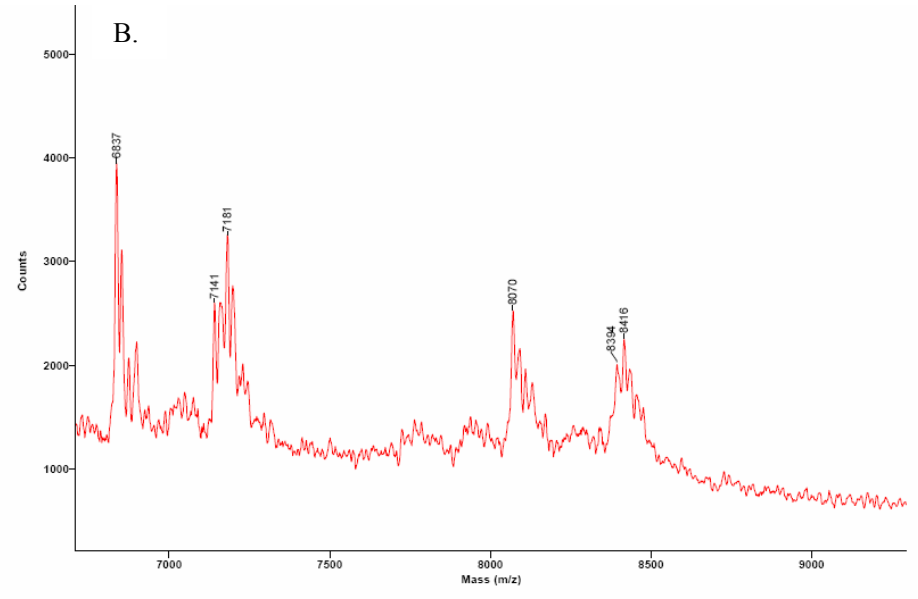

Figure 4.9.B. MALDI-TOF of 4-Se-U 44.1 RNA ($G_{10}A_7C_6U_{se1}$) (calcd. [M] 8130, Observed [M] 8070)

4.4 Discussion

Colored DNA/RNA could have many applications, such as biotechnology research tools and diagnostic tools. Incorporation of 4-Se-thymidine or 4-Se-uridine into nucleic acid through solid phase synthesis has proved to be successful. The incorporation of 4-Se-UTP into RNA through enzymatic reaction is still a problem; because the environments of organic synthesis and enzymatic reaction buffer system are totally different.

It was suspected that the stability of 4-Se-UTP was related to the presence of cation ions and DTT (research results from other lab member, which are not included in this dissertation. These studies showed that selenium modification in 4 position of the base was not very stable in the presence of some divalent ions. Divalent ions can chelate with selenium and result in dimerization and oxidization of the 4-Se-nucleoside.) The dimerized substrate most likely would not be accepted by T7 RNA polymerase. However, DTT and the divalent ions (either Mg^{2+} or Mn^{2+}) have to be used in the transcription buffer to keep RNA polymerase activity. The instability of 4-Se-UTP may answer the question why no mass spectrum result for 4-Se-RNA has been observed. Unlike the highly sensitive radioactive labeling, to prepare mass spectrum sample, a relatively higher quantity of 4-Se-RNA sample needs be prepared and then purified. If the substrate was dimerized, the yield of RNA transcription will be very low and make it very difficult to purify.

Although it was exciting to discover the hydrogen bond in the crystal structure of 4-Se-thymidine synthesized by solid phase synthesizer,[80] it is quite

challenging to put 4-Se-UTP into RNA through enzymatic incorporation. Further investigation is needed for using 4-SeUTP for X-ray Crystallography purposes. The stability of selenium on nucleic acids is an important factor on choosing the right selenium derivatization for nucleic acid X-ray crystallography. Due to stability issue, other sites of UTP, like 2 position on the base, probably are better choices for base selenium modification of uridine for X-ray crystallography.

5. FACILE SYNTHESIS AND ANTI-TUMOR CELL ACTIVITY OF SE-CONTAINING NUCLEOSIDES

(This work has been published on Nucleosides, Nucleotides and Nucleic Acids, 2009, 28 (1): 56-66, Jia Sheng Razin K.Momin, and Zhen Huang are listed as co-authors.)

5.1 Introduction

Due to the recent discovery that selenium is an essential trace element,[60, 121-122] tremendous attention has been paid to the selenium research, including chemical, biochemical, and biological investigations.[56, 122-124] Though selenium is the most noticeable for its antioxidant properties,[123] the biological activities of selenium are not just limited to its antioxidant abilities. The extensive research results have indicated an inverse relationship between the selenium level in body and the abnormalities of HIV and HPV infection, cardiomyopathy, rheumatoid arthritis, and asthma,[125-129] although most of the mechanisms are unclear. In addition, the clinic trial, conducted by Clark and coworkers using the selenium-enriched yeast, revealed approximately 50% reduction of the occurrence and re-occurrence of many types of cancers.[49, 122, 130] Though selenium can be accessed from a variety of food sources,[131] such as broccoli, Brazil nut, and garlic,[132] Se-containing compounds have also been used as the supplements for people with infectious diseases, such as tuberculosis or AIDS,[133-135] as these diseases usually coincide with nutritional deficiencies.

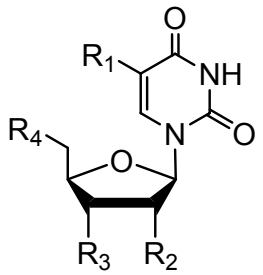

1: R_1= H, R_2= MeSe-, R_3= OH, R_4= OH
2: R_1= CH_3, R_2= H, R_3= MeSe-, R_4= OH
3: R_1= CH_3, R_2= H, R_3= OH, R_4= MeSe-

Figure 5.1. Se-modified nucleosides.

Selenium level in the body is basically dependent on its absorption,[136-137] though the amount of selenium in diet also plays a role. The form and oxidative state of selenium in diet can also significantly affect its absorption and activity.[138-139] Various selenium compounds, in both inorganic and organic forms, have been reported to have biological activities.[60, 140] For instance, selenite and selenomethionine are the most commonly used Se-containing compounds in the experimental and clinic studies.[122] Development of Se-containing organic compounds that can be used as micronutrient supplements is an important approach to improve the disease prevention and treatment. Considering the toxicity and absorption, it is better to synthesize organic seleno-compounds in the forms of the naturally occurring products and the derivatives. Furthermore, Ip and coworkers have demonstrated that methylselenol is an active metabolite of the Se-containing compounds, such as methylselenocysteine and seleno-methionine.[60, 141-143] Methylselenol, offering the high anticancer activity, can be generated via in vivo reduction of the methylseleno-containing compounds.[57, 142] Therefore, the organic compounds containing methylseleno (MeSe) functionality are potential agents for anticancer application and chemoprevention.[142]

It has been well-demonstrated that selenomethionine, containing MeSe functionality, is better absorbed and retained in body than inorganic selenite.[139] Though selenomethionine is commonly used as a food additive and Se-carrier, its cytotoxicity is relatively high.[144] In addition to the Se-amino acids, it was shown that several selenonucleobases and 8- seleno-cGMPs had anticancer activities,[145-146] and that many natural tRNAs contain selenium-modified nucleosides.[61, 147] Recently, our research group has pioneered and developed selenium-derivatized nucleic acids (SeNA) for function and x-ray crystal structure studies.[20, 69-70, 79-80] Therefore, by taking advantage of our experiences in selenium chemistry, we have designed and synthesized novel nucleosides derivatized with MeSe functionality at various positions (Figure 5.1) in order to evaluate the MeSe effect and to develop better Se-carriers for anticancer application and chemoprevention. We describe here the simple synthesis of the new 3'-MeSe-thymidine nucleoside and the other uridine and thymidine derivatives modified with MeSe at the 2'and 5' positions, and report their activity against prostate tumor cell lines.

5.2 Material and method

5.2.1 Synthesis of MeSe-nucleosides

Most solvents and reagents were purchased and used without purification unless mentioned otherwise. Pyridine was dried over KOH (s) and distilled under argon. When necessary, solid reagents were dried under high vacuum. Reactions with compounds sensitive to air or moisture were performed under argon.

Solvent mixtures are indicated as volume/volume ratios. Thin layer chromatography (TLC) was run on Merck 60 F254 plates (0.25 mm thick; Rf values in the text are for the title products), and visualized under UV-light or by a Ce-Mo staining solution (phosphomolybdate, 25 g; $Ce(SO_4)2.4H_2O$, 10 g; H_2SO_4, 60 mL, conc.; H_2O, 940 mL) with heating. Preparative TLC was performed using Merck 60 F254 pre-coated plates (2 mm thick). Flash chromatography was performed using Fluka silica gel 60 (mesh size 0.040–0.063 mm) using a silica gel:crude compound weight ratio of ca. 30:1. ^{1}H and ^{13}C-NMR spectra were recorded usingBruker-300 or 400 (300 or 400 MHz). All chemical shifts (δ) are in ppm relative to tetramethylsilane and all coupling constants (J) are in Hz.

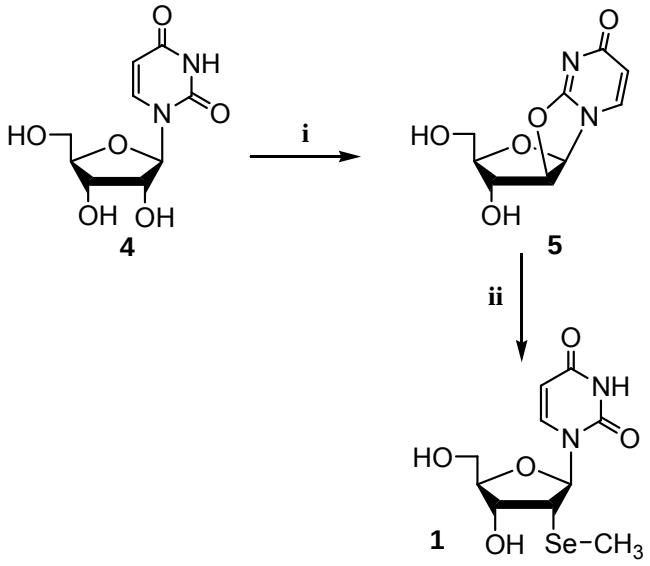

Figure 5.2. Synthesis of 2'-MeSe-uridine (**1**). Reagents and conditions: (i) diphenyl carbonate and $NaHCO_3$ in DMF, heated at 120 ^{o}C for 2 hr; (ii) dimethyl diselenide and $NaBH_4$ in EtOH:MeOH (8:1), heated at 50^{o}C for 3-4 hr.

2'-methylseleno-2'-deoxyuridine (1). Uridine (4.17 g, 17.1 mmol) and diphenyl

carbonate (4.0 g, 18.7 mmol) were placed in a round-bottom flask, and N,N-dimethylformamide (5.0 mL) was added. The slurry was heated in an oil bath at 100◦C. Dry sodium bicarbonate (33 mg) was then added, and a watch glass was used to cover the flask. The reaction mixture was heated at 120–130 ◦C for 1 hour while being monitored on TLC (methanol/methylene chloride, 2:8). After completion, the reaction was cooled to room temperature. The precipitated product was filtered and washed by cold methanol three times (each time 1.5 mL). The white powdered product (**5**) was dried on high vacuum overnight. (3.31 g, 86%). Compound [**5**, 2,2'-O-anhydro-1-(*β*-D-arabinofuranosyl)-uracil]: ^{1}HNMR (d6-DMSO) *δ* (ppm): 3.11–3.23 (m, 2H, H-5'), 3.97–4.11 (m, 1H,H-4'), 4.25–4.41 (m, 1H, H-3'), 4.91 (m, HO), 5.18 (d, J = 5.8 Hz, 1H, H-2'), 5.81 (m, HO), 5.96 (d, J = 7.5 Hz, 1H, H-5), 6.22 (d, J = 5.8 Hz,1H, H-1'), 7.78 (d, J = 7.5 Hz, 1H, H-6). ^{1}H-NMR spectrum is consistent with the literature.[38,39] A suspension of sodium borohydride (148 mg) in ethanol (1 mL) was added drop wisely to dimethyldiselenide (0.33 g, 1.75 mmol) dissolved in ethanol (3 mL) under argon. After the yellow solution turned colorless and there was no more bubble formation in the reaction, the suspension of 2, 2'-anhydrouridine (**5**, 200 mg, 0.88 mmol) in ethanol (4 mL) was added slowly, followed by addition of methanol (2 mL). The reaction was heated at 50 ◦C for 3–4 hours before it was completed (monitored by TLC, 10% MeOH in CH_2Cl_2). After evaporating all solvents, the crude product was purified by silica-gel column chromatography (7% MeOH in CH_2Cl_2). Pure product (258.5 mg, 91%) was obtained. Compound **1**: ^{1}H-NMR (MeOD, 400 MHz): *δ* 1.99 (s, 3H, 2'-Se-CH_3), 3.18–3.55 (m, 1H, 2'-H), 3.74–3.83

(m, 2H, 5'-H), 4.03–4.06 (m, 1H, 3'-H), 4.35–4.37 (m, 1H, 4'-H), 5.76 (d, 1H, J = 8.1 Hz, 5-H), 6.28 (d, 1H, J = 8.4 Hz, 1'-H), 7.99 (d, 1H, J = 8.1 Hz, 6-H); ^{13}C-NMR (100 MHz, $CDCl_3$+DMSO-d6) *δ*: 8.21 (SeCH3), 53.10 (C-2'), 67.28 (C-5'), 77.46 (C-3'), 91.48 (C-4'), 94.38 (C-1'), 107.39 (C-5), 145.51 (C-6), 155.66 (C-2), 168.51 (C-4); ESI-MS: molecular formular $C_{10}H_{14}N_2O_5Se$, observed ($M+Na^+$): 344.9950 (calc. 344.9966).

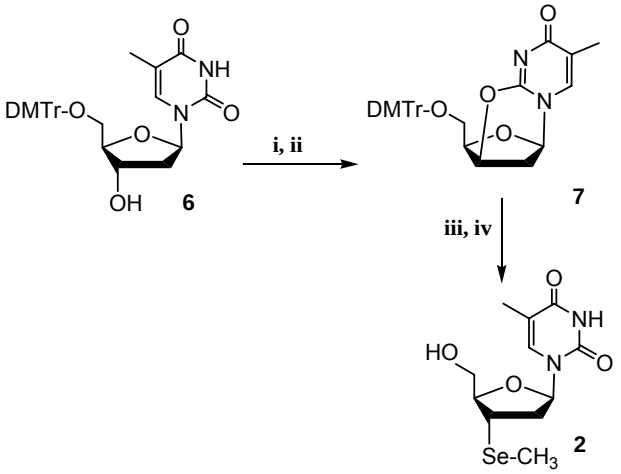

Figure 5.3. Synthesis of 3'-MeSe-thymidine (**2**). Reagents and conditions: (i) MsCl/TEA/THF, at room temperature for 30 min; (ii) dilute NaOH (aq) in EtOH, reflux for 2.5 hr; (iii) dimetheyl diselenide and $NaBH_4$ in dioxane, heated at 93 ^oC for 2 hr; (iv) 80% HOAc (aq) treatment.

3'-methylseleno-3'-deoxythymidine (2). This compound was synthesized from 5'-DMT thymidine in four steps. The first step (**I**) was mesylation of the 3' position of 5'-DMT thymidine. Without purification of the mesylate intermediate, the second step (**II**) allowed the intramolecular cyclization, thereby forming compound **7**. This cyclic compound was purified by flash chromatography. The

third step (**III**) involved the introduction of the methylseleno group at the 3' position. After the detritylation with trichloroacetic acid (**IV**), the target compound **2** was purified by chromatography. Step (**I**): After placing **6** (1.44 g, 2.69 mmol) in a round-bottom flask and drying it under high vacuum for 30 minutes, dry THF (26.4 mL) and triethylamine (1.1 mL, 7.95 mmol, 3 equiv.) were injected into the flask under argon. Methanesulfonyl chloride (247 μL, 3.18 mmol, 1.2 equiv.) was slowly injected into the flask in an ice bath and under dry argon. After stirring the reaction for 10 minutes at 0 °C, the reaction flask was placed and stirred at room temperature for 30 minutes. After monitoring the reaction by TLC to confirm its completion, methanol (1 mL) was added to quench the reaction. After evaporation of all solvents under reduced pressure, the crude product was redissolved in ethyl acetate and the salts were filtered out. The solvent was evaporated again under reduced pressure to afford the crude product.

Step (**II**): The crude product from step (**I**) was redissolved in ethanol (250 mL), and NaOH (13.75 mL, 0.2 M aqueous solution, 2.75 mmol, 1.04 eq.) was added subsequently. The reaction was completed after 2.5-hour reflux (monitored by TLC, 5% MeOH in CH_2Cl_2). The 90% solvent was evaporated under reduced pressure, and water (100 mL) was subsequently added. The crude product was then extracted with EtOAc (3 × 25 mL). The organic phases were combined and dried over anhydrous $MgSO_4$ for 20 minutes. After the filtration and solvent evaporation under reduced pressure, the crude product was purified by flash chromatography (0 to 5% methanol in CH_2Cl_2, gradient). The pure product was dried on high vacuum to afford compound **7** as a fine white powder (1.25 g, 2.42

mmol, 90% yield over two steps).

Step (**III** and **IV**): **7** (50 mg, 0.096 mmol) and $NaBH_4$ (18 mg) were dried separately on high vacuum. Dry dioxane (2.0 mL) was injected into each round bottom flask. A brown liquid of dimethyl diselenide (13 μL, 13.4 mg, 0.071 mmol, 1.5 equiv.) was carefully injected into the flask containing NaBH4. Afterward, a few drops of ethanol were injected into the same flask dropwise until bubble appeared. The reaction was kept running at room temperature for 15 minutes until the solution became colorless, followed by injecting the dioxane solution of compound **7** into this reaction. The mixture was refluxed under argon for 2 hours before its completion (monitoring by TLC). The solvent was evaporated under reduced pressure and the residue was dissolved in CH_2Cl_2 (25mL), followed by washing with brine (3 × 10 mL). The combined organic layers were dried with anhydrous $MgSO_4$, filtered and evaporated to dryness. Without further purifications, the crude product was redissolved in CH_2Cl_2 (5 mL) and treated with trichloroacetic acid (0.19 g, 1.14 mmol). The mixture was stirred (0.5–1 hour) and followed by adding several drops of CH_3CH_2SH to quench the DMTr cation. The reaction was monitored by TLC, and triethylamine was added to neutralize the acid. After evaporation of CH_2Cl_2, the crude product was purified by silica gel column chromatography using 10% methanol inmethylene chloride as eluent. The pure product (27.8 mg) was obtained with 89% yield over two steps. Compound **2**: ^{1}H-NMR ($CDCl_3$,400 MHz): δ 1.90 (s, 5 -CH_3), 2.07 (s, 3H, $SeCH_3$), 2.46–2.56 (m, 2H, 2'-H), 3.44–3.55 (m, 1H, 3'-H), 3.86–4.10 (m, 2H, 5'-H), 3.96–4.00 (m, 1H, 4'-H), 6.10 (m, 1H, 1'-H), 7.59 (s, 1H, 6-H); ^{13}C-NMR ($CDCl_3$, 100

MHz), δ 3.52 (3'-$SeCH_3$), 12.69 (5-CH_3), 32.48 (C-3'), 40.14 (C-2'), 61.18 (C-5'), 85.66 (C-1') 86.71 (C-4'), 110.82 (C-5), 136.65 (C-6), 150.48 (C-2), 164.04 (C-4); ESI-MS: molecular formular $C_{11}H_{16}N_2O_4Se$, observed ($M + Na^+$): 343.0167 (calc. 343.0173).

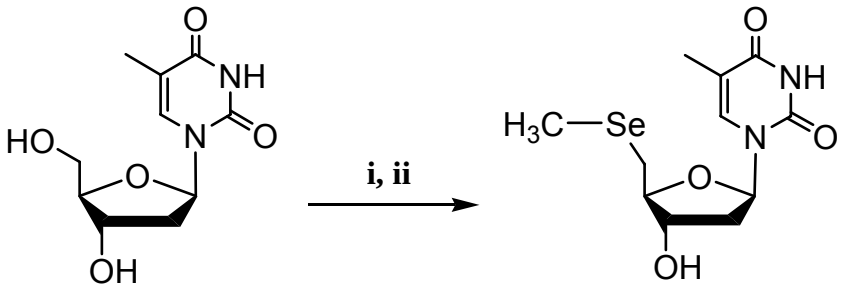

Figure 5.4 Synthesis of 5'-MeSe-thymidine (**3**). Reagents and conditions: (i) p-toluenesulfonyl chloride, DMAP, anhydrous pyridine, 22 hr; (ii) dimethyl diselenide, $NaBH_4$.

5'-methylseleno-5'-deoxythymidine (3). Step (**I**): Thymidine (60.6 mg, 0.25 mmol), p-toluenesulfonyl chloride (97.3 mg) and DMAP (2 mg) were dried under high vacuum in a 10-mL flask for 1 hour, and then dry pyridine (1.25 mL) was added into the flask under argon. The reaction mixture was stirred under argon at room temperature overnight. Step (**II**): To a round-bottom flask containing $NaBH_4$ (111 mg) under argon, ethanol (1.0 mL) was added, followed by addition of dimethyl diselenide (47.0 μL, 93 mg, 0.50 mmol). This reaction was stirred for 30 minutes in an ice-water bath and under dry argon, and the solution turned from yellow to colorless. The tosylate suspension from Step **I** was injected to the methyl selenol solution, followed by stirring at room temperature overnight. The

solvents were evaporated under reduced pressure. The crude product was purified by silica gel plate using 7% methanol in methylene chloride as the eluent. The white foamy product (53.1 mg) was obtained with 80% yield (recovered thymidine, 10.4 mg). Compound **3**: ^{1}H-NMR ($CDCl_3$, 400 MHz): δ 1.96 (s,H, 5-CH_3), 2.09 (s, 3H, 2'-$SeCH_3$), 2.26–2.33 (m, 2H, 2'-H), 2.79–2.96 (m,2H, 5'-H), 4.05–4.10 (m, 1H, 3'-H), 4.38–4.45 (m, 1H, 4'-H), 6.26 (t, 1H,J = 6.7 Hz, 1'-H), 7.29 (s, 1H, 6-H), 8.13–8.18 (br, 1H, NH, exchangeable in D_2O); ^{13}C-NMR ($CDCl_3$, 100 MHz): δ 5.63 (2'-$SeCH_3$), 12.46 (5-CH_3),27.69 (C-2'), 40.04 (C-5'), 73.39 (C-3'), 84.52 (C-4'), 85.21 (C-1'), 111.19 (C-5), 135.64 (C-6), 150.57 (C-2), 164.15 (C-4); ESI-MS: molecular formular $C_{11}H_{16}N_2O_4Se$, observed $(M-H)^-$: 319.0194 (calc. 319.0197).

5.2.2 Anti-prostate tumor cell assays.

Approximately 100,000 cells of each tumor cell line were plated onto six-well plates in duplicate and allowed 24 hours to adhere. Old media was aspirated and the fresh media (2 mL, containing various concentrations (1.0, 10, 100, 1000, 10,000 nM) of compound **1**, **2**, or **3**) was added. A control group with no additives was also prepared. These plates were incubated at 37 ^{o}C in an environment containing 5% CO_2. After 96-hour incubation, the cells were trypsinized and counted. For each test sample with a Se-nucleoside, the number of live cells was normalized to that of the control group and plotted against the concentration of the Se-nucleoside. IC_{50} values of cell growth inhibition were determined by least squares curve fitting.

5.3 Result and Discussion

5.3.1. Synthesis of MeSe-nucleosides

Table 5.1: Synthesized MeSe-nucleosides (1-3)

Compound	R_1	R_2	R_3	R_4	Yield%
1	-H	$-SeCH_3$	-OH	-OH	78[a]
2	$-CH_3$	-H	$-SeCH_3$	-OH	81[a]
3	$-CH_3$	-H	-OH	$-SeCH_3$	80[a]

[a]overall yield.

In this work, we have developed convenient synthetic routes for synthesis of the new 3'-MeSe-thymidine nucleoside and the other uridine and thymidine derivatives modified with MeSe at the 2' and 5' positions, and their overall synthetic yields are high (MeSe-nucleosides, **1–3**; Table 5.1).The synthetic route for 2'-methylseleno-2'-deoxyuridine (**1**) is shown in Figure 5.2. After converting uridine (**4**) to 2,2'-anhydrouridine (**5**) using diphenyl carbonate in hot DMF,[38,39] we normally protected the 5'-OH of **5** to increase the anhydrouridine solubility for the MeSe incorporation, followed by removal of the 5'-protection. In order to avoid the 5' protection and deprotection steps, we explored several conditions, including hot alcohol solvent, to increase the solubility of 2,2'-anhydrouridine while controlling the reaction regioselectivity at the 2'-*α*-position instead of the 2-position. Without the formation of the 2-MeSe-uridine isomer, methylselenol formed by reduction of dimethyl diselenide with $NaBH_4$ was incorporated, in high yield, into the anhydrouridine (**5**) at the 2' *α*-position under the elevated temperature. Thus, the target compound (**1**) was conveniently synthesized in two steps (78% overall yield). Because of the successful MeSe incorporation to the 2'

position of 2, 2'-anhydrouridine without the 5'-protection, we planned to use the similar strategy to introduce MeSe functionality to the 3'-position of the 2, 2'-anhydrothymidine (**7**).

We started the synthesis of 3'-methylseleno-3'-deoxythymidine (**2**) from the partially protected thymidine, 5'-DMTrthymidine (**6**; Figure 5.3). After activating the 3'-hydroxyl group of **6** through a quantitative mesylation reaction, the mesylate intermediate (without purification) was converted to the 2, 3'-anhydrothymidine derivative (**7**) under reflux in ethanol solvent. This intramolecular cyclization was almost quantitative when a low concentration of the mesylate intermediate (10 mM) was used in the presence of dilute NaOH (10.4 mM). Via the intramolecular SN_2 substitution, the *α*-3'-mesyl group was displaced by the 2-oxide formed under the basic condition to give 2, 3'-anhydrothymidine (**7**). Under higher concentrations of the mesylate or NaOH, many by-products were formed probably due to the 3', 2'- or 3', 4'-mesylate elimination. After purification of the generated 2, 3'-anhydrothymidine (**7**), thymidine was functionized with MeSe functionality using a procedure analogous to the synthesis of 2'-MeSe-U (**1**). Due to the higher stability of 2,3'-anhydrothymidine, which has much less ring strain comparing with 2,2'-anhydrouridine, higher reaction temperature was required to allow successful incorporation of the methylseleno functionality. Without the formation of the 2-MeSe-thymidine isomer, MeSe functionality was almost quantitatively introduced to the 3'-*α*-position of **7**. Without further purification of this Se-containing

intermediate, its 5'-dimethoxytrityl group was quantitatively removed by 80% acetic acid, offering the target compound (**2**) with 81% overall yield (four steps).

5'-Methylseleno-5'-deoxythymidine (**3**) was synthesized, in the pyridineethanol mixed solution, through a two-step reaction shown in Figure 5.4. Since it is possible to differentiate the primary and secondary hydroxyl groups, we used p-toluenesulfonyl chloride to selectively activate the 5' position in pyridine. The 5' p-toluenesulfonyl group, a good leaving group, was displaced by methylselenol via a SN_2 substitution, thereby generating target compound **3** (80% yield in two steps).

5.3.2. Anti-Prostate Tumor Cell Evaluation

Table 5.2 Inhibition results of tumor cell growth by compound 1-3

Tumor cell lines	IC_{50} of cell growth inhibition and average cell death (ACD) at the Se-nucleoside concentration (10 μM)	1	2	3	Control ACD (%) (no Se-nucleosides)
DU145	IC_{50} (nM)	25	22	15	3.2
	ACD (%)	3.9	3.4	2.6	
CWR22	IC_{50} (nM)	63	58	25	4.6
	ACD (%)	3.6	2.1	3.7	
PC3	IC_{50} (nM)	76	21	15	5.0
	ACD (%)	6.9	7.4	7.4	
LNCaP	IC_{50} (nM)	200	150	50	1.8
	ACD (%)	2.1	1.1	2.2	

Compounds **1–3**, with relatively good solubility in aqueous solution, were screened for their anticancer activity against prostate cancer cell lines (DU145, CWR22, PC3, and LNCaP). We found that these MeSe-nucleosides have anticancer effects and can generally inhibit cancer cell growth. Their IC_{50} values

for the cell growth inhibition and the average cell death caused by these nucleosides at 10 μM concentration are shown in Table 5.2. Their IC_{50} values against these prostate cancer cells varied from 15 to 200 nM. Our experimental results indicated that 5'-Se-thymidine (**3**) is generally more active than the other 2' and 3' Se-nucleosides against these prostate cancer cell lines. It is probably easier to metabolize the Se-nucleoside containing the primary MeSe than the secondary MeSe, thereby generating more methylselenol from **3**. It was observed that the inhibition of the tumor cell growth was proportional to the concentrations of these MSe-nucleosides.

PUBLICATIONS AND MANUSCRIPTS IN PREPARATION

1. Lina Lin, Andres M. Patino, Jia Sheng, Jaya Punetha, Jullianne Caton-Williams and Zhen Huang. “Simple Synthesis and Characterizations of Nucleoside 5’-(alpha-P-seleno) triphosphates Diastereomers and Its Incorporation into RNA”. (2010). *Manuscript in preparation.*

2. Lina Lin, Jia Sheng, Abdur Rob and Zhen Huang, “Chemical Biology of Natural and Unnatural Selenium-Containing Nucleic Acids, Proteins and Small Molecules”, (2010) review. *Manuscript in preparation.*

3. Sarah M. Spencer, **Lina Lin**, Chenfeng Jian, Zhengchun Peng, Peter Hesketh and Zhen Huang, “RNA Microchip for Rapid, Direct and Specific Detection of Biological RNA”. (2010) *Manuscript in preparation.*

4. Jozef Salon, Julianne Caton-Williams, **Lina Lin** and Zhen Huang, “UV-damage Resistant DNAs and Plasmids Containing TT Dimer Modified by 4-Se-Thymidine”. (2010). *Manuscript in preparation.*

5. Lina Lin, Jia Sheng Razin K.Momin, Zhen Huang, “Facile synthesis and anti-tumor cell activity of se-containing nucleosides”. (2009) Nucleosides, Nucleotides and Nucleic Acids. Volume 28. Issue 1, page 56-66.

APPENDIX: Natrix (Nucleic acid sparse matrix screen)

Tube #	Salt	Buffer ◊	Precipitant
1.	0.01 M Magnesium chloride hexahydrate	0.05 M MES monohydrate pH 5.6	1.8 M Lithium sulfate monohydrate
2.	0.01 M Magnesium acetate tetrahydrate	0.05 M MES monohydrate pH 5.6	2.5 M Ammonium sulfate
3.	0.1 M Magnesium acetate tetrahydrate	0.05 M MES monohydrate pH 5.6	20% v/v (+/-)-2-Methyl-2,4-pentanediol
4.	0.2 M Potassium chloride, 0.01 M Magnesium sulfate heptahydrate	0.05 M MES monohydrate pH 5.6	10% v/v Polyethylene glycol 400
5.	0.2 M Potassium chloride, 0.01 M Magnesium chloride hexahydrate	0.05 M MES monohydrate pH 5.6	5% w/v Polyethylene glycol 8,000
6.	0.1 M Ammonium sulfate, 0.01 M Magnesium chloride hexahydrate	0.05 M MES monohydrate pH 5.6	20% w/v Polyethylene glycol 8,000
7.	0.02 M Magnesium chloride hexahydrate	0.05 M MES monohydrate pH 6.0	15% v/v 2-Propanol
8.	0.1 M Ammonium acetate, 0.005 M Magnesium sulfate heptahydrate	0.05 M MES monohydrate pH 6.0	0.6 M Sodium chloride
9.	0.1 M Potassium chloride, 0.01 M Magnesium chloride hexahydrate	0.05 M MES monohydrate pH 6.0	10% v/v Polyethylene glycol 400
10.	0.005 M Magnesium sulfate heptahydrate	0.05 M MES monohydrate pH 6.0	5% w/v Polyethylene glycol 4,000
11.	0.01 M Magnesium chloride hexahydrate	0.05 M Sodium cacodylate trihydrate pH 6.0	1.0 M Lithium sulfate monohydrate
12.	0.01 M Magnesium sulfate heptahydrate	0.05 M Sodium cacodylate trihydrate pH 6.0	1.8 M Lithium sulfate monohydrate
13.	0.015 M Magnesium acetate tetrahydrate	0.05 M Sodium cacodylate trihydrate pH 6.0	1.7 M Ammonium sulfate
14.	0.1 M Potassium chloride, 0.025 M Magnesium chloride hexahydrate	0.05 M Sodium cacodylate trihydrate pH 6.0	15% v/v 2-Propanol
15.	0.04 M Magnesium chloride hexahydrate	0.05 M Sodium cacodylate trihydrate pH 6.0	5% v/v (+/-)-2-Methyl-2,4-pentanediol
16.	0.04 M Magnesium acetate tetrahydrate	0.05 M Sodium cacodylate trihydrate pH 6.0	30% v/v (+/-)-2-Methyl-2,4-pentanediol
17.	0.2 M Potassium chloride, 0.01 M Calcium chloride dihydrate	0.05 M Sodium cacodylate trihydrate pH 6.0	10% w/v Polyethylene glycol 4,000
18.	0.01 M Magnesium acetate tetrahydrate	0.05 M Sodium cacodylate trihydrate pH 6.5	1.3 M Lithium sulfate monohydrate
19.	0.01 M Magnesium sulfate heptahydrate	0.05 M Sodium cacodylate trihydrate pH 6.5	2.0 M Ammonium sulfate
20.	0.1 M Ammonium acetate, 0.015 M Magnesium acetate tetrahydrate	0.05 M Sodium cacodylate trihydrate pH 6.5	10% v/v 2-Propanol
21.	0.2 M Potassium chloride, 0.005 M Magnesium chloride hexahydrate	0.05 M Sodium cacodylate trihydrate pH 6.5	0.9 M 1,6-Hexanediol
22.	0.08 M Magnesium acetate tetrahydrate	0.05 M Sodium cacodylate trihydrate pH 6.5	15% v/v Polyethylene glycol 400
23.	0.2 M Potassium chloride, 0.01 Magnesium chloride hexahydrate	0.05 M Sodium cacodylate trihydrate pH 6.5	10% w/v Polyethylene glycol 4,000
24.	0.2 M Ammonium acetate, 0.01 M Calcium chloride dihydrate	0.05 M Sodium cacodylate trihydrate pH 6.5	10% w/v Polyethylene glycol 4,000
25.	0.08 M Magnesium acetate tetrahydrate	0.05 M Sodium cacodylate trihydrate pH 6.5	30% w/v Polyethylene glycol 4,000
26.	0.2 M Potassium chloride, 0.1 M Magnesium acetate tetrahydrate	0.05 M Sodium cacodylate trihydrate pH 6.5	10% w/v Polyethylene glycol 8,000
27.	0.2 M Ammonium acetate, 0.01 M Magnesium acetate tetrahydrate	0.05 M Sodium cacodylate trihydrate pH 6.5	30% w/v Polyethylene glycol 8,000
28.	0.05 M Magnesium sulfate hydrate	0.05 M HEPES sodium pH 7.0	1.6 M Lithium sulfate monohydrate
29.	0.01 M Magnesium chloride hexahydrate	0.05 M HEPES sodium pH 7.0	4.0 M Lithium chloride
30.	0.01 M Magnesium chloride hexahydrate	0.05 M HEPES sodium pH 7.0	1.6 M Ammonium sulfate
31.	0.005 M Magnesium chloride hexahydrate	0.05 M HEPES sodium pH 7.0	25% v/v Polyethylene glycol monomethyl ether 550
32.	0.2 M Potassium chloride, 0.01 M Magnesium chloride hexahydrate	0.05 M HEPES sodium pH 7.0	1.7 M 1,6-Hexanediol
33.	0.2 M Ammonium chloride, 0.01 M Magnesium chloride hexahydrate	0.05 M HEPES sodium pH 7.0	2.5 M 1,6-Hexanediol
34.	0.1 M Potassium chloride, 0.005 M Magnesium sulfate hydrate	0.05 M HEPES sodium pH 7.0	15% v/v (+/-)-2-Methyl-2,4-pentanediol
35.	0.1 M Potassium chloride, 0.01 M Magnesium chloride hexahydrate	0.05 M HEPES sodium pH 7.0	5% v/v Polyethylene glycol 400
36.	0.1 M Potassium chloride, 0.01 M Calcium chloride dihydrate	0.05 M HEPES sodium pH 7.0	10% v/v Polyethylene glycol 400
37.	0.2 M Potassium chloride, 0.025 M Magnesium sulfate hydrate	0.05 M HEPES sodium pH 7.0	20% v/v Polyethylene glycol 200
38.	0.2 M Ammonium acetate, 0.15 M Magnesium acetate tetrahydrate	0.05 M HEPES sodium pH 7.0	5% w/v Polyethylene glycol 4,000
39.	0.1 M Ammonium acetate, 0.02 M Magnesium chloride hexahydrate	0.05 M HEPES sodium pH 7.0	5% w/v Polyethylene glycol 8,000
40.	0.01 M Magnesium chloride hexahydrate	0.05 M TRIS hydrochloride pH 7.5	1.6 M Ammonium sulfate
41.	0.1 M Potassium chloride, 0.015 M Magnesium chloride hexahydrate	0.05 M TRIS hydrochloride pH 7.5	10% v/v Polyethylene glycol monomethyl ether 550
42.	0.01 M Magnesium chloride hexahydrate	0.05 M TRIS hydrochloride pH 7.5	5% v/v 2-Propanol
43.	0.05 M Ammonium acetate, 0.01 M Magnesium chloride hexahydrate	0.05 M TRIS hydrochloride pH 7.5	10% v/v (+/-)-2-Methyl-2,4-pentanediol
44.	0.2 M Potassium chloride, 0.05 M Magnesium chloride hexahydrate	0.05 M TRIS hydrochloride pH 7.5	10% w/v Polyethylene glycol 4,000
45.	0.025 M Magnesium sulfate hydrate	0.05 M TRIS hydrochloride pH 8.5	1.8 M Ammonium sulfate
46.	0.005 M Magnesium sulfate hydrate	0.05 M TRIS hydrochloride pH 8.5	2.9 M 1,6-Hexanediol
47.	0.1 M Potassium chloride, 0.01 M Magnesium chloride hexahydrate	0.05 M TRIS hydrochloride pH 8.5	30% v/v Polyethylene glycol 400
48.	0.2 M Ammonium chloride, 0.01 M Calcium chloride dihydrate	0.05 M TRIS hydrochloride pH 8.5	30% w/v Polyethylene glycol 4,000

REFERENCES

1. Rich, A., *The era of RNA awakening: structural biology of RNA in the early years.* Q Rev Biophys, 2009. **42**(2): p. 117-37.
2. Lee, R.C., R.L. Feinbaum, and V. Ambros, *The C. elegans heterochronic gene lin-4 encodes small RNAs with antisense complementarity to lin-14.* Cell, 1993. **75**(5): p. 843-54.
3. Gelfand, M.S., et al., *A conserved RNA structure element involved in the regulation of bacterial riboflavin synthesis genes.* Trends Genet, 1999. **15**(11): p. 439-42.
4. Boyd, S.D., *Everything you wanted to know about small RNA but were afraid to ask.* Lab Invest, 2008. **88**(6): p. 569-78.
5. Filipowicz, W., S.N. Bhattacharyya, and N. Sonenberg, *Mechanisms of post-transcriptional regulation by microRNAs: are the answers in sight?* Nat Rev Genet, 2008. **9**(2): p. 102-14.
6. Scott, W.G., M. Martick, and Y.I. Chi, *Structure and function of regulatory RNA elements: ribozymes that regulate gene expression.* Biochim Biophys Acta, 2009. **1789**(9-10): p. 634-41.
7. Pley, H.W., K.M. Flaherty, and D.B. McKay, *Three-dimensional structure of a hammerhead ribozyme.* Nature, 1994. **372**(6501): p. 68-74.
8. Cate, J.H., et al., *Crystal structure of a group I ribozyme domain: principles of RNA packing.* Science, 1996. **273**(5282): p. 1678-85.
9. Ferre-D'Amare, A.R., K. Zhou, and J.A. Doudna, *Crystal structure of a hepatitis delta virus ribozyme.* Nature, 1998. **395**(6702): p. 567-74.

10. Ban, N., et al., *The complete atomic structure of the large ribosomal subunit at 2.4 A resolution.* Science, 2000. **289**(5481): p. 905-20.

11. Kieft, J.S., et al., *The hepatitis C virus internal ribosome entry site adopts an ion-dependent tertiary fold.* J Mol Biol, 1999. **292**(3): p. 513-29.

12. Batey, R.T., S.D. Gilbert, and R.K. Montange, *Structure of a natural guanine-responsive riboswitch complexed with the metabolite hypoxanthine.* Nature, 2004. **432**(7015): p. 411-5.

13. Ke, A. and J.A. Doudna, *Crystallization of RNA and RNA-protein complexes.* Methods, 2004. **34**(3): p. 408-14.

14. Campbell, N.H. and G.N. Parkinson, *Crystallographic studies of quadruplex nucleic acids.* Methods, 2007. **43**(4): p. 252-63.

15. Taylor, G., *The phase problem.* Acta Crystallogr D Biol Crystallogr, 2003. **59**(Pt 11): p. 1881-90.

16. Hendrickson, W.A., *Determination of macromolecular structures from anomalous diffraction of synchrotron radiation.* Science, 1991. **254**(5028): p. 51-8.

17. Messerchmidt, A., *X-ray Crystallography of Biomicromolecules: A Practical guide*. 2007, Weinheim: Wiley-VCH Verlag GmbH & co. KGaA.

18. LV, G. and Z. Hua, *Fundamentals of Biomicromolecules X-ray Crystallography*. Second ed. 2006: Peking University Press.

19. Deacon, A.M. and S.E. Ealick, *Selenium-based MAD phasing: setting the sites on larger structures.* Structure, 1999. **7**(7): p. R161-6.

20. Jiang, J., et al., *Selenium derivatization of nucleic acids for crystallography.*

Nucleic Acids Res, 2007. **35**(2): p. 477-85.

21. Boosalis, M.G., *The role of selenium in chronic disease.* Nutr Clin Pract, 2008. **23**(2): p. 152-60.
22. Ealick, S.E., *Advances in multiple wavelength anomalous diffraction crystallography.* Curr Opin Chem Biol, 2000. **4**(5): p. 495-9.
23. Rupert, P.B. and A.R. Ferre-D'Amare, *Crystal structure of a hairpin ribozyme-inhibitor complex with implications for catalysis.* Nature, 2001. **410**(6830): p. 780-6.
24. Egli, M., *Nucleic acid crystallography: current progress.* Curr Opin Chem Biol, 2004. **8**(6): p. 580-91.
25. Olieric, V., et al., *A fast selenium derivatization strategy for crystallization and phasing of RNA structures.* Rna, 2009. **15**(4): p. 707-15.
26. Teplova, M., et al., *Covalent incorporation of selenium into oligonucleotides for X-ray crystal structure determination via MAD: proof of principle. Multiwavelength anomalous dispersion.* Biochimie, 2002. **84**(9): p. 849-58.
27. Wilds, C.J., et al., *Selenium-assisted nucleic acid crystallography: use of phosphoroselenoates for MAD phasing of a DNA structure.* J.Am.Chem.Soc., 2002. **124**(50): p. 14910-14916.
28. Mooers, B.H., *Crystallographic studies of DNA and RNA.* Methods, 2009. **47**(3): p. 168-76.
29. Srivatsan, S.G. and Y. Tor, *Enzymatic incorporation of emissive pyrimidine ribonucleotides.* Chem Asian J, 2009. **4**(3): p. 419-27.

30. Steitz, T.A., *Visualizing polynucleotide polymerase machines at work.* Embo J, 2006. **25**(15): p. 3458-68.

31. Castro, C., et al., *Two proton transfers in the transition state for nucleotidyl transfer catalyzed by RNA- and DNA-dependent RNA and DNA polymerases.* Proc Natl Acad Sci U S A, 2007. **104**(11): p. 4267-72.

32. Yang, W., *An equivalent metal ion in one- and two-metal-ion catalysis.* Nat Struct Mol Biol, 2008. **15**(11): p. 1228-31.

33. Thommes, P. and U. Hubscher, *Eukaryotic DNA replication. Enzymes and proteins acting at the fork.* Eur J Biochem, 1990. **194**(3): p. 699-712.

34. Ji, X., *The mechanism of RNase III action: how dicer dices.* Curr Top Microbiol Immunol, 2008. **320**: p. 99-116.

35. Nichols, N.M. and D. Yue, *Ribonucleases.* Curr Protoc Mol Biol, 2008. **Chapter 3**: p. Unit3 13.

36. Nowotny, M. and W. Yang, *Stepwise analyses of metal ions in RNase H catalysis from substrate destabilization to product release.* Embo J, 2006. **25**(9): p. 1924-33.

37. Braasch, D.A., et al., *RNA interference in mammalian cells by chemically-modified RNA.* Biochemistry, 2003. **42**(26): p. 7967-75.

38. Brandt, G., N. Carrasco, and Z. Huang, *Efficient substrate cleavage catalyzed by hammerhead ribozymes derivatized with selenium for X-ray crystallography.* Biochemistry, 2006. **45**(29): p. 8972-7.

39. Doherty, E.A. and J.A. Doudna, *Ribozyme structures and mechanisms.* Annu Rev Biochem, 2000. **69**: p. 597-615.

40. Martick, M. and W.G. Scott, *Tertiary contacts distant from the active site prime a ribozyme for catalysis.* Cell, 2006. **126**(2): p. 309-20.

41. Lee, T.S., et al., *Role of Mg2+ in hammerhead ribozyme catalysis from molecular simulation.* J Am Chem Soc, 2008. **130**(10): p. 3053-64.

42. Raines, K. and P.A. Gottlieb, *Enzymatic incorporation of 2'-thio-CTP into the HDV ribozyme.* Rna, 1998. **4**(3): p. 340-5.

43. Nelson, J.A. and O.C. Uhlenbeck, *Hammerhead redux: does the new structure fit the old biochemical data?* Rna, 2008. **14**(4): p. 605-15.

44. Zhou, D.M., et al., *Explanation by a putative triester-like mechanism for the thio effects and Mn2+ rescues in reactions catalyzed by a hammerhead ribozyme.* FEBS Lett, 1998. **431**(2): p. 154-60.

45. Wang, S., et al., *Identification of the hammerhead ribozyme metal ion binding site responsible for rescue of the deleterious effect of a cleavage site phosphorothioate.* Biochemistry, 1999. **38**(43): p. 14363-78.

46. Flohe, L., *The labour pains of biochemical selenology: The history of selenoprotein biosynthesis.* Biochim Biophys Acta, 2009.

47. Li, C., *Selenium deficiency and endemic heart failure in China: a case study of biogeochemistry for human health.* Ambio, 2007. **36**(1): p. 90-3.

48. *Selenium. Monograph.* Altern Med Rev, 2003. **8**(1): p. 63-71.

49. Clark, L.C., et al., *Effects of selenium supplementation for cancer prevention in patients with carcinoma of the skin. A randomized controlled trial. Nutritional Prevention of Cancer Study Group.* JAMA, 1996. **276**(24): p. 1957-63.

50. Lippman, S.M., et al., *Effect of selenium and vitamin E on risk of prostate cancer and other cancers: the Selenium and Vitamin E Cancer Prevention Trial (SELECT).* JAMA, 2009. **301**(1): p. 39-51.

51. Kryukov, G.V., et al., *Characterization of mammalian selenoproteomes.* Science, 2003. **300**(5624): p. 1439-43.

52. Surh, Y.-J., *Dietary modulation of cell signaling pathways*. 2009, Boca Raton: CRC Press. xxii, 477 p.

53. Flohe, L., W.A. Gunzler, and H.H. Schock, *Glutathione peroxidase: a selenoenzyme.* FEBS Lett, 1973. **32**(1): p. 132-4.

54. Reeves, M.A. and P.R. Hoffmann, *The human selenoproteome: recent insights into functions and regulation.* Cell Mol Life Sci, 2009.

55. Rayman, M.P., H.G. Infante, and M. Sargent, *Food-chain selenium and human health: spotlight on speciation.* Br J Nutr, 2008. **100**(2): p. 238-53.

56. Burk, R.F., K.E. Hill, and A.K. Motley, *Selenoprotein metabolism and function: evidence for more than one function for selenoprotein P.* J Nutr, 2003. **133**(5 Suppl 1): p. 1517S-20S.

57. Letavayova, L., V. Vlckova, and J. Brozmanova, *Selenium: from cancer prevention to DNA damage.* Toxicology, 2006. **227**(1-2): p. 1-14.

58. Suzuki, K.T. and Y. Ogra, *Metabolic pathway for selenium in the body: speciation by HPLC-ICP MS with enriched Se.* Food Addit Contam, 2002. **19**(10): p. 974-83.

59. Glass, R.S., et al., *Monoselenophosphate: synthesis, characterization, and identity with the prokaryotic biological selenium donor, compound*

SePX. Biochemistry, 1993. **32**(47): p. 12555-9.

60. Ip, C., et al., *Chemical form of selenium, critical metabolites, and cancer prevention.* Cancer Res, 1991. **51**(2): p. 595-600.
61. Caton-Williams, J. and Z. Huang, *Biochemistry of selenium-derivatized naturally occurring and unnatural nucleic acids.* Chem Biodivers, 2008. **5**(3): p. 396-407.
62. Chen, C.S. and T.C. Stadtman, *Selenium-containing tRNAs from Clostridium sticklandii: cochromatography of one species with L-prolyl-tRNA.* Proc Natl Acad Sci U S A, 1980. **77**(3): p. 1403-7.
63. Veres, Z. and T.C. Stadtman, *A purified selenophosphate-dependent enzyme from Salmonella typhimurium catalyzes the replacement of sulfur in 2-thiouridine residues in tRNAs with selenium.* Proc Natl Acad Sci U S A, 1994. **91**(17): p. 8092-6.
64. Wolfe, M.D., et al., *Functional diversity of the rhodanese homology domain: the Escherichia coli ybbB gene encodes a selenophosphate-dependent tRNA 2-selenouridine synthase.* J Biol Chem, 2004. **279**(3): p. 1801-9.
65. Politino, M., et al., *Biosynthesis of selenium-modified tRNAs in Methanococcus vannielii.* Proc Natl Acad Sci U S A, 1990. **87**(16): p. 6345-8.
66. Ching, W.M., *Occurrence of selenium-containing tRNAs in mouse leukemia cells.* Proc Natl Acad Sci U S A, 1984. **81**(10): p. 3010-3.
67. Mizutani, T., et al., *Trace 5-methylaminomethyl-2-selenouridine in bovine tRNA and the selenouridine synthase activity in bovine liver.* Mol Biol Rep,

1999. **26**(3): p. 167-72.

68. Lin, L., et al., *Facile synthesis and anti-tumor cell activity of Se-containing nucleosides.* Nucleosides Nucleotides Nucleic Acids, 2009. **28**(1): p. 56-66.
69. Carrasco, N., et al., *Synthesis of selenium-derivatized nucleosides and oligonucleotides for X-ray crystallography.* Nucleosides Nucleotides Nucleic Acids, 2001. **20**(9): p. 1723-34.
70. Du, Q., et al., *Internal derivatization of oligonucleotides with selenium for X-ray crystallography using MAD.* J Am Chem Soc, 2002. **124**(1): p. 24-5.
71. Carrasco, N., et al., *Selenium derivatization and crystallization of DNA and RNA oligonucleotides for X-ray crystallography using multiple anomalous dispersion.* Nucleic Acids Res, 2004. **32**(5): p. 1638-46.
72. Buzin, Y., N. Carrasco, and Z. Huang, *Synthesis of selenium-derivatized cytidine and oligonucleotides for X-ray crystallography using MAD.* Org Lett, 2004. **6**(7): p. 1099-102.
73. Sheng, J., et al., *Synthesis of a 2'-Se-thymidine phosphoramidite and its incorporation into oligonucleotides for crystal structure study.* Org Lett, 2007. **9**(5): p. 749-52.
74. Hobartner, C. and R. Micura, *Chemical synthesis of selenium-modified oligoribonucleotides and their enzymatic ligation leading to an U6 SnRNA stem-loop segment.* J Am Chem Soc, 2004. **126**(4): p. 1141-9.
75. Hobartner, C., et al., *Syntheses of RNAs with up to 100 nucleotides containing site-specific 2'-methylseleno labels for use in X-ray crystallography.* J Am Chem Soc, 2005. **127**(34): p. 12035-45.

76. Moroder, H., et al., *Synthesis, oxidation behavior, crystallization and structure of 2'-methylseleno guanosine containing RNAs.* J Am Chem Soc, 2006. **128**(30): p. 9909-18.

77. Carrasco, N. and Z. Huang, *Enzymatic synthesis of phosphoroselenoate DNA using thymidine 5'-(alpha-P-seleno)triphosphate and DNA polymerase for X-ray crystallography via MAD.* J Am Chem Soc, 2004. **126**(2): p. 448-9.

78. Carrasco, N., et al., *Efficient enzymatic synthesis of phosphoroselenoate RNA by using adenosine 5'-(alpha-P-seleno)triphosphate.* Angew Chem Int Ed Engl, 2005. **45**(1): p. 94-7.

79. Caton-Williams, J. and Z. Huang, *Synthesis and DNA-polymerase incorporation of colored 4-selenothymidine triphosphate for polymerase recognition and DNA visualization.* Angew Chem Int Ed Engl, 2008. **47**(9): p. 1723-5.

80. Salon, J., et al., *Oxygen replacement with selenium at the thymidine 4-position for the Se base pairing and crystal structure studies.* J Am Chem Soc, 2007. **129**(16): p. 4862-3.

81. Hassan, A.E., et al., *Synthesis and crystallographic analysis of 5-Se-thymidine DNAs.* Org Lett, 2009. **11**(12): p. 2503-6.

82. Salon, J., et al., *Derivatization of DNAs with selenium at 6-position of guanine for function and crystal structure studies.* Nucleic Acids Res, 2008. **36**(22): p. 7009-18.

83. Makarova, J.A. and D.A. Kramerov, *Noncoding RNAs.* Biochemistry

(Mosc), 2007. **72**(11): p. 1161-78.

84. Osborne, E.M., J.E. Schaak, and V.J. Derose, *Characterization of a native hammerhead ribozyme derived from schistosomes.* Rna, 2005. **11**(2): p. 187-96.

85. Doudna, J.A., *Hammerhead ribozyme structure: U-turn for RNA structural biology.* Structure, 1995. **3**(8): p. 747-50.

86. Brinton, M.A., *The molecular biology of West Nile Virus: a new invader of the western hemisphere.* Annu Rev Microbiol, 2002. **56**: p. 371-402.

87. Emara, M.M., et al., *Mutation of mapped TIA-1/TIAR binding sites in the 3' terminal stem-loop of West Nile virus minus-strand RNA in an infectious clone negatively affects genomic RNA amplification.* J Virol, 2008. **82**(21): p. 10657-70.

88. Shi, P.Y., W. Li, and M.A. Brinton, *Cell proteins bind specifically to West Nile virus minus-strand 3' stem-loop RNA.* J Virol, 1996. **70**(9): p. 6278-87.

89. Saldanha, R., A. Ellington, and A.M. Lambowitz, *Analysis of the CYT-18 protein binding site at the junction of stacked helices in a group I intron RNA by quantitative binding assays and in vitro selection.* J Mol Biol, 1996. **261**(1): p. 23-42.

90. Szewczak, A.A., et al., *Thermodynamic stability of the P4-P6 domain RNA tertiary structure measured by temperature gradient gel electrophoresis.* Biochemistry, 1998. **37**(32): p. 11162-70.

91. Juneau, K., et al., *Structural basis of the enhanced stability of a mutant ribozyme domain and a detailed view of RNA--solvent interactions.*

Structure, 2001. **9**(3): p. 221-31.

92. Stawinski, J. and M. Thelin, *Nucleoside H-phosphonates. 14. Synthesis of nucleoside phosphoroselenoates and phosphorothioselenoates via stereospecific selenization of the corresponding H-phosphonate and H-phosphonothioate diesters with the aid of new selenium-transfer reagent, 3H-1,2-benzothiaselenol-3-one.* J. Org. Chem., 1994. **59**: p. 130-136.

93. Ludwig, J. and F. Eckstein, *Rapid and efficient synthesis of nucleoside 5'-0-(1-thiotriphosphates), 5'-triphosphates and 2',3'-cyclophosphorothioates using 2-chloro-4H-1,3,2-benzodioxaphosphorin-4-one.* J. Org. Chem., 1989. **54**(3): p. 631-635.

94. Kao, C., M. Zheng, and S. Rudisser, *A simple and efficient method to reduce nontemplated nucleotide addition at the 3 terminus of RNAs transcribed by T7 RNA polymerase.* Rna, 1999. **5**(9): p. 1268-72.

95. Kim, R., et al., *High-resolution crystals and preliminary X-ray diffraction studies of a catalytic RNA.* Acta Crystallogr D Biol Crystallogr, 1994. **50**(Pt 3): p. 290-2.

96. Li, P., et al., *Synthesis of alpha-P-modified nucleoside diphosphates with ethylenediamine.* J Am Chem Soc, 2005. **127**(48): p. 16782-3.

97. Wilson, C. and A.D. Keefe, *Building oligonucleotide therapeutics using non-natural chemistries.* Curr Opin Chem Biol, 2006. **10**(6): p. 607-14.

98. Jagannadham, M.V., *Identifying the Sequence and Distinguishing the Oxidized—Methionine from Phenylalanine Peptides by MALDI TOF/TOF Mass Spectrometry in an Antarctic Bacterium Pseudomonas Syringae.*

Proteomics Insights, 2009. **2**: p. 27-31.

99. Hall, A.H., et al., *RNA interference using boranophosphate siRNAs: structure-activity relationships.* Nucleic Acids Res, 2004. **32**(20): p. 5991-6000.

100. Terrazas, M. and E.T. Kool, *RNA major groove modifications improve siRNA stability and biological activity.* Nucleic Acids Res, 2009. **37**(2): p. 346-53.

101. Kusenda, B., et al., *MicroRNA biogenesis, functionality and cancer relevance.* Biomed Pap Med Fac Univ Palacky Olomouc Czech Repub, 2006. **150**(2): p. 205-15.

102. Ambros, V., *The functions of animal microRNAs.* Nature, 2004. **431**(7006): p. 350-5.

103. Ozpolat, B., A.K. Sood, and G. Lopez-Berestein, *Nanomedicine based approaches for the delivery of siRNA in cancer.* J Intern Med, 2010. **267**(1): p. 44-53.

104. Schroeder, A., et al., *Lipid-based nanotherapeutics for siRNA delivery.* J Intern Med, 2010. **267**(1): p. 9-21.

105. Takahashi, M., N. Minakawa, and A. Matsuda, *Synthesis and characterization of 2'-modified-4'-thioRNA: a comprehensive comparison of nuclease stability.* Nucleic Acids Res, 2009. **37**(4): p. 1353-62.

106. Chiu, Y.L. and T.M. Rana, *RNAi in human cells: basic structural and functional features of small interfering RNA.* Mol Cell, 2002. **10**(3): p. 549-61.

107. Sioud, M. and P.O. Iversen, *Ribozymes, DNAzymes and small interfering RNAs as therapeutics.* Curr Drug Targets, 2005. **6**(6): p. 647-53.

108. Chiu, Y.L. and T.M. Rana, *siRNA function in RNAi: a chemical modification analysis.* Rna, 2003. **9**(9): p. 1034-48.

109. Yang, M. and J. Mattes, *Discovery, biology and therapeutic potential of RNA interference, microRNA and antagomirs.* Pharmacol Ther, 2008. **117**(1): p. 94-104.

110. Kim, D.H., et al., *Interferon induction by siRNAs and ssRNAs synthesized by phage polymerase.* Nat Biotechnol, 2004. **22**(3): p. 321-5.

111. Mazurek, S., *Pyruvate kinase type M2: a key regulator within the tumour metabolome and a tool for metabolic profiling of tumours.* Ernst Schering Found Symp Proc, 2007(4): p. 99-124.

112. Elbashir, S.M., et al., *Duplexes of 21-nucleotide RNAs mediate RNA interference in cultured mammalian cells.* Nature, 2001. **411**(6836): p. 494-8.

113. Prakash, T.P., et al., *Activity of siRNAs with 2-thio-2'-O-methyluridine modification in mammalian cells.* Nucleosides Nucleotides Nucleic Acids, 2009. **28**(10): p. 902-10.

114. Chow, C.S., S.K. Mahto, and T.N. Lamichhane, *Combined Approaches to Site-Specific Modification of RNA.* ACS Chem Biol, 2008. **3**(1): p. 30-37.

115. Baudin-Baillieu, A., et al., *Nucleotide modifications in three functionally important regions of the Saccharomyces cerevisiae ribosome affect translation accuracy.* Nucleic Acids Res, 2009. **37**(22): p. 7665-77.

116. Onizuka, K., Y. Taniguchi, and S. Sasaki, *Site-specific covalent modification of RNA guided by functionality-transfer oligodeoxynucleotides.* Bioconjug Chem, 2009. **20**(4): p. 799-803.

117. Peracchi, A., et al., *Structure-function relationships in the hammerhead ribozyme probed by base rescue.* Rna, 1998. **4**(11): p. 1332-46.

118. Williams, A.A., et al., *Impact of sugar pucker on base pair and mispair stability.* Biochemistry, 2009. **48**(50): p. 11994-2004.

119. Wittwer, A.J., et al., *Identification and synthesis of a naturally occurring selenonucleoside in bacterial tRNAs: 5-[(methylamino)methyl]-2-selenouridine.* Biochemistry, 1984. **23**(20): p. 4650-5.

120. Yoshikawa, M., T. Kato, and T. Takenishi, *A novel method for phosphorylation of nucleosides to 5'-nucleotides.* Tetrahedron Lett, 1967. **50**: p. 5065-8.

121. Barceloux, D.G., *Selenium.* J Toxicol Clin Toxicol, 1999. **37**(2): p. 145-72.

122. El-Bayoumy, K. and R. Sinha, *Mechanisms of mammary cancer chemoprevention by organoselenium compounds.* Mutat Res, 2004. **551**(1-2): p. 181-97.

123. Gladyshev, V.N. and D.L. Hatfield, *Selenocysteine-containing proteins in mammals.* J Biomed Sci, 1999. **6**(3): p. 151-60.

124. Sinha, R., et al., *Effects of naturally occurring and synthetic organoselenium compounds on protein profiling in androgen responsive and androgen independent human prostate cancer cells.* Nutr Cancer, 2008. **60**(2): p. 267-75.

125. Cirelli, A., et al., *Serum selenium concentration and disease progress in patients with HIV infection.* Clin Biochem, 1991. **24**(2): p. 211-4.

126. Thompson, F.E., et al., *Serum selenium and the risk of cervical cancer among women in the United States.* Cancer Causes Control, 2002. **13**(6): p. 517-26.

127. Cheng, T.O., *Selenium deficiency and cardiomyopathy.* J R Soc Med, 2002. **95**(4): p. 219-20.

128. Tarp, U., *Selenium and the selenium-dependent glutathione peroxidase in rheumatoid arthritis.* Dan Med Bull, 1994. **41**(3): p. 264-74.

129. Allam, M.F. and R.A. Lucane, *Selenium supplementation for asthma.* Cochrane Database Syst Rev, 2004(2): p. CD003538.

130. Duffield-Lillico, A.J., et al., *Baseline characteristics and the effect of selenium supplementation on cancer incidence in a randomized clinical trial: a summary report of the Nutritional Prevention of Cancer Trial.* Cancer Epidemiol Biomarkers Prev, 2002. **11**(7): p. 630-9.

131. Dumont, E., F. Vanhaecke, and R. Cornelis, *Selenium speciation from food source to metabolites: a critical review.* Anal Bioanal Chem, 2006. **385**(7): p. 1304-23.

132. El-Bayoumy, K., et al., *Cancer chemoprevention by garlic and garlic-containing sulfur and selenium compounds.* J Nutr, 2006. **136**(3 Suppl): p. 864S-869S.

133. Hurwitz, B.E., et al., *Suppression of human immunodeficiency virus type 1 viral load with selenium supplementation: a randomized controlled trial.*

Arch Intern Med, 2007. **167**(2): p. 148-54.

134. Kupka, R., et al., *Randomized, double-blind, placebo-controlled trial of selenium supplements among HIV-infected pregnant women in Tanzania: effects on maternal and child outcomes.* Am J Clin Nutr, 2008. **87**(6): p. 1802-8.

135. Villamor, E., et al., *A trial of the effect of micronutrient supplementation on treatment outcome, T cell counts, morbidity, and mortality in adults with pulmonary tuberculosis.* J Infect Dis, 2008. **197**(11): p. 1499-505.

136. Sohni, O.S., et al., *Contrasting patterns of selenium excretion by female CD rats treated with chemically related chemopreventive organic selenocyanate compounds.* Anticancer Res, 1995. **15**(5B): p. 1849-56.

137. Sohn, O.S., et al., *Comparative effects of phenylenebis(methylene)selenocyanate isomers on xenobiotic metabolizing enzymes in organs of female CD rats.* Carcinogenesis, 1999. **20**(4): p. 615-21.

138. Deagen, J.T., et al., *Effects of dietary selenite, selenocystine and selenomethionine on selenocysteine lyase and glutathione peroxidase activities and on selenium levels in rat tissues.* J Nutr, 1987. **117**(1): p. 91-8.

139. Swanson, C.A., et al., *Human [74Se]selenomethionine metabolism: a kinetic model.* Am J Clin Nutr, 1991. **54**(5): p. 917-26.

140. Brown, K.M., et al., *Effects of organic and inorganic selenium supplementation on selenoenzyme activity in blood lymphocytes,*

granulocytes, platelets and erythrocytes. Clin Sci (Lond), 2000. **98**(5): p. 593-9.

141. Ip, C., et al., *In vitro and in vivo studies of methylseleninic acid: evidence that a monomethylated selenium metabolite is critical for cancer chemoprevention.* Cancer Res, 2000. **60**(11): p. 2882-6.

142. Ip, C., Y. Dong, and H.E. Ganther, *New concepts in selenium chemoprevention.* Cancer Metastasis Rev, 2002. **21**(3-4): p. 281-9.

143. Lee, J.S., et al., *Neural network-based analysis of thiol proteomics data in identifying potential selenium targets.* Prep Biochem Biotechnol, 2006. **36**(1): p. 37-64.

144. Kajander, E.O., et al., *Metabolism, cellular actions, and cytotoxicity of selenomethionine in cultured cells.* Biol Trace Elem Res, 1991. **28**(1): p. 57-68.

145. Chu, S.H., C.Y. Shiue, and M.Y. Chu, *Synthesis and biological activity of some 8-substituted selenoguanosine cyclic 3',5'-phosphates and related compounds.* J Med Chem, 1975. **18**(6): p. 559-64.

146. Mautner, H.G., et al., *The Synthesis and Antineoplastic Properties of Selenoguanine, Selenocytosine and Related Compounds.* J Med Chem, 1963. **6**: p. 36-9.

147. Ching, W.M., B. Alzner-DeWeerd, and T.C. Stadtman, *A selenium-containing nucleoside at the first position of the anticodon in seleno-tRNAGlu from Clostridium sticklandii.* Proc Natl Acad Sci U S A, 1985. **82**(2): p. 347-50.